АВТОМАТИКА
И
ТЕЛЕМЕХАНИКА

Volume 19, No. 4

April 1958

SOVIET INSTRUMENTATION AND
CONTROL TRANSLATION SERIES

Automation and Remote Control

(The Soviet Journal *Avtomatika i Telemekhanika* in English Translation)

■ This translation of a Soviet journal on automatic control is published as a service to American science and industry. It is sponsored by the Instrument Society of America under a grant in aid from the National Science Foundation, continuing a program initiated by the Massachusetts Institute of Technology.

SOVIET INSTRUMENTATION AND CONTROL TRANSLATION SERIES

■ This translation of the Soviet Journal *Avtomatika i Telemekhanika* is published and distributed at nominal subscription rates under a grant in aid to the Instrument Society of America from the National Science Foundation. This translated journal, and others in the Series (see back cover), will enable American scientists and engineers to be informed of work in the fields of instrumentation, measurement techniques and automatic control reported in the Soviet Union.

The original Russian articles are translated by competent technical personnel. The translations are on a cover-to-cover basis, permitting readers to appraise for themselves the scope, status and importance of the Soviet work.

Publication of *Avtomatika i Telemekhanika* in English translation started under the present auspices in April 1958 with Russian Vol. 18, No. 1 of January 1957. Translation of Vol. 18 has now been completed. The twelve issues of Vol. 19 will be published in English translation by mid-1959.

All views expressed in the translated material are intended to be those of the original authors, and not those of the translators, nor the Instrument Society of America.

Readers are invited to submit communications on the quality of the translations and the content of the articles to ISA headquarters. Pertinent correspondence will be published in the "Letters" section of the ISA Journal. Space will also be made available in the ISA Journal for such replies as may be received from Russian authors to comments or questions by American readers.

Subscription Prices:

Per year (12 issues), starting with Vol. 19, No. 1

General: United States and Canada	$30.00
Elsewhere	33.00
Libraries of non-profit academic institutions:	
United States and Canada	$15.00
Elsewhere	18.00
Single issues to everyone, each	$ 6.00

See back cover for combined subscription to entire Series.

Subscriptions and requests for information on back issues should be addressed to the:

Instrument Society of America
313 Sixth Avenue, Pittsburgh 22, Penna.

Translated and printed by Consultants Bureau, Inc.

Volume XIX No. 4 – April 1958

English Translation Printed February, 1959

Automation and Remote Control

The Soviet Journal Avtomatika i Telemekhanika in English Translation

Avtomatika i Telemekhanika is a Publication of the Academy of Sciences of the USSR

See following page for Table of Contents.

AUTOMATION AND REMOTE CONTROL

Volume 19, Number 4 April 1958

CONTENTS

12-149244
S.O.

GRAPHICO-ANALYTIC METHOD FOR DETERMINING RELAY SYSTEM CHARACTERISTICS

L. P. Kuz'min

(Moscow)

A graphico-analytic method is presented for the determination of relay system characteristics $J_1(\omega)$ and $J_\gamma(\omega)$, necessary in the investigation of periodic regimens in relay systems when the frequency method is used. There will be given an example of the determination of the characteristics $J_1(\omega)$ and $J_\gamma(\omega)$, using the actual frequency characteristic of the linear portion of the system.

In the investigation of periodic regimens in relay designs, the schematic diagram is usually given in the form shown in Fig. 1. All the linear (linearized) links are treated as one link, characterized by the transfer function $W_{lp}(p)$. The external controlling function u(t) and the external stimulus f(t) are brought to the input of the relay element. In this case, the controlling signal x(t) at the relay input is made up of the controlling function u(t), f(t) and the feedback signal z(t). As a result of the impression of the controlling signal x(t), a signal y(t) is produced at the relay output, this signal taking the form of a sequence of rectangular pulses of constant amplitude. Acting on the linear link, these signals give rise to the appearance of the output signal z(t) of the closed-loop relay system.

If the system is in a periodic regimen, the quantities x(t), y(t) and z(t) vary periodically with a definite frequency. The investigation of the periodic regimen in relay systems boils down to the determination of the periodic solution of the equation

$$\tilde{z}(t) = W_{lp}(p)\,\tilde{y}(t), \quad * \qquad (1)$$

satisfying the conditions that the given periodic regimen exist [1].

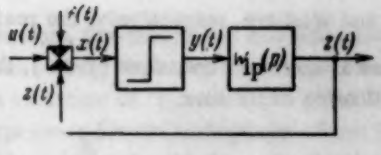

Fig. 1. Schematic diagram of a relay system.

In the majority of cases, the direct determination of the periodic solution of Equation (1) is a quite difficult problem. Therefore, it is generally solved by means of various special methods [2-5].

The investigation of periodic regimens in relay systems by the frequency method [2] is carried out by means of the so-called characteristic of the relay system

$$J(\omega) = -\frac{1}{\omega}\tilde{z}\left(\frac{\pi}{\omega}\right) - j\tilde{z}'\left(\frac{\pi}{\omega}\right). \qquad (2)$$

If the relay element possesses an insensitive zone, then the periodic regimen is characterized not only by the frequency ω, but also by the relative time during which the relay contact is in the closed state, $\gamma = t_{cl}/T$.

*Here and in the sequel, the sign ~ over the symbol for a quantity indicates that the quantity varies periodically.

where T is the half-period of the given periodic regimen.

In this case, the investigation of the relay system is carried out by means of two characteristics:

$$J_1(\omega) = -\frac{1}{\omega}\tilde{z}\left(\frac{\pi}{\omega}\right) - \tilde{z}\left(\frac{\pi}{\omega}\right), \quad J_\gamma(\omega) = -\frac{1}{\omega}\tilde{z}\left(\gamma\frac{\pi}{\omega}\right) - \tilde{z}\left(\gamma\frac{\pi}{\omega}\right), \tag{3}$$

which are functions of two parameters: the frequency ω and the relative time the contact is in the closed state, γ.

The characteristics (2) and (3) of the relay system are closely related to the transfer function of the linear portion, $W_{lp}(p)$, and, in those cases where the poles of $W_{lp}(p)$ are known, may be calculated from this transfer function. Moreover, $J(\omega)$, $J_1(\omega)$ and $J_\gamma(\omega)$ may be computed from the transient (timewise) and from the amplitude-phase characteristics of the linear portion [1].

The latter method is used the most frequently since, in practice, it has no limitations from the point of view of structure of the system, parameters, stability of the linear portion, etc. It provides the possibility of calculation of the characteristics (2) and (3) from empirically determined amplitude-phase characteristics of the systems being investigated.

The relay system characteristics are connected to the amplitude-phase characteristic of the linear portion by the following expressions, given in the form of series:

$$\begin{aligned} J_1(\omega) &= \frac{2k_p}{\pi}\sum_{m=1}^{\infty}\Big[\{[1-\cos(2m-1)\gamma\pi]u[(2m-1)\omega]-\sin(2m-1)\gamma\pi v[(2m-1)\omega]\}+ \\ &+ j\left\{\frac{\sin(2m-1)\gamma\pi}{2m-1}u[(2m-1)\omega]+\frac{1-\cos(2m-1)\gamma\pi}{2m-1}v[(2m-1)\omega]\right\}\Big], \\ J_\gamma(\omega) &= \frac{2k_p}{\pi}\sum_{m=1}^{\infty}\Big[\{[1-\cos(2m-1)\gamma\pi]u[(2m-1)\omega]+\sin(2m-1)\gamma\pi v[(2m-1)\omega]\}- \\ &- j\left\{\frac{\sin(2m-1)\gamma\pi}{2m-1}u[(2m-1)\omega]-\frac{1-\cos(2m-1)\gamma\pi}{2m-1}v[(2m-1)\omega]\right\}\Big], \end{aligned} \tag{4}$$

where $u(\omega)$ and $v(\omega)$ are, respectively, the real and imaginary parts of the amplitude-phase characteristic.

If there is no intensitive zone ($\gamma = 1$), then the characteristics $J_1(\omega)$ and $J_\gamma(\omega)$ coincide, and are determined from the following expression:

$$J(\omega) = \frac{4k_p}{\pi}\sum_{m=1}^{\infty}\left[u[(2m-1)\omega]+j\frac{v[(2m-1)\omega]}{2m-1}\right]. \tag{5}$$

Analysis of Expressions (4) and (5) shows that the determination of the relay system characteristic and, in the former case, of the characteristics $J_1(\omega)$ and $J_\gamma(\omega)$, entails a great deal of computational work. In fact, to determine $J_1(\omega)$ or $J_\gamma(\omega)$ from Formula (4) it is necessary, for each fixed value of the frequency, to compute mp terms of each series (here, m is the number of terms taken, and p is the number of fixed values of the parameter γ). There is thus the constant necessity to compute mpq terms in Expression (4), where q is the minimum quantity of fixed frequencies necessary for the construction of the characteristics $J_1(\omega)$ and $J_\gamma(\omega)$.

The magnitude of the computing job essentially complicates the use of the frequency method in investigating relay systems. This is particularly the case when a choice of parameters for the periodic regimen is being made, with concomitant variations of the structure of the design (introduction of feedback, etc.), since here the expressions $J_1(\omega)$ and $J_\gamma(\omega)$ are repeated more than once.

The problem of investigation is essentially simplified if a graphico-analytic method is used for determining the characteristic. In essence, the graphico-analytic method of computing the characteristics $J_1(\omega)$ and

$J_\gamma(\omega)$ consists of picturing their components, corresponding to the values m = 1, 2,..., ∞ and $\gamma = 1$, in the form of vectors, for each fixed value of frequency, determining the hodographs of these vectors when γ varies within the limits $0 < \gamma \leq 1$, and summing the vectors for equal values of the parameter γ. The resulting vectors determine the points of the characteristics $J_1(\omega)$ and $J_\gamma(\omega)$ for the given frequencies and for all values of γ in the interval $0 < \gamma \leq 1$.

As will be shown below, the hodographs of these vectors are determined by an uncomplicated geometric construction, which also gives the possibility of facilitating the determination of the relay system characteristic.

As a basis for our method, we transform Equation (4). Considering that, in practice, the determination of $J_1(\omega)$ and $J_\gamma(\omega)$ is usually restricted to n terms of the series, we present Expressions (4) in the following form:

$$\begin{aligned} J_1(\omega) &= J_{1_1}(\omega) + J_{1_2}(3\omega) + \cdots + J_{1_n}((2n-1)\omega), \\ J_\gamma(\omega) &= J_{\gamma_1}(\omega) + J_{\gamma_2}(3\omega) + \cdots + J_{\gamma_n}((2n-1)\omega). \end{aligned} \tag{6}$$

Here, the complex terms $J_{1_1}(\omega)$, $J_{1_2}(3\omega)$,..., $J_{\gamma_1}(\omega)$, $J_{\gamma_2}(3\omega)$... corresponding to the values m = 1, 2,..., n, are determined by substituting the corresponding values of m in the expression

$$\begin{aligned} J_{1_m}\left((2m-1)\omega\right) &= \frac{2k_p}{\pi}\left[\left\{[1-\cos(2m-1)\gamma\pi]\,u\left((2m-1)\omega\right)-\right.\right. \\ &-\left.\sin(2m-1)\gamma\pi v\left((2m-1)\omega\right)\right\} + j\left\{\frac{\sin(2m-1)\gamma\pi}{2m-1}u\left((2m-1)\omega\right)+\right. \\ &+\left.\left.\frac{1-\cos(2m-1)\gamma\pi}{2m-1}v\left((2m-1)\omega\right)\right\}\right], \\ J_{\gamma_m}\left((2m-1)\omega\right) &= \frac{2k_p}{\pi}\left[\left\{[1-\cos(2m-1)\gamma\pi]\,u\left((2m-1)\omega\right)+\right.\right. \\ &+\left.\sin(2m-1)\gamma\pi v\left((2m-1)\omega\right)\right\} - j\left\{\frac{\sin(2m-1)\gamma\pi}{2m-1}u\left((2m-1)\omega\right)-\right. \\ &-\left.\left.\frac{1-\cos(2m-1)\gamma\pi}{2m-1}v\left((2m-1)\omega\right)\right\}\right]. \end{aligned} \tag{7}$$

The expressions in (7) correspond, in the complex plane, to vectors, the magnitude and direction of which are determined by the frequency ω and the relative time of contact closure γ, but for fixed values of the frequency, $\omega = \omega_k$, depend only on the parameter γ. With continuous variation of γ within the limits $0 < \gamma \leq 1$, the ends of each of these vectors describe hodographs. The analytic expression for the hodographs of the vectors J_{1m} and $J_{\gamma m}$ may be determined immediately from Equations (7) by substituting in them the fixed value of frequency, $\omega = \omega_k$.

Transforming Formulas (7), we present the analytic expression for the hodographs J_{1m} and $J_{\gamma m}$ in a clearer form.

First, we consider the hodographs of the vectors J_{1m} and $J_{\gamma m}$ for m = 1. In this case, substituting in Expression (7) m = 1 and $\omega = \omega_k$ and carrying out a simple transformation, we obtain

$$\begin{aligned} J_{1_1}(\gamma,\ \omega_k) &= \frac{2k_p}{\pi}\{[u(\omega_k) + jv(\omega_k)] - [u(\omega_k) + jv(\omega_k)](\cos\gamma\pi - j\sin\gamma\pi)\}, \\ J_{\gamma_1}(\gamma,\ \omega_k) &= \frac{2k_p}{\pi}\{[u(\omega_k) + jv(\omega_k)] - [u(\omega_k) + jv(\omega_k)](\cos\gamma\pi + j\sin\gamma\pi)\}. \end{aligned} \tag{8}$$

Letting

$$z(\omega_k) = \frac{2k_p}{\pi}[u(\omega_k) + jv(\omega_k)] = \frac{2k_p}{\pi}W(j\omega_k), \tag{9}$$

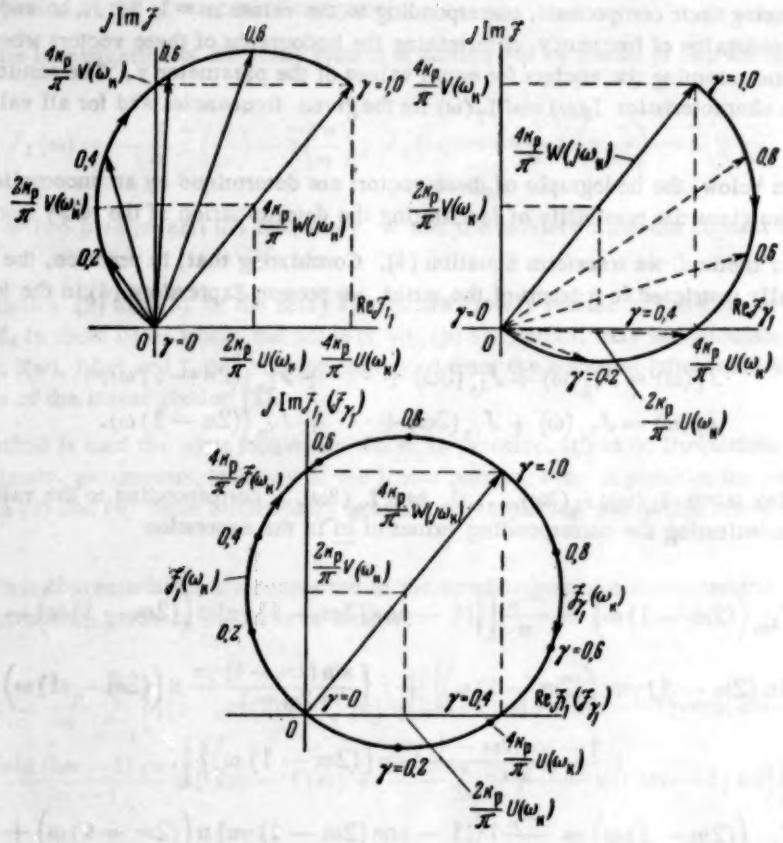

Fig. 2. Hodographs of the vectors $J_{1m}[(2m-1)\omega_k]$ and $J_{\gamma m}[(2m-1)\omega_k]$ for m = 1.

and also taking into account the Euler equations, we can write the equations for the hodographs of $J_{1_1}(\gamma, \omega_k)$ and $J_{\gamma_1}(\gamma, \omega_k)$ in the following form:

$$J_{1_1}(\gamma, \omega_k) = z(\omega_k) - z(\omega_k) e^{-j\gamma\pi}, \quad J_{\gamma_1}(\gamma, \omega_k) = z(\omega_k) - z(\omega_k) e^{j\gamma\pi}. \tag{8'}$$

An equation of the type (8) or (8') is the equation of a circle of radius $z(\omega_k)$ whose center has been displaced to the point $z(\omega_k)$. Bearing in mind that in Equations (8') the argument varies from 0 to π, and that the displacement from its center to the origin of coordinates is equal to its radius, we see that the hodographs of $J_{1_1}(\gamma, \omega_k)$ and $J_{\gamma_1}(\gamma, \omega_k)$ are semicircles, cutting the origin of coordinates when $\gamma = 0$ (Fig. 2). The sum of the hodographs of $J_{1_1}(\gamma, \omega_k)$ and $J_{\gamma_1}(\gamma, \omega_k)$ is a full circle whose diameter is $4k_p/\pi$, the modulus of the amplitude-phase characteristic of the linear portion of the system. In fact, we find from Equation (8) that, for $\gamma = 1$,

$$J_{1_1}(\gamma, \omega_k) = J_{\gamma_1}(\gamma, \omega_k) = \frac{4k_p}{\pi} \overline{W}(j\omega_k) = \frac{4k_p}{\pi} W_0(\omega_k) e^{j\varphi_k},$$

where $W_0(\omega_k)$ is the modulus of the amplitude-phase characteristic when $\omega = \omega_k$.

By analogous transformation, we can put the equations for the hodographs $J_{1m}(\gamma, \omega_k)$ and $J_{\gamma m}(\gamma, \omega_k)$, for m > 1, in the form

$$J_{1_m}(\gamma, (2m-1)\omega_k) = z_{1_m} - \frac{z_{1_m} - z_{2_m}}{2} e^{j(2m-1)\gamma\pi} - \frac{z_{1_m} + z_{2_m}}{2} e^{-j(2m-1)\gamma\pi},$$

$$J_{\gamma_m}(\gamma, (2m-1)\omega_k) = z_{1_m} - \frac{z_{1_m} + z_{2_m}}{2} e^{j(2m-1)\gamma\pi} - \frac{z_{1_m} - z_{2_m}}{2} e^{-j(2m-1)\gamma\pi}, \tag{10}$$

where

$$z_{1_m} = \frac{2k_p}{\pi}\left[u\left((2m-1)\,\omega_k\right) + j\,\frac{v\left((2m-1)\,\omega_k\right)}{2m-1}\right],$$
$$z_{2_m} = \frac{2k_p}{\pi}\left[\frac{u\left((2m-1)\,\omega_k\right)}{2m-1} + jv\left((2m-1)\,\omega_k\right)\right]. \qquad (11)$$

Equations (10) represent ellipses with centers displaced to the point z_{1m} (Fig. 3), determined from Expressions (11).

It is easy to see from Equations (10) that the hodographs of vectors $J_{1m}(\gamma, \omega_k)$ and $J_{\gamma m}(\gamma, \omega_k)$ coincide, differing only in the direction of rotation of the vectors J_{1m} and $J_{\gamma m}$.*

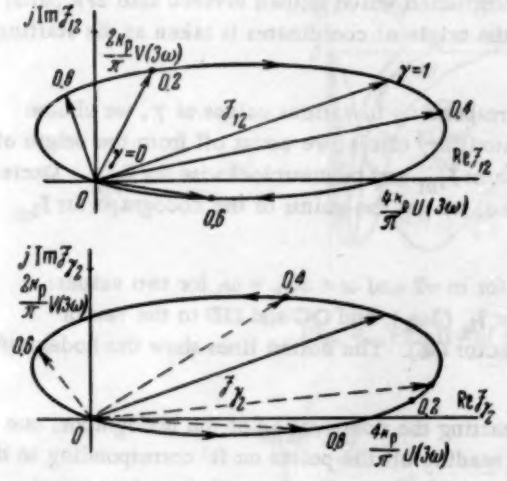

Fig. 3. Hodographs of the vectors $J_{1_m}[(2m-1)\omega_k]$ and $J_{\gamma_m}[(2m-1)\,\omega_k]$ for m = 2.

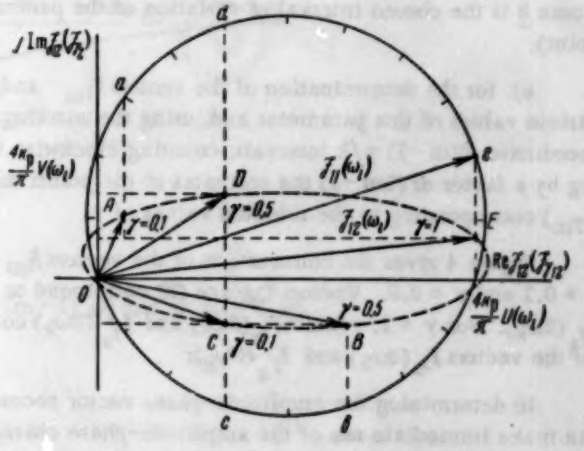

Fig. 4. Construction of the hodographs for the vectors $J_{1m}[(2m-1)\,\omega_k]$ and $J_{\gamma_m}[(2m-1)\,\omega_k]$ for m = 2.

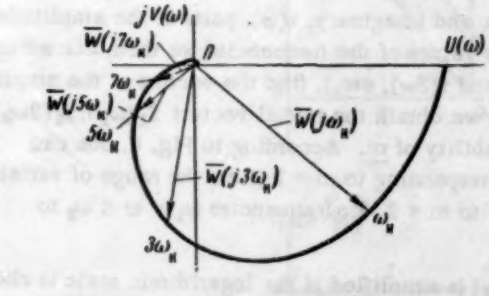

Fig. 5. Determination of the vectors $W[j(2m-1)\,\omega_k]$ from the amplitude-phase characteristic of the linear portion.

For m = 1, the equations for the ellipses, (10), degenerate into those for the circles (8'). Considering circles as particular cases of ellipses whose semi-axes are equal, we are led to the conclusion that the hodographs of the vectors J_{1_m} and J_{γ_m} are ellipses, the magnitude and position of which are determined, for fixed frequency, by the magnitude of the real and imaginary parts of the amplitude-phase characteristic of the linear portion of the system.

It follows from this that, in the determination of $J_1(\omega)$ and $J_\gamma(\omega)$, it is not necessary to compute, for every value of the frequency, the magnitude of the components J_{1_m} and J_{γ_m} for different values of the parameter γ. It is sufficient just to find the components of J_{1_m} and J_{γ_m} for $\gamma = 1$, and all the remaining ones, corresponding to other values of γ, may be found from the hodographs determined by Expressions (10) and (8').

The construction of the hodographs of the vectors J_{1_m} and J_{γ_m} and the determination of the points of these hodographs corresponding to different values of γ, is carried out according to Equations (10). However, it is

* When γ varies between the limits $0 < \gamma \leq 1$, the vector J_{1_m} rotates clockwise, and the vector J_{γ_m} rotates counterclockwise (Fig. 3).

simpler to carry out these operations graphically.

In analyzing Expressions (7) for m> 1, and in comparing them with the corresponding expressions for m = 1, we note that, for m > 1, there is a decrease in the imaginary parts of J_{1m} and $J_{\gamma m}$, and also an increase in the arguments of trigonometric functions sin and cos by a factor of (2m −1). The first condition entails a deformation of the hodograph in amplitude, and the second entails an increase in the argument of the vector J_{1m} (J_{γ_m}) with a change of the parameter γ in comparison with the increase of the argument of the vector J_{1_1} (J_{γ_1}), again by a factor of (2m −1).

Bearing these in mind, and also taking into account that, for m = 1, the hodograph of the vectors J_{1m} and $J_{\gamma m}$ is a circle, we establish the following sequence for constructing the hodographs of these vectors for m > 1:

a) on the complex plane the amplitude-phase characteristic corresponding to the frequency (2m −1) ω is constructed, magnified by the factor $4k_p/\pi$;

b) with this vector as a diameter, an auxiliary circle is constructed which is then divided into 2/k parts, where k is the chosen interval of variation of the parameter γ (the origin of coordinates is taken as the starting point);

c) for the determination of the vectors J_{1m} and $J_{\gamma m}$, corresponding to various values of γ, we choose various values of this parameter and, using the markings on the auxiliary circle, we count off from the origin of coordinates (2m −1) γ/k intervals, counting clockwise for the vector J_{1m} and counterclockwise for $J_{\gamma m}$. Decreasing by a factor of (2m −1) the ordinates of the points thus obtained, we get the points of the hodograph for J_{1m} ($J_{\gamma m}$) corresponding to the selected values of γ.

Figure 4 gives the construction of the vectors J_{1m} and $J_{\gamma m}$ for m =2 and $\omega = 3\omega_k = \omega_i$ for two values: γ = 0.1 and γ = 0.5. Vectors OA and OB correspond to the vector $J_{1_2}(3\omega_k)$, and OC and OD to the vector $J_{\gamma_2}(3\omega_k)$. For γ = 1, vectors $J_{1_2}(3\omega_k)$ and $J_{\gamma_2}(3\omega_k)$ coincide (vector OE). The dotted lines show the hodograph for the vectors $J_{1_2}(3\omega_k)$ and $J_{\gamma_2}(3\omega_k)$:

In determining the amplitude-phase vector necessary for starting the construction of the hodographs, one can make immediate use of the amplitude-phase characteristic, reading off the points on it corresponding to the frequencies ω_k, $3\omega_k$, $5\omega_k$, ... (2m −1) ω_k. The vectors from the origin of coordinates to these points are proportional to $J_1(\omega_k)$, $J_2(3\omega_k)$, $J_3(5\omega_k)$, ... $J_m[(2m-1)\omega_k]$ (Fig. 5).

It is more convenient to carry out the determination of the starting vectors from the family of curves for the real, $u[(2m-1)\omega]$, and imaginary, $v[(2m-1)\omega]$, parts of the amplitude-phase characteristic (Fig. 6), from which the range of variation of m for all computed frequencies may also be determined. The family of curves $u[(2m-1)\omega]$ and $v[(2m-1)\omega]$ are constructed from the real, $u(\omega)$, and imaginary, $v(\omega)$, parts of the amplitude-phase characteristic by recomputing the arguments. By setting the values of the frequencies we then, according to the ordinates of the corresponding curves ($u(\omega)$ and $v(\omega)$, $u(3\omega)$ and $v(3\omega)$, etc.), find the vectors of the amplitude-phase characteristic. Multiplying these by the factor $4k_p/\pi$, we obtain the initial vectors $J_1(\omega_k)$, $J_2(3\omega_k)$, ... $J_m[(2m-1)\omega_k]$. After this, we determine the range of variability of m. According to Fig. 6, one can limit ones consideration to the components of $J_1(\omega)$ and $J_\gamma(\omega)$ corresponding to m = 1 (i.e., the range of variability is m = 1). For frequencies $\omega_2 < \omega \leq \omega_3$ one can limit oneself to m = 2, for frequencies $\omega_1 < \omega \leq \omega_2$ to m = 3, etc.

The construction of the curves $u[(2m-1)\omega]$ and $v[(2m-1)\omega]$ is simplified if the logarithmic scale is chosen for the frequency [1]. Bearing in mind that one octave corresponds to a doubling of the frequency, these curves are simply constructed by translating the curves of $u(\omega)$ and $v(\omega)$ to the left 1.6 octaves for m = 2, 2.3 octaves for m = 3, etc. (Fig. 7).

Taking all of the above into consideration, we can set up the sequence of steps for the determination of the characteristics $J_\chi(\omega)$ and $J_\gamma(\omega)$:

1) the amplitude-phase characteristic of the linear portion of the system is computed, and the curves $u(\omega)$ and $v(\omega)$ are constructed;

2) from the curves $u(\omega)$ and $v(\omega)$ are constructed the families of curves $u[(2m-1)\omega]$ and $v[(2m-1)\omega]$ for m = 2, 3, ..., n;

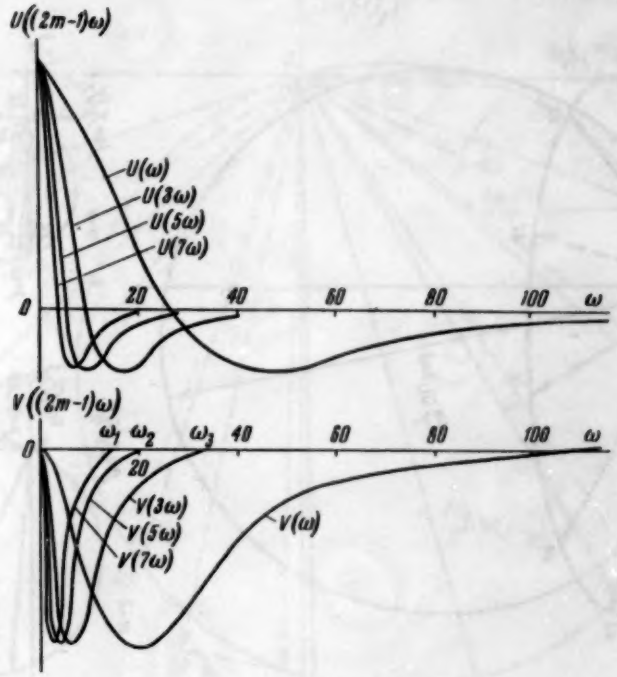

Fig. 6. Family of curves u[(2m −1) ω] and v[(2m −1) ω].

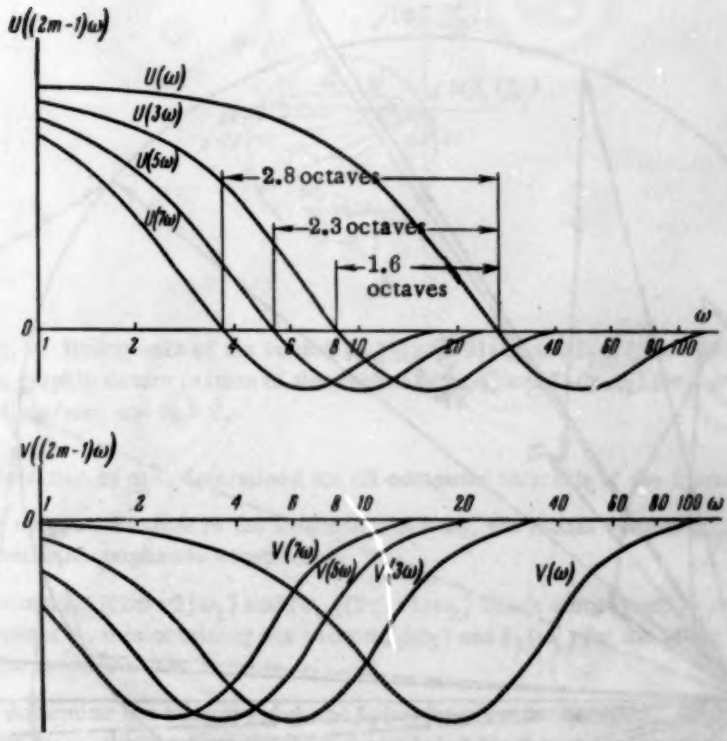

Fig. 7. Construction of the curves u[(2m −1) ω] and v[(2m −1) ω] for m = 2, 3... from the curves u(ω) and v(ω).

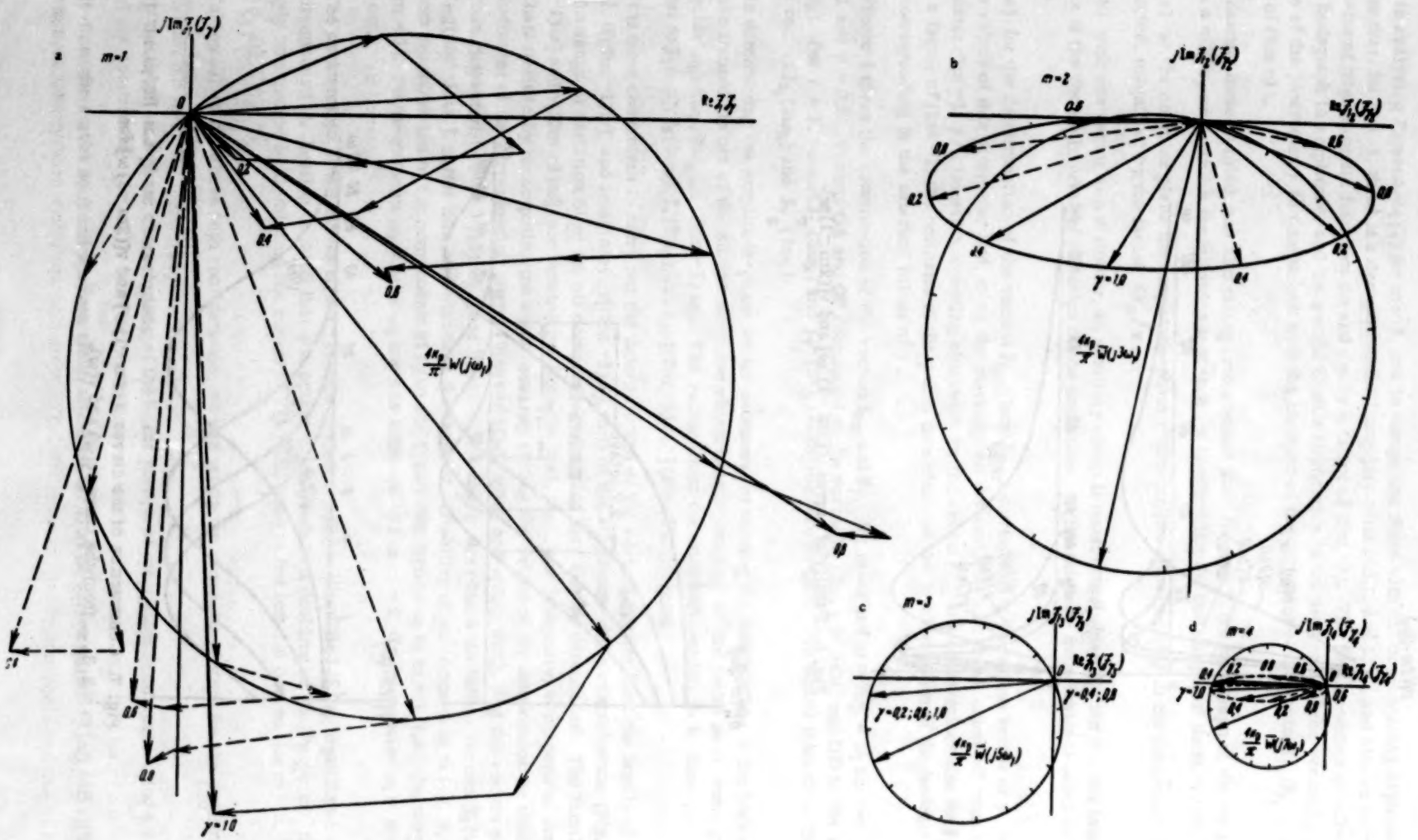

Fig. 8. Hodographs of the vectors $\mathbf{J}_{1m}[(2m-1)\,\omega_1]$ and $\mathbf{J}_{\gamma m}[(2m-1)\,\omega_1]$ and the graphic determination of the vectors $\mathbf{J}_1(\gamma, \omega_1)$ and $\mathbf{I}_\gamma(\gamma, \omega_1)$ for $\omega_1 = 10$ radians/sec., $m = 4$.

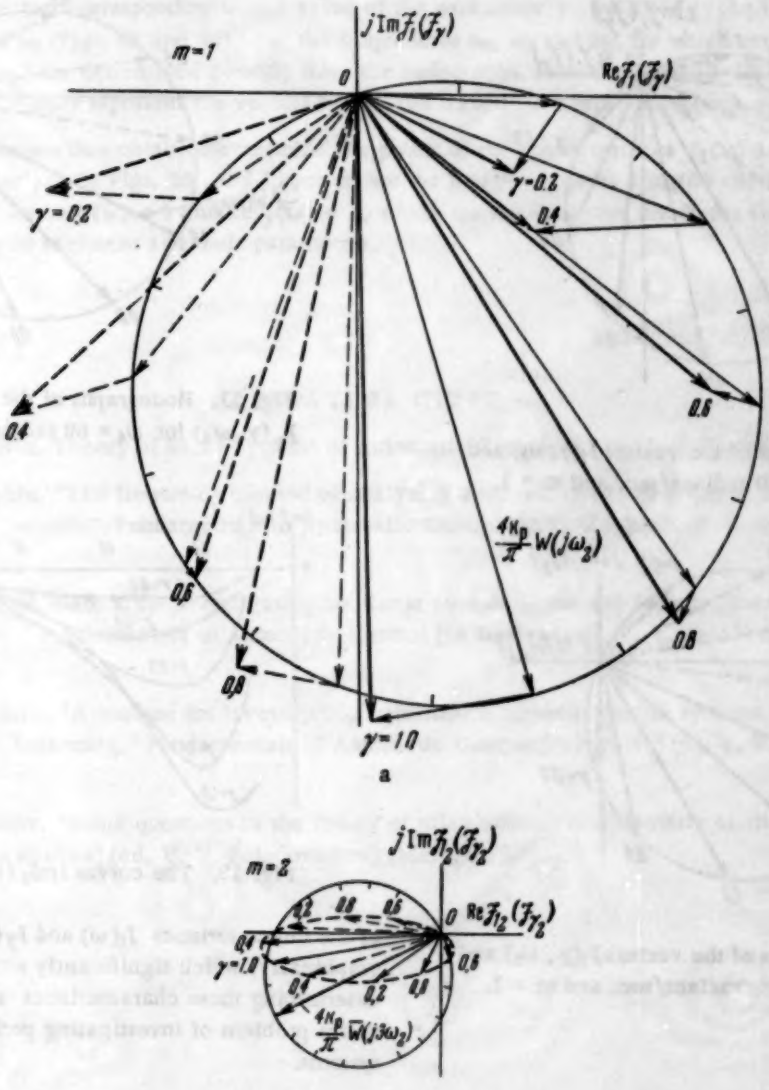

Fig. 9. Hodographs of the vectors $\mathbf{J}_{1m}[(2m-1)\omega_2]$ and $\mathbf{J}_{\gamma m}[(2m-1)\omega_2]$ and the graphic determination of the vectors $\mathbf{J}_1(\gamma,\omega_2)$ and $\mathbf{J}_\gamma(\gamma,\omega_2)$ for $\omega_2 = 20$ radians/sec. and m = 2.

3) the range of variation of m is determined for all computed intervals of the frequency ω;

4) for the chosen computed values of the frequency, $\omega = \omega_k$, the initial vectors $\mathbf{J}_{1m}[(2m-1)\omega_k) = \mathbf{J}_{\gamma m}[(2m-1)\omega_k]$ and their hodographs are constructed;

5) we add the vectors $\mathbf{J}_{1m}[(2m-1)\omega_k]$ and $\mathbf{J}_{\gamma m}[(2m-1)\omega_k]$ which correspond to m = 1, 2, . . . , n and to the same value of the parameter γ, thus obtaining the vectors $\mathbf{J}_1(\omega_k)$ and $\mathbf{J}_\gamma(\omega_k)$ for the given frequency and for various values of γ in the range $0 < \gamma \leq 1$;

6) similarly, we determine the vectors $\mathbf{J}_1(\omega)$ and $\mathbf{J}_\gamma(\omega)$ for all other computed values of the frequency, after which we construct from them the characteristics $J_1(\omega)$ and $J_\gamma(\omega)$ [or their imaginary parts, $\mathrm{Im}J_1(\omega)$ and $\mathrm{Im}J_\gamma(\omega)$], necessary for the investigation of periodic regimens in relay systems.

Thus, using the graphico-analytic method for determining the characteristics of relay systems involves the computation of just one amplitude-phase characteristic. The remaining operations necessary for the determination

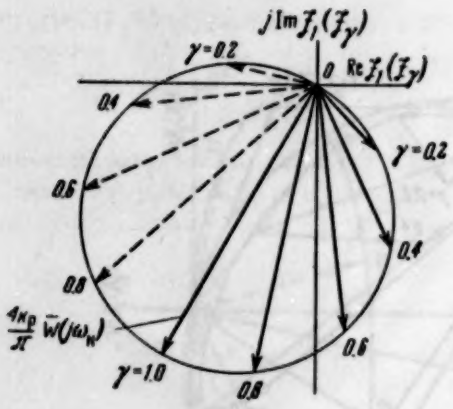

Fig. 10. Hodographs of the vectors $\mathbf{J}_1(\gamma, \omega_3)$ and $\mathbf{J}_\gamma(\gamma, \omega_3)$ for $\omega_3 = 40$ radians/sec. and m = 1.

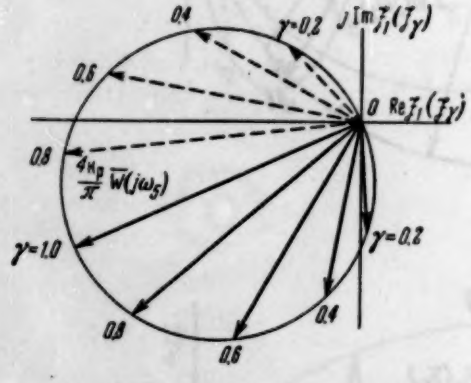

Fig. 12. Hodographs of the vectors $\mathbf{J}_1(\gamma, \omega_5)$ and $\mathbf{J}_\gamma(\gamma, \omega_5)$ for $\omega_5 = 80$ radians/sec. and m = 1.

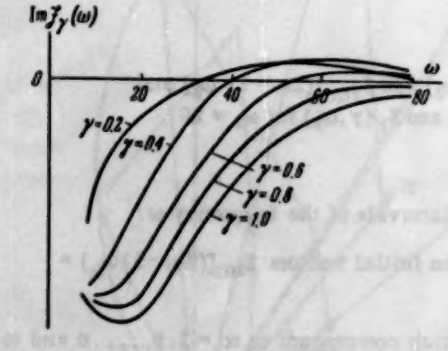

Fig. 14. The curves $\mathrm{Im}J_\gamma(\omega)$.

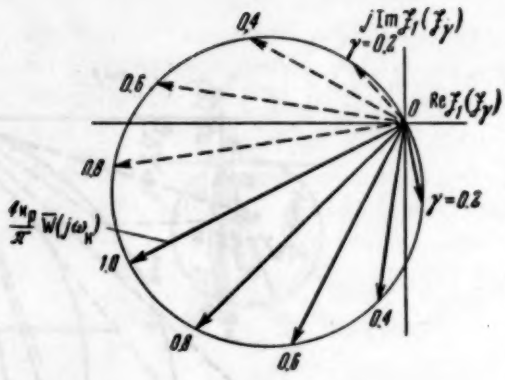

Fig. 11. Hodographs of the vectors $\mathbf{J}_1(\gamma, \omega_4)$ and $\mathbf{J}_\gamma(\gamma, \omega_4)$ for $\omega_4 = 60$ radians/sec. and m = 1.

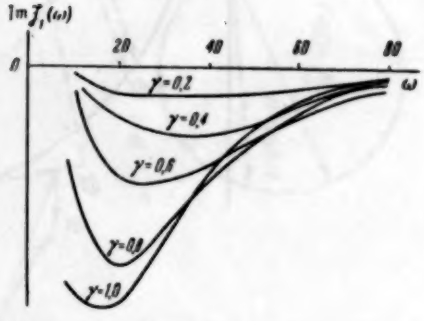

Fig. 13. The curves $\mathrm{Im}J_1(\omega)$.

of the characteristics $J_1(\omega)$ and $J_\gamma(\omega)$ are carried out graphically, which significantly simplifies the problem of determining these characteristics and, consequently, the entire problem of investigating periodic regimens in relay systems.

As an example, we compute the characteristics $J_1(\omega)$ and $J_\gamma(\omega)$ for the relay system for which the families of curves $u[(2m-1)\omega]$ and $v[(2m-1)\omega]$ are shown in Fig. 7.

We determine the range of variation of m for various values of the frequency: m = 1 for $\omega \geq 30$ radians/sec.; m = 2 for 20 radians/sec. $\leq \omega <$ 30 radians/sec.; m = 3 for 15 radians/sec. $\leq \omega <$ 20 radians/sec.; m = 4 for $\omega <$ 15 radians/sec.

We set the values of the frequency: $\omega_1 = 10$ radians/sec. for m = 4, $\omega_2 = 20$ radians/sec. for m = 2; $\omega_3 = 40$ radians/sec., $\omega_4 = 60$ radians/sec., $\omega_5 = 80$ radians/sec. for m = 1.

We set the values of the parameter γ: $\gamma_1 = 0.2$, $\gamma_2 = 0.4$, $\gamma_3 = 0.6$, $\gamma_4 = 0.8$, $\gamma_5 = 1.0$.

Using the method described above, we determine the starting vectors $\mathbf{J}_{1m}[(2m-1)\omega_k]$ and construct the hodographs (Figs. 8-12).

Summing the vectors corresponding to one value of the parameter γ, we find $J_1(\gamma, \omega_k)$ and $J_\gamma(\gamma, \omega_k)$ for the frequencies ω_1 and ω_2 (Figs. 8a and 9a). For the frequencies ω_3, ω_4 and ω_5, for which m = 1, the vectors $J_1(\gamma, \omega_k)$ and $J_\gamma(\gamma, \omega_k)$ are determined directly from the hodographs, shown in Figs. 10-12. On Figs. 8a, 9a, 10, 11 and 12, the solid lines represent the vectors $J_1(\omega_k)$, the dotted lines represent $J_\gamma(\omega_k)$.

The resulting vectors thus obtained determine the points of the characteristics $J_1(\omega)$ and $J_\gamma(\omega)$ for various values of the parameter γ. On Figs. 13 and 14 are shown the imaginary parts $\mathrm{Im}J_1(\omega)$ and $\mathrm{IM}J_\gamma(\omega)$ of these characteristics for values $\mathrm{Re}J_1(\omega) < 0$ and $\mathrm{Re}J_\gamma(\omega) < 0$, which are necessary for the direct determination of the existence of the periodic regimens and their parameters.

Received July 24, 1957

LITERATURE CITED

[1] Ia. Z. Tsypkin, Theory of Relay Systems of Automatic Control [In Russian] (Gostekhizdat, 1955).

[2] Ia. Z. Tsypkin, "The frequency method of analyzing auto-oscillation and forced oscillation in relay systems of automatic control," Fundamentals of Automatic Control [In Russian] (ed. V. V. Solodovnikov) (Mashgiz, 1954).

[3] A. I. Lur'e, "A method for investigating nonlinear automatic control systems, based on the principle of harmonic balancing," Fundamentals of Automatic Control [In Russian] (ed. V. V. Solodovnikov) (Mashgiz, 1954).

[4] L. S. Gol'dfarb, "A method for investigating nonlinear automatic control systems, based on the principle of harmonic balancing," Fundamentals of Automatic Control [In Russian] (ed. V. V. Solodovnikov) (Mashgiz, 1954).

[5] G. S. Pospelov, "Some questions in the theory of relay systems of automatic control," Fundamentals of Automatic Control [In Russian] (ed. V. V. Solodovnikov) (Mashgiz, 1954).

CONCERNING A METHOD FOR ANALYZING SAMPLED-DATA SYSTEMS

Fan Chun-Wui

(Moscow)

Based on the discrete Laplace transform, a well-known method [1, 2] for analyzing continuous linear systems is generalized to sampled-data systems and applied to the qualitative prediction of their forced motion.

It is well known that the output coordinates of a linear system are completely determined by the distribution of the zeroes and poles of the closed-loop system's transfer function, the initial conditions and the external forcing function. The applicability of such an approach to continuous linear systems was asserted by S. P. Strelkov [1, 2]. In articles [3-5] attempts were described to investigate sampled-data systems in an analogous manner. However, the case of an arbitrary forcing function was not investigated there. This paper considers the accuracy of a sampled-data system to which a discrete forcing function of a very general form is applied.

Preliminary Remarks

We consider the sampled-data control, or regulating, system, the schematic for which is shown in Fig. 1, where $f[n]$, $E[n]$ and $x[n, \epsilon]$ are some step functions.

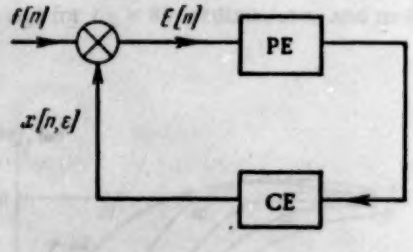

Fig. 1.

The transfer function for the closed-loop sampled-data system has the following form [6]:

$$\Phi_{xj}^{*}(q,\ \varepsilon) = \frac{X_j^{*}(q, \varepsilon)}{F^{*}(q)} = \frac{b_0 + b_1 e^{q} + \ldots + b_m e^{qm}}{a_0 + a_1 e^{q} + \ldots + a_l e^{ql}} = \frac{H_j^{*}(q, \varepsilon)}{G^{*}(q)}, \quad (j = \mathrm{I}, \mathrm{II}) \tag{1}$$

where $X_j^{*}(q, \epsilon)$ and $F^{*}(q)$ represent the discrete transformations of the step functions $x[n, \epsilon]$ and $f[n]$.

In Equation (1), $m \leq l$, and the quantity ϵ, which can vary within the intervals from 0 to γ and from γ to 1 (γ is the "porosity"), enter into the coefficients $b_0, b_1, \ldots, b_m$.

We assume that the discrete forcing function $f[n]$ can be represented in the form

$$f[n] = \sum_{k=1}^{s} c_k[n]\, e^{\rho_k n} \tag{2}$$

where $c_k[n]$ is a polynomial in n and ρ_k is a real or complex number.

We write the expression for the output function, $X_j^*(q, \epsilon)$, in the general form:

$$X_j^*(q, \varepsilon) = \frac{H_j^*(q, \varepsilon)}{G^*(q)} F^*(q) = \frac{H_j^*(q, \varepsilon)}{G^*(q)} \frac{F_1^*(q)}{F_2^*(q)} =$$

$$= \frac{H_j^*(q, \varepsilon)}{(e^q - e^{\lambda_1})(e^q - e^{\lambda_2}) \ldots (e^q - e^{\lambda_l})} \frac{F_1^*(q)}{(e^q - e^{\rho_1})(e^q - e^{\rho_2}) \ldots (e^q - e^{\rho_s})} \tag{3}$$

Here $\lambda_1, \lambda_2, \ldots, \lambda_l$ and $\rho_1, \rho_2, \ldots, \rho_s$ are the poles of the transfer function of the system itself and of the transformation $F^*(q)$ of the forcing function. Initially, for simplicity in the argument, we shall assume that all the poles are distinct. Then, by the usual formulae, we find the step function at the output in the following form:

$$x_j[n, \varepsilon] = \sum_{i=1}^{l} \frac{H_j^*(\lambda_{i1}\varepsilon)}{e^{\lambda_i} \dot{G}^*(\lambda_i)} \frac{F_1^*(\lambda_i)}{F_2^*(\lambda_i)} e^{\lambda_i n} + \sum_{k=1}^{s} \frac{H_j^*(\rho_k, \varepsilon)}{G^*(\rho_k)} \frac{F_1^*(\rho_k)}{e^{\rho_k} \dot{F}_2^*(\rho_k)} e^{\rho_k n} =$$

$$= \sum_i S_i e^{\lambda_i n} + \sum_k R_k e^{\rho_k n} = x_I[n] + x_F[n]. \tag{4}$$

Here x_I may be called the "inherent" and x_F the "forced" components.

It is clear from Equation (4) that both these components depend on the distribution of the zeroes and poles of the transfer functions of the system itself and of the function $F^*(q)$. Obviously, the inherent motion of the system always entails a necessary error of reproduction. For stability of the system, the real parts of all λ_i certainly must be negative. Moreover, it is clear from Equation (4) that the quantities R_k are not always proportional or equal to the quantities c_k of Equation (2). This means that the forced motion of the system is different from the controlling signal $f[n]$, i.e., it is distorted. Thus, for accurate transmission of the signals, it is necessary to decrease these two components of distortion.

We shall consider the conditions for a distortion-free forcing part, figuring the inherent motion as having a certain error, which will be investigated later.

Conditions for Distortion-Free Forced Motion

Initially we shall assume that the inherent motions of the system die out after a certain time. In this case, the accuracy of signal reproduction is completely determined by the system's forced motion. We consider the following cases.

1. The poles of the system's transfer function are simple, different from its zeroes, and none of them coincides with a pole of $F^*(q)$. In this case, it is clear from Equation (4) that the sequence of polynomials at the discrete moments $R_k[n]$ will equal the sequence of polynomials $c_k[n]$. Hence, the conditions for distortion-free forced motion will be

$$\frac{H_j^*(\rho_k, \varepsilon)}{G^*(\rho_k)} = \text{const} = C. \tag{5}$$

Condition (5) is not sufficient if $F^*(q)$ has multiple poles. For example, if $F^*(q)$ has two multiple roots, $\rho_{1,2}$, i.e.,

$$F^*(q) = \frac{F_1^*(q)}{(e^q - e^{\rho_{1,2}})^2 F_2^*(q)},$$

then $f[n]$ takes the form

$$f[n] = D^{-1}[F^*(q)] = \frac{F_1^*(\rho_{1.2})}{F_2^*(\rho_{1.2})}(n-1)\,e^{(n-2)\rho_{1.2}} + \\ + \frac{d}{de^q}\frac{F_1^*(q)}{F_2^*(q)}\bigg|_{q=\rho_{1.2}} e^{(n-1)\rho_{1.2}} + \sum_{k=3}^{s}\frac{F_1^*(\rho_k)}{(e^{\rho k}-e^{\rho_{1.2}})^2\,e^{\rho k}\dot{F}_2^*(\rho_k)}\,e^{\rho_k n} \tag{6}$$

for $n \geq 1$.

The transform of the output function $X_j^*(q, \epsilon)$ will be

$$X_j^*(q,\ \varepsilon) = \frac{H_j^*(q, \varepsilon)}{G^*(q)}\,\frac{F_1^*(q)}{F_2^*(q)\,(e^q - e^{\rho_{1.2}})^2}\,. \tag{7}$$

In this case, the forced motion at the system output will be

$$x_F[n,\ \varepsilon] = \frac{H_j^*(\rho_{1.2}, \varepsilon)}{G^*(\rho_{1.2})}\frac{F_1^*(\rho_{1.2})}{F_2^*(\rho_{1.2})}(n-1)\,e^{(n-2)\rho_{1.2}} + \\ + \frac{d}{de^q}\frac{F_1^*(q)}{F_2^*(q)}\frac{H_j^*(q, \varepsilon)}{G^*(q)}\bigg|_{q=\rho_{1.2}} e^{(n-1)\rho_{1.2}} + \\ + \sum_{k=3}^{s}\frac{H_j^*(\rho_k,\ \varepsilon)}{G^*(\rho_k)}\,\frac{F_1^*(\rho_k)}{(e^{\rho k}-e^{\rho_{1.2}})^2\,e^{\rho k}\dot{F}_2^*(\rho_k)}\,e^{\rho k n} \tag{8}$$

for $n \geq 1$.

It is clear from (6) that, in this case, the conditions for distortion-free forced motion will be

$$\frac{H_j^*(\rho_k,\ \varepsilon)}{G^*(\rho_k)} = \frac{H_j^*(\rho_{1.2},\ \varepsilon)}{G^*(\rho_{1.2})} = \text{const} = C, \tag{9}$$

$$\frac{d}{de^q}\frac{F_1^*(q)}{F_2^*(q)}\,\frac{H_j^*(q, \varepsilon)}{G^*(q)}\bigg|_{q=\rho_{1.2}} = C\,\frac{d}{de^q}\,\frac{F_1^*(q)}{F_2^*(q)}\bigg|_{q=\rho_{1.2}}\,. \tag{10}$$

If $F_1^*(q)/F_2^*(q) = \text{const}$, then (10) reduces to an equation of the form

$$\frac{d}{de^q}\,\frac{H_j^*(q, \varepsilon)}{G^*(q)}\bigg|_{\rho_{1.2}} = 0. \tag{11}$$

If the poles of $F^*(q)$ have multiplicity m ($m > 1$), then the conditions for distortion-free motion, in addition to Equation (5), will be the following equations:

$$\frac{d^{m-1}}{de^{qm-1}}\,\frac{H_j^*(q,\ \varepsilon)}{G^*(q)}\,\frac{F_1^*(q)}{F_2^*(q)}\bigg|_{\rho_{1+m}} = C\,\frac{d^{m-1}}{de^{qm-1}}\,\frac{F_1^*(q)}{F_2^*(q)}\bigg|_{\rho_{1+m}}\,, \tag{12 (cont'd)}$$

$$\frac{d^{m-2}}{de^{q_{m-2}}}\left.\frac{H_j^*(q,\varepsilon)}{G^*(q)}\frac{F_1^*(q)}{F_2^*(q)}\right|_{\rho_{1+m}} = C\left.\frac{d^{m-2}}{de^{q_{m-2}}}\frac{F_1^*(q)}{F_2^*(q)}\right|_{\rho_{1+m}},$$

$$\cdots\cdots\cdots\cdots\cdots\cdots\cdots\cdots \tag{12}$$

$$\frac{d}{de^q}\left.\frac{H_j^*(q,\varepsilon)}{G^*(q)}\frac{F_1^*(q)}{F_2^*(q)}\right|_{\rho_{1+m}} = C\left.\frac{d}{de^q}\frac{F_1^*(q)}{F_2^*(q)}\right|_{\rho_{1+m}}.$$

In particular, if $F_1^*(q)/F_2^*(q) = \text{const}$, then the System (12) takes the form:

$$\begin{aligned}
&\left.\frac{d^{m-1}}{de^{q_{m-1}}}\frac{H_j^*(q,\varepsilon)}{G^*(q)}\right|_{\rho_{1+m}} = 0,\\
&\left.\frac{d^{m-2}}{de^{q_{m-2}}}\frac{H_j^*(q,\varepsilon)}{G^*(q)}\right|_{\rho_{1+m}} = 0,\\
&\cdots\cdots\cdots\cdots\\
&\left.\frac{d}{de^q}\frac{H_j^*(q,\varepsilon)}{G^*(q)}\right|_{\rho_{1+m}} = 0.
\end{aligned} \tag{13}$$

Conditions analogous to (13) were obtained in [8].

2. Poles of $F^*(q)$ coincide with poles of the system's transfer function, for example, $\rho_1 = \lambda_1$. For simplicity of exposition, we shall assume that the poles of $F^*(q)$ and of the system's transfer function are simple and different from their zeroes. In this case, the forcing function $f[n]$ may be put in the form

$$f[n] = \frac{1}{2\pi j}\int_{c-j\pi}^{c+j\pi} F^*(q)\,e^{qn}\,dq = \sum_{k=1}^{s}\frac{F_1^*(q)}{e^{\rho_k}\dot{F}_2^*(q)}\,e^{\rho_k n}, \tag{14}$$

and the forced motion at the system output will be

$$\begin{aligned}
x_F[n,\varepsilon] = {}& \frac{H_j^*(\rho_1,\varepsilon)}{\dot{G}^*(\rho_1)}\frac{F_1^*(\rho_1)}{F_2^*(\rho_1)}(n-1)\,e^{(n-2)\rho_1} +\\
&+\left.\frac{d}{de^q}\frac{H_j^*(q,\varepsilon)}{\dot{G}^*(q)}\frac{F_1^*(q)}{F_2^*(q)}\right|_{q=\rho_1} e^{(n-1)\rho_1} + \sum_{k=2}^{s}\frac{H_j^*(\rho_k,\varepsilon)}{G^*(\rho_k)}\frac{F_1^*(\rho_k)}{e^{\rho_k}\dot{F}_2^*(\rho_k)}\,e^{\rho_k n}.
\end{aligned} \tag{15}$$

It is clear from a comparison of Equations (14) and (15) that for such systems it is not possible to have accurate reproduction of the forcing function $f[n]$. Therefore, we add to the conditions for absence of distortion the condition that there be no resonance, i e., we impose the requirement that the poles of $F^*(q)$ do not coincide with the poles of the system's transfer function.

3. The poles of $F^*(q)$ coincide with the zeroes of the system's transfer function for errors. The transfer function for closed-loop sampled-data systems for errors will be

$$\Phi_{3\varepsilon}^*(q) = \frac{E_{in}^*(q)}{F^*(q)} = \frac{D^*(q)}{G^*(q)}. \tag{16}$$

The step function for the errors, E[n], will be

$$E[n] = \frac{1}{2\pi j}\int_{c-j\pi}^{c+j\pi}\frac{D^*(q)}{G^*(q)}\,F^*(q)\,e^{qn}\,dq = \tag{17}$$

(cont'd)

$$= \sum_{k=1}^{s} \frac{D^*(\rho_k)}{G^*(\rho_k)} \frac{F_1^*(q)}{e^{\rho_k} \dot{F}_2^*(\rho_k)} e^{\rho_k n} + \sum_{i=1}^{l} \frac{F_1^*(\lambda_i)}{F_2^*(\lambda_i)} \frac{D^*(\lambda_i)}{\dot{G}^*(\lambda_i)} e^{\lambda_i n}. \quad (17)$$

It is clear from (17) that for accurate reproduction of the effective signals, the system must be such that the poles of $F^*(q)$ coincide with the zeroes of the transfer function of the system for errors, i.e., that

$$D^*(\rho_k) = 0. \quad (18)$$

In particular, if $F^*(q) = F_1^*(q)/(e^q - 1)^\gamma$, then the system's transfer function for errors must be

$$\Phi_{s\varepsilon}^*(q) = \frac{D_1^*(q)(e^q - 1)^\gamma}{G^*(q)}. \quad (19)$$

Inherent Motion

In order to decrease the error in reproduction, it is necessary to shorten the interval of time in which, after initiation of the process, there is an appreciable inherent motion. According to (4), the inherent motions take the form:

$$x_I[n] = \sum_{i=1}^{l} \frac{H_j^*(\lambda_i, \varepsilon)}{e^{\lambda_i} \dot{G}^*(\lambda_i)} F^*(\lambda_i) e^{\lambda_i n}. \quad (20)$$

We will understand by the "transient response" that regimen in which there is still noticeable inherent motion. It is obvious that to shorten this regimen it is necessary that the absolute values of the real parts of all λ_i be as large as possible. In the limit we shall have $|\mathrm{Re}\,\lambda_i| = \infty$ for all λ_i, i.e., the degree of system stability is infinite. In this case, the system's transfer function will be

$$\Phi_s^*(q, \varepsilon) = \frac{H_j^*(q, \varepsilon)}{G^*(q)} = \frac{H_j^*(q, \varepsilon)}{a_l e^{ql}}, \quad (21)$$

that is, $a_0 = a_1 = \ldots = a_{l-1} = 0$, and the transfer function of the system for errors, using Condition (19), will have the form:

$$\Phi_s^*(q) = \frac{D^*(q)}{G^*(q)} = \frac{D_1^*(q)(e^q - 1)^\gamma}{a_n e^{qn}}. \quad (22)$$

Expression (22) coincides with the results in [8].

On the Oscillations of Sampled-Data Systems Between Sampling Times

If $\gamma \neq 1$, the system's forced motion, on the basis of Expression (4), is written in the form

$$x_{FI}[n, \varepsilon] = \sum_{k=1}^{s} \frac{H_I^*(\rho_k, \varepsilon)}{G^*(\rho_k)} \frac{F_2^*(\rho_k)}{e^{\rho_k} \dot{F}_1(\rho_k)} e^{\rho_k n} \quad \text{for} \quad 0 \leqslant \varepsilon < \gamma,$$

$$x_{FII}[n, \varepsilon] = \sum_{k=1}^{s} \frac{H_{II}^*(\rho_k, \varepsilon)}{G^*(\rho_k)} \frac{F_2^*(\rho_k)}{e^{\rho_k} \dot{F}_1(\rho_k)} e^{\rho_k n} \quad \text{for} \quad \gamma \leqslant \varepsilon < 1. \quad (23)$$

In the intervals $0 \leq \epsilon < \gamma$ and $\gamma \leq \epsilon < 1$, the function $x_F[n, \epsilon]$ varies exponentially [6], i.e., in the general case the process will have an oscillatory character. But for some systems, given a definite form of forcing function, the system oscillations may not appear. For example, in first-order astatic sampled-data systems, system oscillations between sampling times are not present for unit forcing functions, since in this case $H^*_I(0,\epsilon) = H^*_{II}(0, \epsilon) = \text{const.}$, i.e., in the steady state, the system's output function will always be constant, and not depend upon ϵ. But for more complex forcing functions of the general form (2), $H^*_I(\rho_k, \epsilon)$ and $H^*_{II}(\rho_k, \epsilon)$ of Expression (23) cannot equal one another, and will depend upon ϵ. Consequently, in spite of the fact that Condition (5) for distortion-free forced motion does hold between sampling times, the output magnitude as a whole will have an oscillatory character. If there is a fixing element in the system, then this is equivalent to $\gamma = 1$. In this case, $\Phi^*_{sI}(q) = \Phi^*_{sII}(q) = \Phi^*_s(q)$, and there will be no oscillations in the system (if the system is stable).

Estimating the Reproduction Error of the Forcing Function

We shall assume that the relative reproduction error of the system is determined in the following fashion:

$$\varepsilon = \frac{|x[n] - k_{se} f[n]|}{k_{se} |f[n]|}. \tag{24}$$

Among the problems of designing a sampled-data system is that a limitation is placed on the system parameters by the inequality

$$|\varepsilon| \leqslant \varepsilon_0, \tag{25}$$

where ϵ_0 is the given maximum error. The error in reproducing the forcing function $f[n]$ by the forced component $x_F[n, \epsilon]$ may be written in the form

$$\varepsilon_F[n, \varepsilon] = \frac{1}{k_{se}} \frac{|x_F[n, \varepsilon]|}{|f[n]|} - 1. \tag{26}$$

Finally, we introduce the reproduction error of the individual elementary excitations

$$\varepsilon(\rho_k) = \frac{1}{k_{se}} \frac{H^*(\rho_k, \varepsilon)}{G^*(\rho_k)} - 1, \tag{27}$$

where

$$k_{se} = \frac{H^*(0, \varepsilon)}{G^*(0)}. \tag{28}$$

We find from (27) and (28)

$$\frac{H^*(\rho_k, \varepsilon)}{G^*(\rho_k)} = \frac{H^*(0, \varepsilon)}{G^*(0)} [1 + \varepsilon(\rho_k)]. \tag{29}$$

After some simple transformations, we find from (4), (26) and (29)

$$\varepsilon_F[n, \varepsilon] = \frac{1}{|f(n)|} \left| \sum_{k=1}^{s} \frac{F_1^*(\rho_k)}{e^{\rho_k} \dot{F}_2^*(\rho_k)} \varepsilon(\rho_k) e^{\rho_k n} \right|. \tag{30}$$

This formula shows that to improve the quality of reproduction of the forcing function it is necessary to strive to reduce $\epsilon(\rho_k)$.

We now turn to the investigation of ways to reduce $\epsilon(\rho_k)$. Initially we set

$$e^q = z. \tag{31}$$

Then, $G^*(\rho_k)$ and $H^*(\rho_k, \epsilon)$ may be put in the form

$$G^*(\rho_k) = a_l (e^{\rho_k} - e^{\lambda_1})(e^{\rho_k} - e^{\lambda_2}) \dots (e^{\rho_k} - e^{\lambda_l}) =$$

$$= a_l (z_{\rho_k} - z_{\lambda_1})(z_{\rho_k} - z_{\lambda_2}) \dots (z_{\rho_k} - z_{\lambda_l}) = a_l \prod_{i=1}^{l} R_i^{pk}, \quad (32)$$

$$H^*(\rho_k, \varepsilon) = b_m (e^{\rho_k} - e^{\gamma_1})(e^{\rho_k} - e^{\gamma_2}) \dots (e^{\rho_k} - e^{\gamma_m}) =$$

$$= b_m (z_{\rho_k} - z_{\gamma_1})(z_{\rho_k} - z_{\gamma_2}) \dots (z_{\rho_k} - z_{\gamma_m}) = b_m \prod_{i=1}^{m} R_i^{zk}. \quad (33)$$

Here, R_i^{pk} is a vector in the Z plane drawn from the i'th pole of the system's transfer function to the k'th pole of $F^*(q)$, and R_i^{zk} is the vector drawn from the i'th zero of the transfer function of the k'th pole of $F^*(q)$ (Fig. 2). Since $F^*(q + j2k\pi) = F^*(q)$ due to the periodicity [6, 7], we will consider $F^*(q)$ in the strip $-\pi < \mathrm{Im} q \leq \pi$. The strip $-\pi < \mathrm{Im} q \leq \pi$ corresponds to the region lying to the right of the imaginary axis in the Z plane (Fig. 2).

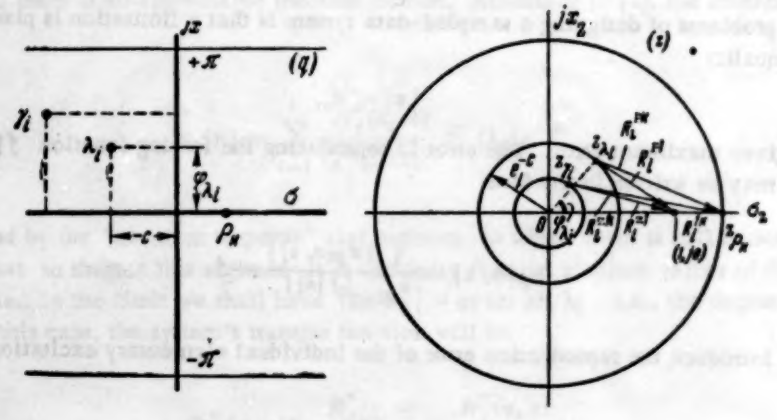

Fig. 2.

It is clear from Fig. 2 that $R_i^{pk} = R_i^{p1} + R_i^{1k}$ and $R_i^{zk} = R_i^{z1} + R_i^{1k}$. Making these substitutions in Equations (32) and (33), we obtain

$$G^*(\rho_k) = a_l \prod_{i=1}^{l} (R_i^{p1} + R_i^{1k}), \quad (34)$$

$$H^*(\rho_k, \varepsilon) = b_m \prod_{i=1}^{m} (R_i^{z1} + R_i^{1k}), \quad (35)$$

where R_i^{z1}, R_i^{p1}, and R_i^{1k} are the vectors shown in Fig. 2. Substituting these quantities in the expression for $\epsilon(\rho_k)$ (27), we get

$$\varepsilon(\rho_k) = \frac{G^*(0)}{H^*(0, \varepsilon)} \frac{b_m \prod_{i=1}^{m} (R_i^{z1} + R_i^{1k})}{a_l \prod_{i=1}^{l} (R_i^{p1} + R_i^{1k})} - 1. \quad (36)$$

Considering that

$$G^*(0) = a_l(1 - z_{\lambda_1})(1 - z_{\lambda_2}) \ldots (1 - z_{\lambda_l}) = a_l \prod_{i=1}^{l} R_i^{p1}, \tag{37}$$

$$H^*(0, \varepsilon) = b_m \prod_{i=1}^{m} R_i^{z1} \tag{38}$$

and substituting (37) and (38) in (36), we find

$$\varepsilon(\rho_k) = \frac{\prod_{i=1}^{l} R_i^{p1} \prod_{i=1}^{m} (R_i^{z1} + R_i^{1k})}{\prod_{i=1}^{m} R_i^{z1} \prod_{i=1}^{l} (R_i^{p1} + R_i^{1k})} - 1 = \frac{\prod_{i=1}^{m} \left(1 + \frac{R_i^{1k}}{R_i^{z1}}\right)}{\prod_{i=1}^{l} \left(1 + \frac{R_i^{1k}}{R_i^{p1}}\right)} - 1. \tag{39}$$

This formula allows one to estimate the error of reproduction of each elementary excitation, defined by a pole z_{ρ_k}, in the Z plane. From this it is clear that to reduce the error in reproducing the forcing function it is necessary that the zeroes and poles of the system's transfer function be removed from the region in which the poles of $F^*(q)$ are to be found, and that to the greatest extent possible the zeroes of the transfer function should be close to its poles. Since, in the majority of cases, the number of zeroes of the transfer function is always less than the number of its poles, it is expeditious to try to place the zeroes close to those poles of the transfer function which are closest to the region in which the poles of $F^*(q)$ lie.

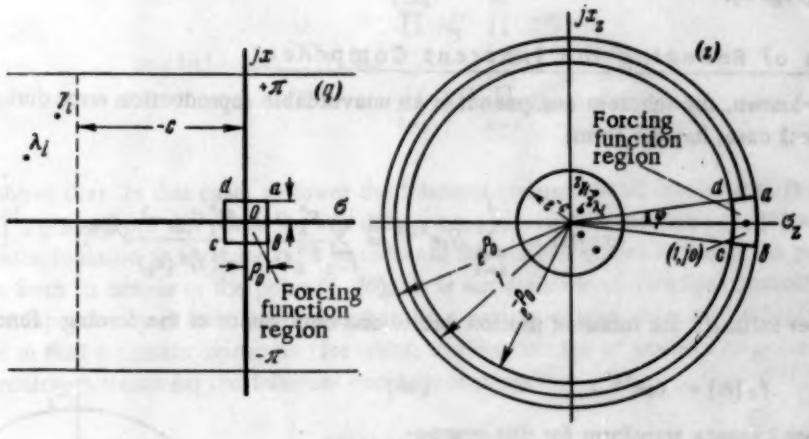

Fig. 3.

If the region in which the poles of $F^*(q)$ lie is sufficiently small, and sufficiently remote from the region in which the poles and zeroes of the system's transfer function lie (Fig. 3), it is possible in this case to consider that $R_i^{1k}/R_i^{p1} \ll 1$, and $R_i^{1k}/R_i^{z1} \ll 1$, and Equation (39) is replaced by the simple approximate formula

$$\varepsilon(\rho_k) \approx R^{1k} \left[\sum_{i=1}^{m} \frac{1}{R_i^{z1}} - \sum_{i=1}^{l} \frac{1}{R_i^{p1}} \right] \tag{40}$$

In this case, Expression (33) is also significantly simplified:

$$\varepsilon_F[n] \approx \frac{1}{|f|n||} \left| \sum_{k=1}^{\circ} \frac{F_1^*(\rho_k)}{e^{\rho_k} F_2^*(\rho_k)} SR^{1k} e^{\rho_k n} \right|, \tag{41}$$

where

$$S = \sum_{i=1}^{m} \frac{1}{R_i^{z1}} - \sum_{i=1}^{l} \frac{1}{R_i^{p1}}, \quad R^{1k} = (e^{\rho_k} - 1).$$

We transform Expression (41), noting that

$$\Delta f[n] = f[n+1] - f[n] = \sum_{k=1}^{s} \frac{F_1^*(\rho_k)}{e^{\rho_k} F_2^*(\rho_k)} (e^{\rho_k} - 1) e^{\rho_k n}.$$

As a result, we obtain

$$\varepsilon_F[n] = \frac{1}{|f[n]|} |S\Delta f[n]| = \frac{D|\Delta f[n]|}{R_0 |f[n]|}, \tag{42}$$

where $R_0 = (e^{\rho_0} - 1)$, $D = SR_0$.

Thus, to reduce the reproduction error, it is necessary to reduce the quantity

$$D = R_0 \left[\sum_{i=1}^{m} \frac{1}{R_i^{z1}} - \sum_{i=1}^{l} \frac{1}{R_i^{p1}} \right], \tag{43}$$

which depends only on the mutual distribution of the zeroes and poles of the system's transfer function, and on the quantity ρ_0 (Fig. 3).

The Problem of Reducing the Innerent Component

As is well-known, the inherent component is an unavoidable reproduction error during the transient response and, in the general case, has the form:

$$x_i[n] = \sum_{i=1}^{l} S_i e^{\lambda_i n} = \sum_{i=1}^{l} \frac{F_1^*(\lambda_i)}{F_2^*(\lambda_i)} \frac{H_j^*(\lambda_i, \varepsilon)}{e^{\lambda_i} \dot{G}^*(\lambda_i)} e^{\lambda_i n}. \tag{44}$$

We consider initially the inherent motion due to one component of the forcing function

$$f_k[n] = c_k e^{\rho_k n}. \tag{45}$$

The discrete Laplace transform for this component will be

$$F_k^*(q) = \frac{c_k e^q}{e^q - e^{\rho_k}}, \tag{46}$$

and the component of motion, $x_{1k}[n]$, has the expression

$$x_{1k}[n] = \sum_{i=1}^{l} \frac{c_k e^{\lambda_i}}{e^{\lambda_i} - e^{\rho_k}} \frac{H_j^*(\lambda_i \varepsilon)}{e^{\lambda_i} \dot{G}^*(\lambda_i)} e^{\lambda_i n}. \tag{47}$$

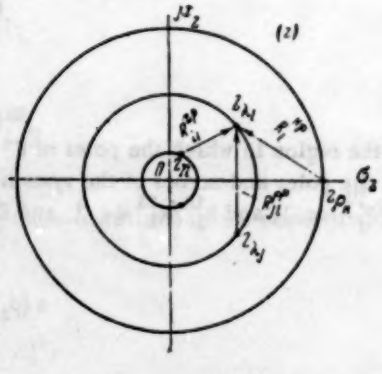

Fig. 4.

Here,

$$\dot{G}^*[\lambda_i] = a_l (z_{\lambda_i} - z_{\lambda_1})(z_{\lambda_i} - z_{\lambda_2}) \ldots (z_{\lambda_i} - z_{\lambda_{i-1}})(z_{\lambda_i} - z_{\lambda_{i+1}}) \ldots (z_{\lambda_i} - z_{\lambda_l}). \tag{48}$$

Thus,

$$x_{1k}[n] = \sum_{i=1}^{l} \frac{c_k b_m}{a_m} \frac{(z_{\lambda_i} - z_{\gamma_1})(z_{\lambda_i} - z_{\gamma_2}) \dots (z_{\lambda_i} - z_{\gamma_m})\, e^{\lambda_i n}}{(z_{\lambda_i} - z_{p_k})(z_{\lambda_k} - z_{\lambda_1}) \dots (z_{\lambda_i} - z_{\lambda_{i-1}})(z_{\lambda i} - z_{\lambda_{i+1}}) \dots (z_{\lambda_i} - z_{\lambda_l})} \tag{49}$$

We emphasize that here the sum extends over all poles of the system's transfer function. The expression obtained may be given a vector interpretation (Fig. 4). It is not difficult to see that each parentheses of the numerator of Expression (49) may be represented by a vector R_{il}^{zp} drawn from a zero, z_{γ_1}, of the transfer function to its i'th pole, z_{λ_1}, and the parentheses of the denominator of Expression (49) may be represented by the product of vectors R_{jl}^{pp}, drawn to the i'th pole of the system's transfer function from all other poles, multiplied by the vector R_i^{kp}, drawn from the given k'th pole of the forcing function to the i'th pole of the system's transfer function (Fig. 4).

Using the foregoing notation, we can write (49) as:

$$x_{1k}[n] = \sum_{i=1}^{l} c_k \frac{b_m}{a_l} \frac{\prod_{l=1}^{m} R_{il}^{zp}}{R_i^{kp} \prod_{j=1}^{l-1} R_{ji}^{pp}} e^{\lambda_i n} = \sum_{i=1}^{l} c_k k_{se} \frac{\prod_{j=1}^{l} R_j^{p1}}{\prod_{l=1}^{m} R_l^{z1}} \frac{\prod_{l=1}^{m} R_{il}^{zp}}{R_i^{kp} \prod_{j=1}^{l-1} R_{ji}^{pp}} e^{\lambda_i n}. \tag{50}$$

In the case where the poles of the forcing function lie in a small region about the point (1, j0) in the Z plane (Fig. 3), it is possible, with sufficient accuracy, to take $R_1^{kp} \approx R_1^{1p} = -R_1^{p1}$ (Figs. 2 and 3). In this case, Expression (50) may be written in the form

$$x_{1k}[n] = -\sum_{i=1}^{l} c_k k_{se} \frac{\prod_{j=1}^{l-1} R_j^{p1} \prod_{l=1}^{m} R_{il}^{zp}}{\prod_{l=1}^{m} R_l^{z1} \prod_{j=1}^{l-1} R_{ji}^{pp}} e^{\lambda_i n}. \tag{51}$$

Expression (51) shows that in this case to lower the inherent component of oscillation, it is necessary to decrease the vectors R_j^{p1}, going from the poles z_λ of the transfer function to the point (1, j0) and from the zeroes z_γ of the transfer function to its poles, and to increase the vectors drawn between the poles of the transfer function and drawn from its zeroes to the point (1, j0). It is not difficult to convince oneself that these requirements cannot be met independently of each other and that to a certain extent they are mutually contradictory. However, it is possible to find a certain optimum for which the distribution of zeroes and poles of the transfer function permit of a minimum value for the inherent component of motion.

SUMMARY

1. From the technical conditions imposed on the system, the limits should be determined for the region in which lie the poles of the transform of the forcing function which is to be reproduced with some permissible error.

2. The conditions for distortion-free forced motion may be formulated as follows: a) the system must be stable, b) the poles of the system's transfer function may not coincide with the poles of the transform of the forcing function, c) the spectrum of the system must be constant for all poles of the forcing function.

If the transform of the forcing function has multiple poles, then the condition for distortion-free forced motion is given by Equation (12).

3. The poles of the system's transfer function must be distant from the region in which the poles of the forcing function's spectrum lie.

4. The zeroes of the transfer function are best situated close to its poles, placed as far as possible from the origin of the Z plane. With an increase of the distance of the transfer function's zeroes from its poles goes an increase in the oscillation of the inherent component.

5. The poles of the system's transfer function must be placed as close as possible to the origin of the Z plane.

Received June 5, 1957

LITERATURE CITED

[1] S. P. Strelkov, "On the general theory of linear amplifiers, Part I," Automation and Remote Control (USSR) 9, 3 (1948).

[2] S. P. Strelkov, "On the general theory of linear amplifiers, Part II," Automation and Remote Control (USSR) 10, 4 (1949).

[3] Eliahu I.Jury, "The effect of pole and zero locations on the transient response of sampled-data systems," Trans. AIEE, 74, pt. II (1955).

[4] K. Sklansky and J. R. Ragazzini, "Analysis of errors in sampled-data feedback systems," Trans. AIEE, 74 pt. II (1955).

[5] Eliahu I.Jury, "Correlation between root-locus and transient response of sampled-data control systems," Trans. AIEE, 74 pt. II (1955).

[6] Ia. Z. Tsypkin, Transient and Steady-State Processes in Pulsed Links [In Russian] (Gosenergoizdat, 1951).

[7] Ia. Z. Tsypkin ,"Theory of discontinuous regulation, I, II," Automation and Remote Control (USSR) 10, 3 and 5 (1949).

[8] Ia. Z. Tsypkin, "Investigation of steady-state processes in sampled-data systems," Automation and Remote Control (USSR) 17, 12 (1956).*

* See English translation.

ON IMPROVING THE TRANSIENT RESPONSE OF CORRECTING LINKS WITH VARIABLE PARAMETERS

E. K. Shigin

(Moscow)

Some methods are presented for improving the transient responses in fourth-order automatic control systems containing two integrating links. It is shown that when a differentiator with a variable time constant is introduced, the transient response can effectively be improved by the introduction of an integrating link with a variable time constant into the correcting circuit.

The behavior of automatic control systems can sometimes be improved by the introduction of artificial nonlinearities, obtained by varying parameters during the length of the transient response. This artifice allows one to obtain a duration of transient response which, for given regulated object and executive organ characteristics, cannot be attained by linear systems with constant parameters. A better approximation to an aperiodic process may also be obtained [1, 5].

One variable parameter which may be used is the gain of a differentiator, smoothly or step-wise varying during the transient response [2, 3]. The introduction of one such variable-gain differentiator immediately leads to the desired results in systems without integrators in the correcting circuit, but in systems with such integrators the introduction of just one variable differentiator may not suffice to give the requisite improvement.

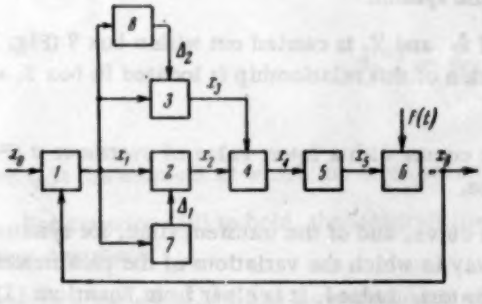

Fig. 1.

To show this, we use a fourth-order automatic control system, the block schematic of which is given in Fig. 1. The system can function either as a following system or as a stabilizing system. The numbered boxes in Fig. 1 are as follows: 1 is the sensing element, 2 is the differentiator, 3 is the integrator, 4 is the amplifier, 5 is the executive organ and 6 is the controlled object. The purposes of boxes 7 and 8 will be given below.

The link equations may be written as follows:

$$x_1 = x_0 - x_6, \tag{1}$$

$$x_2 = (T_1 p + 1)\, x_1, \tag{2}$$

$$x_3 = \frac{x_1}{T_2 p}, \tag{3}$$

$$x_4 = K(x_2 + x_3) = K\left(1 + T_1 p + \frac{1}{T_2 p}\right) x_1, \tag{4}$$

$$(T_3 p + 1)\, x_5 = x_4, \tag{5}$$

$$(T_4 T_5 p^2 + T_5 p)\, x_6 = f(t) + x_5. \tag{6}$$

Here, x_0 is the controlling stimulus, x_1 is the error, x_2 is the differentiator output, x_3 is the integrator output, x_4 is the amplifier output, x_5 is the executive organ output, x_6 is the controlled quantity, T_1 is the differentiator's time constant, T_2 is the integrator time constant, T_3 is the executive organ's time constant, T_4 is the controlled object's time constant, T_5 is the time constant of the damped controlled object, K is the amplifier gain, f(t) is the external disturbance and p is the symbol for differentiation.

Using standard methods [1], let us find acceptable adjustments of the differentiator and integrator with the condition that $\sigma \leq 20\%$, where σ is the magnitude of the first regulating surge following a unit step controlling input ($x_0 = 1$ for $t > 0$). Here, the transient response may be either optimal, in the ordinary sense, or nonoptimal.

The dotted curve on Fig. 2 shows the transient response of the system under consideration for $T_1 = 0.7$ sec, $T_2 = 8$ sec, $T_3 = 0.2$ sec, $T_4 = T_5 = 1$ sec and $K = 2$, the curve being constructed by the Bashkirov method (with unit step excitation). With these settings, the transient time $t_{t_1} = 7.5$ sec (we take the length of the transient response to be the time necessary to establish an error not exceeding 5% of the unit step excitation).

If the differentiator time constant T_1 is decreased to 0.35 sec, the transient time decreases ($t_{t_2} < t_{t_1}$) (Fig. 2, curve A), but the magnitude of the initial overshoot σ increases.

We consider whether, in this case, it is impossible, by stepwise varying of the parameter T_1 during the transient response, to decrease the amount of overshoot without thereby increasing the duration of the transient response.

The rules for introducing step-wise variation of parameter T_1 can be chosen according to the recommendations given in [2, 3]. However, this may more easily be done by considering the relationship, during the course of the transient response, of the signs of the speed and velocity errors of x_1 [4]. Let T_1 depend in the following way on the relationship of the signs of the first and second derivative errors:

$$T_1 = \begin{cases} T_{10} & \text{for } \frac{\dot{x}_1}{\ddot{x}_1} > 0 \text{ ("startup"),} \\ K_{\Delta 1} T_{10} & \text{for } \frac{\dot{x}_1}{\ddot{x}_1} < 0 \text{ ("braking"),} \end{cases} \tag{A}$$

where T_{10} is the basic differentiator time constant ($T_{10} = 0.35$ sec.) on the startup portion and K_{Δ_1} is the coefficient of step-wise variation of T_1 along the braking portion of the system.

The determination of the relationship between the signs of $\dot{x}_1$ and $\ddot{x}_1$ is carried out within box 7 (Fig. 1), and the discriminator which stipulates the effect of Δ_1 as a function of this relationship is located in box 2, where T_1 is varied.

If T_1 is increased at time t_1 (Fig. 2), the transient response occurs with a lower value of overshoot σ (Fig. 2, curve B), but the duration of the transient response t_{t_3} increases.

This type of variation of the form of the transient response curve, and of the transient time, for systems with variable-parameter differentiators does not depend on the way in which the variations of the parameters is introduced, and is inherent in all systems with two or more integrators. Indeed, it is clear from Equations (1)-(6) that, after the new equilibrium state is established ($x_0 = x_6 = 1$ for $t = \infty$), all remaining intermediate quantities vanish:

$$x_1 = x_2 = x_3 = x_4 = x_5 = 0. \tag{7}$$

On the basis of Equation (3), one may write

$$x_3^{(\infty)} = \frac{1}{T_2} \int_0^\infty x_1 dt = 0. \tag{8}$$

For the transient response represented by Fig. 2, curve A, Expression (8) can be written in the form

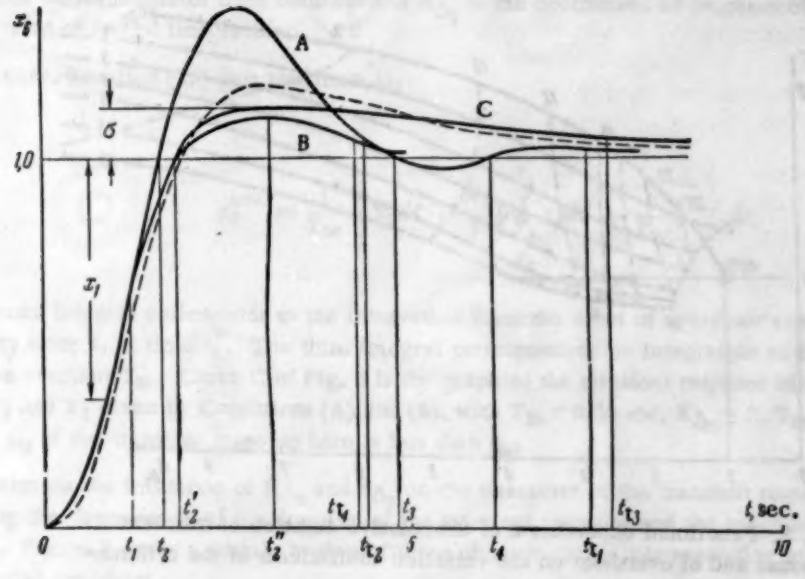

Fig. 2. Graphs of the transient responses in an automatic control system with variable time constants in the differentiator and integrator.

$$x_3^{(\infty)} = \frac{1}{T_2}\int_0^{t_2} x_1 dt + \frac{1}{T_2}\int_{t_2}^{t_3} x_1 dt + \frac{1}{T_2}\int_{t_3}^{t_4} x_1 dt + \frac{1}{T_2}\int_{t_4}^{\infty} x_1 dt = 0, \qquad (9)$$

where t_2, t_3 and t_4 are the instants of time at which the error becomes equal to zero.

The first and third integrals in (9) are positive and the second and fourth are negative. Since Equation (8) must be valid also for systems with variable T_1, it is then possible to write, for the transient response represented by Fig. 2, curve B,

$$x_3^{(\infty)} = \frac{1}{T_2}\int_0^{t_2'} x_1 dt + \frac{1}{T_2}\int_{t_2'}^{\infty} x_1 dt = 0, \qquad (10)$$

where t_2' is the moment at which the error becomes equal to zero.

For Equation (10) to hold, the integrals must be of different sign. Thus, the transient response cannot occur without overshoot.

Since the error x_1 in the second integral of Equation (9) is greater in absolute value than the error x_1 in the second integral of Equation (10), the value of x_3 in Equation (9) will approximate to its equilibrium value in a shorter time than will the value of x_3 in (10).

It is obvious that in order to decrease the duration of the transient response at the moment t_2', it is necessary to have a step-wise decrease of the integrator time constant, T_2. We stipulate that T_2 will vary as a function of the relationship of the signs of the error and its first derivative:

$$T_2 = \begin{cases} T_{20} & \text{for} \quad \frac{\dot{x}_1}{x_1} < 0, \\ \frac{T_{20}}{K_{\Delta_2}} & \text{for} \quad \frac{\dot{x}_1}{x_1} > 0, \end{cases} \qquad (B)$$

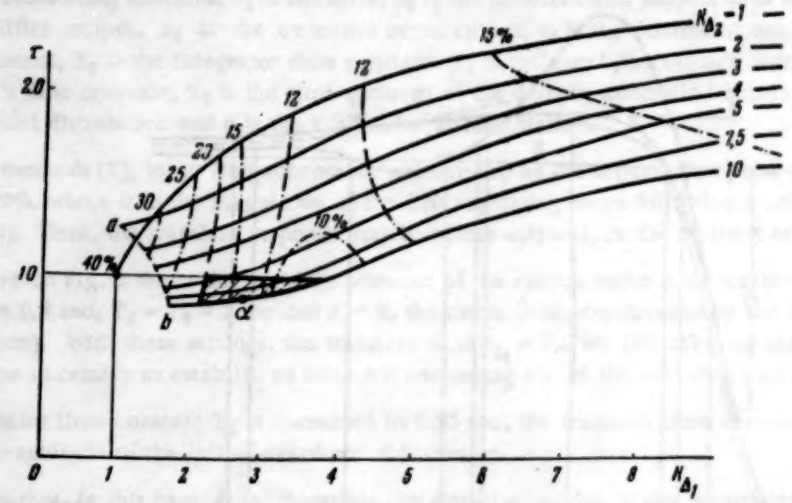

Fig. 3. Functional dependence of the relative duration of transient response and of overshoot on the variation coefficients of the differentiator and integrator time constants.

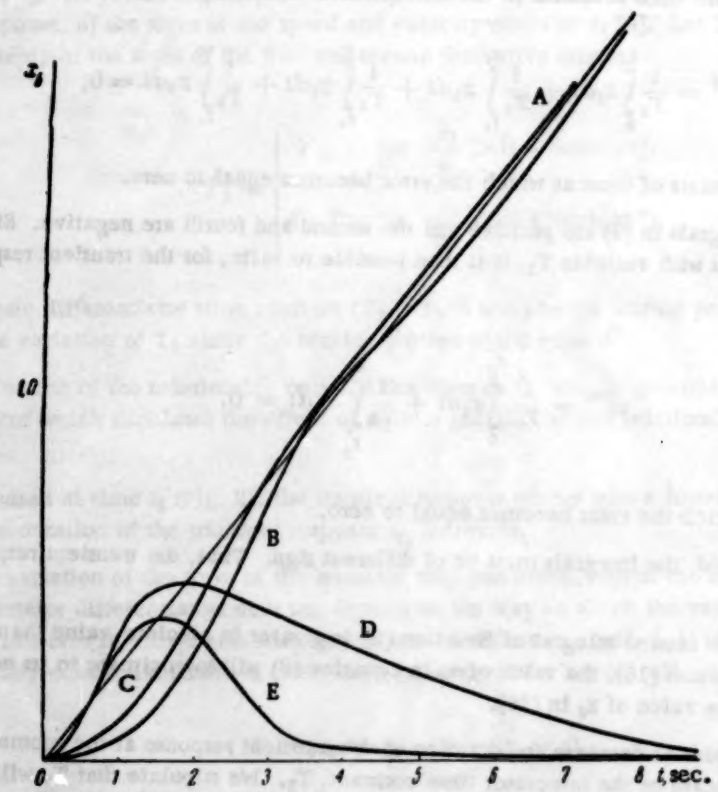

Fig. 4. A is the graph of $x_0 = 0.25$ t, B is the transient response for a constant-parameter system, C for a variable-parameter system, both in the case when $x_0 = 0.25$ t, D and E are the curves for, respectively, constant-parameter and variable-parameter system transient response for a step-wise excitation, $f(t) = 1$, for $t > 0$.

where T_{20} is the basic integrator time constant and K_{Δ_2} is the coefficient of decrease of the integrator time constant along the interval of forced integration.

In this case, Equation (10) gets rewritten as:

$$x_3^{(\infty)} = \frac{1}{T_{20}} \int_0^{t_2'} x_1 dt + \frac{K_{\Delta_2}}{T_{20}} \int_{t_2'}^{t_2''} x_1 dt + \frac{1}{T_{20}} \int_{t_2''}^{\infty} x_1 dt, \tag{11}$$

where the second integral corresponds to the integration from the onset of overshoot at t_2' to the change in sign of the velocity error $\dot{x}_1$ at time t_2''. The third integral corresponds to the integration of the negative error with the basic time constant T_{20}. Curve C of Fig. 2 is the graph of the transient response of a system with variable parameters T_1 and T_2 given by Conditions (A) and (B), with $T_{10} = 0.35$ sec, $K_{\Delta_1} = 3$, $T_{20} = 8$ sec, and $K_{\Delta_2} = 10$. The duration t_{t_4} of the transient response here is less than t_{t_2}.

To determine the influence of K_{Δ_1} and K_{Δ_2} on the character of the transient response, one may construct curves showing the dependence of the duration of the transient response and the magnitude of the overshoot on K_{Δ_1} and K_{Δ_2}. Figure 3 shows a certain region of these characteristics, corresponding to a transient response with just one essential overshoot.

The ordinates of Fig. 3 correspond to the relative time of the transient response $\tau = t_{t\Delta} / t_{t_2}$, where $t_{t\Delta}$ is the duration of the transient response for a system with variable parameters, and t_{t_2} is the duration of the transient response for a system with constant parameters. The solid curves give the dependence $\tau = F(K_{\Delta_1})$ for various values of K_{Δ_2}. The dotted curves join points with equal values of overshoot. The value of this overshoot, in percentages, is given above each curve. The dotted curve a-b bounds the region with just one essential overshoot.

The cross-hatched region represents the zone of allowable values of K_{Δ_1} and K_{Δ_2} satisfying the conditions $\sigma \leq 20\%$ and $\tau \leq 1$.

Real improvements in the transient responses of systems with parameters varying according to Laws (A) and (B) are also observed with linearly varying input quantities ($x_0 = \omega t$, where ω is the speed of variation of the input quantity) and in cases of step-wise varying external excitations, when the system is working as a stabilizer. The corresponding curves for the transient responses are given in Fig. 4 for systems adjusted in accordance with point α of Fig. 3.

SUMMARY

1. The introduction into automatic control systems of given structure and characteristics, and with essentially invariant links, of parameters which vary during the course of the transient response can significantly improve the quality of the transient response.

2. For systems with integrators, this improvement is obtained, not only by the introduction of variable time constants in the differentiators, but also by a mandatory introduction of variable time constants in the integrators.

Received May 18, 1957

LITERATURE CITED

[1] V. V. Solodovnikov (editor), Automatic Control Fundamentals, [In Russian] (Mashgiz, 1954).

[2] G. M. Ostrovskii, "The application of nonlinear correcting devices in second-order automatic control systems," Automation and Remote Control (USSR) 17, 11 (1956) [See English translation].

[3] G. Lewis, "The application of nonlinear feedback for improving transient responses in automatic control systems," [Russian trans.] Voprosy Raketnoi Tekhn. 4, 22 (1954).

[4] E. K. Shigin, "A following system of automatic control," Author's Certificate No. 106167 by claim No. 550384 of April 9, 1956.

[5] Flugge-Lotz and C. F. Taylor, "Synthesis of a nonlinear control system." IRE Transaction on automatic control, Vol. 1, May, 1956.

STATISTICAL INVESTIGATION OF NONSTATIONARY PROCESSES IN LINEAR SYSTEMS BY MEANS OF INVERSE SIMULATING DEVICES

A. V. Solodov

(Moscow)

A general theory is presented for the construction of what may be called inverse circuits. The application of inverse circuits to the investigation of nonstationary random processes by the simulation method is given. It is shown to be possible to couple inverse circuits with real regulators. The application of this methodology is illustrated by an example.

INTRODUCTION

The choice of parameters of a control system of given structure, minimizing the mean-square deviation of the total output signal from the effective signal, leads in general, when the random input signal and the system are nonstationary and the process is observed at time t = 0, to the problem of minimizing the expression

$$\sigma^2_{\text{out}}(t_n) = \int_0^{t_n}\int_0^{t_n} W(t_n, \xi)\, W(t_n, u)\, K_{\text{in}}(u, \xi)\, d\xi du. \qquad (1)$$

This expression defines the relationship between the dispersion σ_{out} of the output signal at a certain fixed moment of time t_n and the correlation function $K_{\text{in}}(u, \xi)$ of the input signal, in terms of the system's impulsive response function $W(t, \xi)$ [1]. Due to the great difficulty of obtaining analytical solutions to this problem, in the majority of practical cases recourse is had to numerical solutions using the resources of modern computing technology. Here, simulating devices merit particular attention since they have been widely used in the design of practical systems, due to the simplicity of the set of problems, the graphical nature of the solutions and the possibility of coupling with actual regulators. However, their use for statistical analysis has heretofore been limited to certain special cases only. If the input signal is a stationary process, of the "white" noise type, then

$$K_{\text{in}}(u, \xi) = S_0 \delta(t - \xi) \text{ and } \sigma^2_{\text{out}}(t_n) = S_0 \int_0^{t_n} W^2(t, \xi)\, d\xi, \qquad (2)$$

where S_0 is the noise spectral density.

Under these conditions, the problem of determining the dispersion of the output signal reduces to the integration of the square of the system's impulsive response function with respect to its second argument, ξ. Since the impulsive response function $W(t, \xi)$ is defined as the reaction of the system to a delta function input applied at time $t = \xi$, then, as obtained experimentally, $W(t, \xi)$ will contain ξ as a parameter, whereas it is necessary, in order to solve (2) by a simulating device, to have the argument t as the parameter, in order that ξ might be

the simulated variable. For this, it suffices to find a differential equation with ξ as the independent variable which would be satisfied by the function $W(t, \xi)$ for a fixed value of t. It is well known that this condition is satisfied by the conjugate equation. By implementing its simulation for a certain fixed value of t, one can obtain an output signal in the form of $W(t, \xi)$ as a function of ξ.

The practical implementation of this idea directly, with the aim of simulating, has still not found widespread use and is to be found only in a few works, although the solution of analogous problems in another domain of technology, the computation of ballistic correction, was carried out by D. A. Venttsel' as early as 1926 (published in 1928 [2]).

In 1952, the conjugate equation was used for determining, on electronic models, integrals of the form

$$\int_0^t |N(t, \tau)| d\tau,$$

connected with the solution of Bulgakov's problem concerning accumulated perturbations. Here, the technical details of solving the problem were worked out, as were the theoretical questions.

Subsequently, in [3], an analogous method of simulating the conjugate equation was presented, to be used in evaluating integrals of type (2). This method differed from the other only in that, instead of an instrument for defining the amplitude of the system's reaction, it required a squaring device to be added to the simulator output. In [3] there was given an excellent formulation of the correct construction of models for a conjugate system whereby the input and output roles are interchanged for each element entering into the system design. For the general case of nonstationary processes, a different methodology was presented for determining the dispersion at the system output, since the method described above was not directly applicable to this problem. Writing Expression (1) in the form

$$\sigma^2_{\text{out}}(t_n) = \int_0^{t_n} W(t_n, \xi)\, d\xi \int_0^{t_n} W(t_n, u)\, K_{\text{in}}(u, \xi)\, du$$

and introducing the notation

$$I(t_n, \xi) = \int_0^{t_n} W(t_n, u)\, K_{\text{in}}(u, \xi)\, du, \tag{3}$$

we obtain

$$\sigma^2_{\text{out}}(t_n) = \int_0^{t_n} W(t_n, \xi)\, I(t_n, \xi)\, d\xi. \tag{4}$$

We see from Expression (3) that if in the system with impulsive response function $W(t, u)$ we introduce by means of some external device the function $K_{\text{in}}(\xi, t)$ for a fixed value of the parameter ξ, then the output signal will be the function $I(t, \xi)$. By repeating this operation for a series of values of ξ we can, after the corresponding reorganization of the results, obtain $I(t, \xi)$ as a function of ξ. If we then reproduce this $I(t, \xi)$ by functional blocks and feed it to the input of the system under investigation then, according to Expression (4), we can obtain the desired dispersion σ^2_{out} at the output. The method just described does not require the use of the conjugate system, and allows the investigation to be carried out with actual regulators. However, even leaving aside the cumbersomeness of the experiments, such a procedure does not entail the mechanization of the bulk of the computational process. Thus, the method of simulating the conjugate equation allows nonstationary processes to be investigated by simulators only when the input signal is stationary, in which case the problem reduces to the simulation of Relationship (2). Here, the entire problem can certainly be simulated. If it is necessary to keep in the simulating design, as a constituent element, an actual linear regulator (the equation for

which might be unknown a priori), then the method of simulating the conjugate equation is obviously inapplicable in general. For the general nonstationary case there is now known only the method of [3] which, however, is essentially based on the use of simulating devices only for the intermediate operations in the computation of Expression (1), and which does not provide complete mechanization of the analysis.

The present work presents a method for applying simulating devices to the investigation of linear systems in the general nonstationary case and is based on the construction of special simulating designs which allow complete mechanization of the bulk of the process of computing Expression (1) and which allows coupling with actual linear regulators with constant parameters (for example, RC circuits). The theory of constructing such designs, the so-called inverse systems, is a development of the idea of the conjugate system as applied to a transformed design.

1. Theory of Constructing Inverse Systems.

Below we shall look for correct transformations of designs to allow us to obtain from them, as reaction to delta function inputs, outputs equivalent to the variation of the corresponding impulsive response function $W(t, \xi)$ with variable ξ, for a fixed value of t. Analytically, this is tantamount to the necessity of finding differential equations for the links, and equations for their interconnections, with ξ as the independent variable, said equations being satisfied by the function $W(t, \xi)$ which would simultaneously satisfy the original link and interconnection equations in terms of the variable t. Henceforth, a system with the impulsive response function $W(t, \xi)$, with t variable and ξ fixed, will be called the original system and the system with impulsive response function $W(t, \xi)$, with variable ξ and fixed t, will be called the inverse system.[1]

All linear systems with variable parameters may be represented as combinations of parallel and series connections, and feedback loops, of two types of links, inertial and forcing. By an "inertial link" is understood a linear system described by the equation

$$\sum_{i=0}^{n} a_i(t) \frac{d^i x_{\text{out}}}{dt^i} = y(t), \tag{5}$$

where x_{out} is the output signal and y is the input signal.

A forcing link is realized by differentiating the input signal in accordance with the relationship

$$x_0(t) = \sum_{j=0}^{m} b_j(t) \frac{d^j x_{\text{in}}}{dt^j}, \tag{6}$$

where x_{in} is the input signal and x_0 is the output signal.

A series connection of the stated two types of links, when $x_0(t) = y(t)$, forms a system of the general type described by the equation

$$\sum_{i=0}^{n} a_i(t) \frac{d^i x_{\text{out}}}{dt^i} = \sum_{j=0}^{m} b_j(t) \frac{d^j x_{\text{in}}}{dt^j}. \tag{7}$$

Thus, the problem consists of finding rules for obtaining the design of the inverse system for the inertial and forcing links, connected in parallel and series, with feedback loops, of the original system. We consider an inertial link. The impulsive response function $G(t, \xi)$ of the original system will satisfy Equation (5) for $y = \delta(t - \xi)$ and the condition of physical realizability

$$G(t, \xi) = \begin{cases} 0 & \text{for } t < \xi, \\ G(t, \xi) & \text{for } t \geqslant \xi, \end{cases} \tag{8}$$

[1] The meaning of the term "inverse system" will be clarified in the sequel.

where the connection between x_{out} and $\underline{y}$ will be defined by the expression

$$x_{out}(t) = \int_0^t G(t, u)\, y(u)\, du. \tag{9}$$

We apply the following technique which, further on, will also determine the rules for constructing the inverse system. We assume that a delta function type signal is produced at the system output. Based on (5) and (9), this gives us

$$\delta(t-\xi) = \int_0^t G(t, u) \sum_{i=0}^{n} a_i(u)\, \delta_u^{(i)}(u-\xi)\, du.$$

After using the well-known identity

$$(-1)^{\nu} \frac{d^{\nu} f(\xi)}{d\xi^{\nu}} = \int_{-\infty}^{+\infty} f(u)\, \delta_u^{(\nu)}(u-\xi)\, du \tag{10}$$

we finally obtain

$$(-1)^n \frac{d^n}{a\xi^n}[G(t, \xi)\, a_n(\xi)] + \ldots - \frac{d}{d\xi}[G(t, \xi)\, a_1(\xi)] + \\ + G(t, \xi)\, a_0(\xi) = \delta(t-\xi). \tag{11}$$

Equation (11), with ξ as the independent variable, is satisfied by the same function $G(t, \xi)$ as the original Equation (5). If, in Equation (11), we replace ξ by $\underline{t}$, we shall have

$$(-1)^n \frac{d^n}{dt^n}[G^*(t, \xi)\, a_n(t)]_t' + \ldots - \frac{d}{dt}[G^*(t, \xi)\, a_1(t)] + \\ + G^*(t, \xi)\, a_0(t) = \delta(\xi - t), \tag{12}$$

where

$$G^*(t, \xi) = G(\xi, t). \tag{13}$$

The role of the fixed moment of observation, t_n, will be played by the quantity ξ. Simulation of Equation (12) does not give the necessary results, since the function $G(t, \xi)$, necessary for further application, will be determined for values $t < \xi$, while the reaction of the real system occurs only for $t \geq \xi$. In fact, interchanging ξ and $\underline{t}$ in Relationship (8), we have

$$G(\xi, t) \begin{cases} 0 & \text{for } \xi < t, \\ G^*(t, \xi) & \text{for } \xi \geqslant t, \end{cases} \tag{14}$$

which confirms what has been stated above. Since, in Equation (12), the role of t_n is played by ξ, by introducing a change of variable

$$\xi - t = t_n - t = \tau,$$

which will be the current time in the model, we shall have from (12)

$$\frac{d^n}{d\tau^n}[G^*(\tau, t_n)\, a_n(t_n - \tau)] + \ldots + G^*(\tau, t_n)\, a_0(t_n - \tau) = \delta(\tau) \tag{15}$$

and Condition (14) will take the form

$$G(t_n, \tau) = \begin{cases} 0 & \text{for } \tau < 0, \\ G^*(\tau, t_n) & \text{for } \tau \geqslant 0, \end{cases} \tag{16}$$

which corresponds to the reaction of a physically realizable system. On the basis of Equations (5) and (15) it is easy to construct the block schematics[2] shown in Fig. 1,a and Fig. 1,b. Comparing these, one can easily form the rules for constructing the modified schematic from the block schematic of the original circuit.

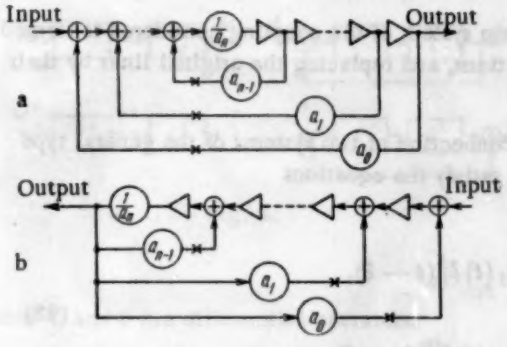

Fig. 1.

If the block schematic of the original design consists of integrators and adders with unit transfer coefficient, and of blocks of variable coefficients, then the inverse of each element is taken (i.e., each element is turned in such a way as to reverse the roles of input and output) and, in the blocks of variable coefficients, instead of the argument t the argument $t_n - \tau$ is introduced, and the result will be the block schematic of the altered, i.e., inverse, design.

Equation (12) is the conjugate of the original Equation (5). Therefore, in those cases when the system under investigation leads to the simulation of an equation of the type of (5) (or the corresponding system of equations written in normal form), the problem reduces to the construction of the conjugate system, the roles for constructing which were formulated above [3].

Consider now a forcing link. The impulsive response function of this link is defined by the expression

$$Y(t, \xi) = b_m(t)\,\delta_t^{(m)}(t-\xi) + \ldots + b_0(t)\,\delta(t-\xi) \tag{17}$$

and is a linear combination of delta functions of various orders. To make ξ the independent variable, we use the identity

$$\frac{d^\nu}{dt^\nu}\delta(t-\xi) = (-1)^\nu \frac{d^\nu}{d\xi^\nu}\delta(t-\xi), \tag{18}$$

application of which to Expression (17) gives

$$Y(t, \xi) = (-1)^m \frac{d^m}{d\xi^m}[b_m(t)\,\delta(t-\xi)] + \ldots + b_0(t)\,\delta(t-\xi).$$

Interchanging ξ and t and introducing, as previously, the new variable $\xi - t = t_n - t = \tau$, we will have

$$Y(\tau, t_n) = \frac{d_m}{d\tau^m}[b_m(t_n-\tau)\,\delta(\tau)] + \ldots + b_0(t_n-\tau)\,\delta(\tau). \tag{19}$$

Comparison of Equations (17) and (19) shows that the correct construction of the inverse of a forcing link remains the same as for an inertial link.

A series connection of the links investigated gives a system of the general type described by Equation (7) (Fig. 2,a). The impulsive response function $W(t, \xi)$ of this system will satisfy Equation (7) for $x_{1n} = \delta(t-\xi)$. On the other hand, the function $W(t, \xi)$ is determined by the function $G(t, \xi)$ from the relationship [4]

$$W(t, \xi) = (-1)^m \frac{d^m}{d\xi^m}[b_m(\xi)\,G(t, \xi)] + \ldots + b_0(\xi)\,G(t, \xi). \tag{20}$$

[2] The crosses on the connecting lines in the schematics indicate that the signals on these lines have had their signs reversed.

Interchanging ξ and t and bearing (13) in mind, we obtain

$$W^*(t, \xi) = (-1)^m \frac{d^m}{dt^m}[b_m(t) G^*(t, \xi)] + \ldots + b_0(t) G^*(t, \xi),$$

where

$$W^*(t, \xi) = W(\xi, t). \tag{21}$$

We now introduce the change of variable $\tau = t_n - t$, finally obtaining

$$W^*(\tau, t_n) = \frac{d^m}{d\tau^m}[b_m(t_n - \tau) G^*(\tau, t_n)] + \ldots + b_0(t_n - \tau) G^*(\tau, t_n), \tag{22}$$

and the corresponding circuit takes the form shown in Fig. 2,b.

Comparing circuits a and b of Fig. 2, we see that the inverse system of the coupling considered is formed from the original system by reversing the direction of the connections, and replacing the original links by their inverses.

We now consider an original system consisting of a series connection of two systems of the general type (Fig. 3,a). Let the impulsive response functions of these systems satisfy the equations

$$\begin{aligned} \sum_{i=0}^{n_1} a_i(t) W_A^i(t, \xi) &= \sum_{j=0}^{m_1} b_j(t) \delta_t^j(t - \xi), \\ \sum_{i=0}^{n_2} a_{1i}(t) W_B^{(i)}(t, \xi) &= \sum_{j=0}^{m_2} b_{1j}(t) \delta_t^{(j)}(t - \xi). \end{aligned} \tag{23}$$

Then, the impulsive response function of the series configuration, based on the integrative connection (9) (in which the role of the input signal will be played by the function $W_A(t, \xi)$), is determined by the relationship

$$W(t, \xi) = \int_{\xi}^{t} W_B(t, u) W_A(u, \xi)\, du. \tag{24}$$

The lower limit of the integral in (24) is affected by the condition on the impulsive response function

$$W(t, \xi) \equiv 0 \quad (t < \xi). \tag{25}$$

We rewrite Expression (24) in the form

$$W(t, \xi) = -\int_{t}^{\xi} W_A(u, \xi) W_B(t, u)\, du$$

and carry out the rearrangement of the arguments t and ξ. Then, based on (21), we shall have

$$W^*(t, \xi) = -\int_{\xi}^{t} W_A^*(t, u) W_B^*(u, \xi)\, du. \tag{26}$$

The block schematic corresponding to Relationship (26)[3] is shown in Fig. 3,b.

For parallel configurations of systems of the general type, the inverse configuration, by virtue of the principle of superposition, is formed by connecting in parallel the inverses of the systems forming the original circuit.

We now consider a feedback loop formed by a system of the general type and an inflexible feedback connection. In this case, the correct equation is

[3] The minus sign in (26) disappears when the change is made to the simulation variable $\tau = t_n - t$.

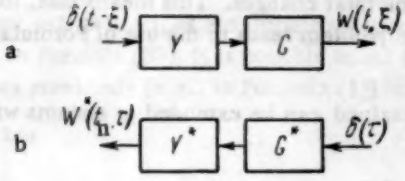

Fig. 2.

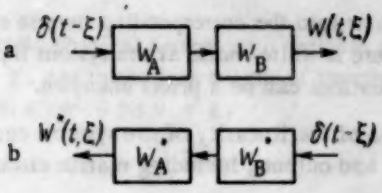

Fig. 3.

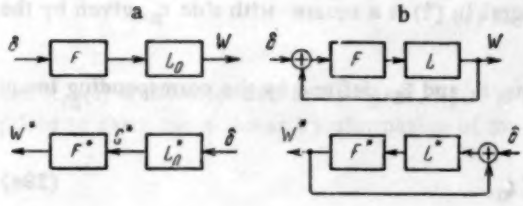

Fig. 4.

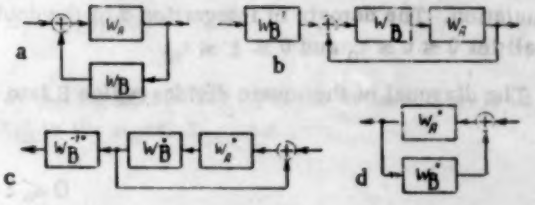

Fig. 5.

$$Lx_{\text{out}} = F(x_{\text{in}} + x_{\text{out}}),$$

where L and F are differential operators.

For $x_{in} = \delta(t-\xi)$ we shall have

$$L_0 W(t, \xi) = F\delta(t-\xi), \quad L_0 = L - F. \tag{27}$$

Equation (27) describes a certain equivalent system consisting of a series configuration of an inertial link, with the operator L_0, and a forcing link, with the operator F. Corresponding to the rules previously obtained, the inverse configuration must satisfy the relationships

$$L_0^* G^*(t, \xi) = \delta(t, \xi), \quad W^*(t, \xi), = F^* G^*(t, \xi), \quad L_0^* = L^* - F^*, \tag{28}$$

where the operators L_0^* and F^* are satisfied by the corresponding inverse systems. The block schematics satisfying Equations (27) and (28) are shown in Fig. 4,a and, in transformed form,[4] in Fig. 4,b. In the case where a system of the general type is already found in the feedback path (Fig. 5,a), it is first necessary to transfer the summing unit to the input of the feedback path[5] (Fig. 5,b), after which the circuit thus obtained will appear as a combination of the previously considered cases of a series connection with an inflexible feedback connection.

We now carry out the construction of the inverse system using the rules studied above, obtaining the circuit shown in Fig. 5,c, after which, by moving the branch point, we obtain the final configuration, shown in Fig. 5,d.

A comparison of the block schematic of the inverse circuit with that of the original circuit in all the cases so far studied allows us to formulate the following general rule.

To construct the block schematic of an inverse system from that of the original system, it suffices, in the latter, to reverse the direction of all connections between the component systems; it is necessary to replace each of the component systems by its inverse, using the rules developed above.

It is easy to show that the inverse system of the general type with constant parameters is equivalent to the original system. It is sufficient for this to set all the coefficients of Equations (15) and (19) constant, and then to apply the inversion of the transfer function to all the circuits under consideration. A consequence of this is the fact that links with constant parameters (for example, RC circuits or actual linear regulators) in the original

[4] Since the operator L−F (or $L^* - F^*$) determines a link consisting of an inertial link shunted by a feedback path containing a forcing link [6].

[5] Here the link W_B^{-1} is the inverse of link W_B, and possesses the property $\int_{\xi}^{t} W_B(t, u) W_B^{-1}(u, \xi) = \delta(t-\xi)$.

system will enter into the corresponding inverse system without any structural changes. This means that, for cases when there is white noise at the system input and solution of the problem leads to the use of Formula (2), the system equations can be a priori unknown.

By virtue of the linearity of the systems considered, all results obtained can be extended to systems with several inputs and outputs, including matrix circuits.

2. Simulating Design for Determining the Mean Square Deviation of the Full Output Signal from the Effective Signal.

We carry out a preliminary transformation of Formula (1) which will allow it to be used for the purpose of simulation. The domain of integration B of the double integral in (1) is a square with side t_n, given by the inequalities $0 \leq u \leq t_n$ and $0 \leq \xi \leq t_n$.

The diagonal of the square divides region B into two parts, B_1 and B_2, defined by the corresponding inequalities

$$0 \leqslant \xi \leqslant u \leqslant t_n, \tag{29a}$$

$$0 \leqslant u \leqslant \xi \leqslant t_n. \tag{29b}$$

Thus, the integral in (1) may be given in the form

$$\iint\limits_B \Phi(u, \xi)\, du\, d\xi = \iint\limits_{B_1} \Phi(u, \xi)\, du\, d\xi + \iint\limits_{B_2} \Phi(u, \xi)\, du\, d\xi, \tag{30}$$

where

$$\Phi(u, \xi) = W(t_n, \xi)\, W(t_n, u)\, K_{in}(u, \xi). \tag{31}$$

It is easy to see that the surface defined by the function $\Phi(u, \xi)$ is symmetric with respect to the diagonal $u = \xi$ since $\Phi(u, \xi) = \Phi(\xi, u)$ which follows immediately from Formula (31). Consequently,

$$\iint\limits_B \Phi(u, \xi)\, du\, d\xi = 2\iint\limits_{B_1} \Phi(u, \xi)\, du\, d\xi = 2\iint\limits_{B_2} \Phi(u, \xi)\, du\, d\xi.$$

Going over from the double integral to a repeated one and bearing inequality (29a) in mind, we obtain

$$\sigma^2_{out}(t_n) = 2\int_0^{t_n} W(t_n\ \xi)\, d\xi \int_\xi^{t_n} W(t_n, u)\, K_{in}(u, \xi)\, du. \tag{32}$$

Setting

$$H(t_n, \xi) = \int_\xi^t W(t_n, u)\, K_{in}(u, \xi)\, du, \tag{33}$$

we shall have

$$\sigma^2_{out}(t_n) = 2\int_0^{t_n} W(t_n, \xi)\, H(t_n, \xi)\, d\xi. \tag{34}$$

A comparison of Expression (33) with Formula (24) for series-connected systems of the general type with variable parameters allows us to make the introduction of the correlation function, $K_{in}(u, \xi)$ (very important

for what will follow), as the impulsive response function of a certain physical system with variable parameters since, in Formula (33), it is possible to set $K_{in}(u, \xi) = 0$ for $u < \xi$, due to the lower limit of integration, and this was previously [e.g., in Formula (1)] impossible, since $K_{in}(u, \xi) \neq 0$ for $u < \xi$.

Let

$$X_1(t) = X_{in}(t) + N_{in}(t)$$

and

$$X_0(t) = \int_0^t W(t, u) X_1(u)\, du,$$

where $X_{in}(t)$ is the effective input signal, $X_0(t)$ is the full output signal and $N_{in}(t)$ is the noise, and let it be required to carry out a linear transformation of the signal X_{in} to the signal X_{out}, i.e.,

$$X_{out}(t) = \int_0^t W_{tr}(t, u) X_{in}(u)\, du,$$

where $W_{tr}(t, u)$ determines the given linear transformation.

Then, the quantity $\epsilon = X_{out} - X_0$ will be defined as the deviation of the full output signal from the effective signal for the given system.

Based on (1), the dispersion of the error, σ_ϵ^2, will be determined by the relationship

$$\begin{aligned}\sigma_\epsilon^2(t_n) = &\int_0^{t_n} W_{tr}(t_n, \xi)\, d\xi \int_0^{t_n} W_{tr}(t_n, u) K_{in}(u, \xi)\, du + \\ &+ \int_0^{t_n} W(t_n, \xi)\, d\xi \left\{ \int_0^{t_n} W(t_n, u) K_1(u, \xi)\, du - \right. \\ &\left. - \int_0^{t_n} W_{tr}(t_n, \eta) [K_{in}(\eta, \xi) + K_{SN}(\eta, \xi)]\, d\eta \right\},\end{aligned} \tag{35}$$

where $K_{in}(u, \xi)$ is the correlation function of the effective input signal, $K_1(u, \xi)$ is the correlation function of the full input signal and $K_{SN}(\eta, \xi)$ is the cross correlation function of the effective input signal and noise.

Due to its simplicity, we carry out the construction of the simulating design for the case when there is no correlation between effective input signal and noise. Here, $K_{SN}(\eta, \xi) = 0$, $K_1(u, \xi) = K_{in}(u, \xi) + K_N(u, \xi)$.

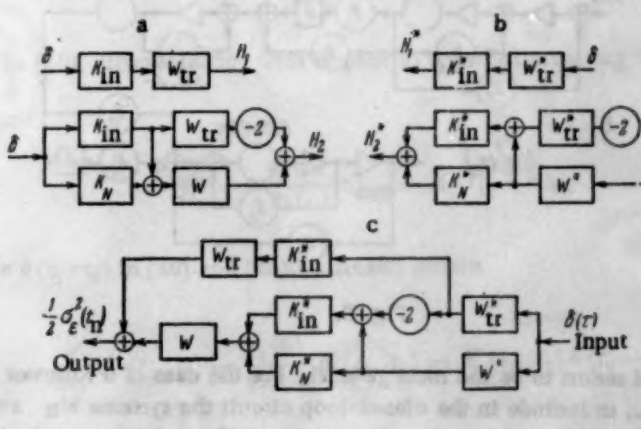

Fig. 6.

Bearing in mind the transformation of the domain of integration considered above, and introducing the functions

$$H_1(t_n, \xi) = \int_{\xi}^{t_n} W_{tr}(t_n, u) K_{in}(u, \xi)\, du,$$
$$H_2(t_n, \xi) = \int_{0}^{t_n} W(t_n, u)\,[K_{in}(u, \xi) + K_N(u, \xi)]\, du - 2H_1(t_n, \xi), \tag{36}$$

we can write Expression (35) in the form

$$\sigma_\varepsilon^2(t_n) = 2\int_0^{t_n} W_{tr}(t_n, \xi) H_1(t_n, \xi)\, d\xi + 2\int_0^{t_n} W(t_n, \xi) H_2(t_n, \xi)\, d\xi. \tag{37}$$

As was shown above, Formulas (36) characterize a series connection of systems with variable parameters, where the correlation functions are considered as the impulsive response functions of certain physical systems. Bearing this in mind, we can set up the design shown in Fig. 6,a. It is clear from (37) that the functions H_1 and H_2 must have ξ as the independent variable, while the circuit of Fig. 6,a must give the reactions H_1 and H_2 as functions of t. To solve this problem it is necessary to construct the inverse circuit for which it suffices to use the rules formulated above. The circuit thus obtained is shown in Fig. 6,b. To determine the dispersion of the error ϵ in accordance with Formula (37), the functions H_1 and H_2 must be used as the input signals to systems with the impulsive response functions $W_{tr}(t_n, \xi)$ and $W(t_n, \xi)$. Introducing into these latter the simulating variable τ we finally obtain the design given in Fig. 6,c. With an impulse at the input at time $\tau = 0$, the dispersion of the error will be observed at the output at time $\tau = t_n$. By varying the parameters of systems W and W^* one can so tune the system being investigated as to obtain the minimum dispersion of the error.

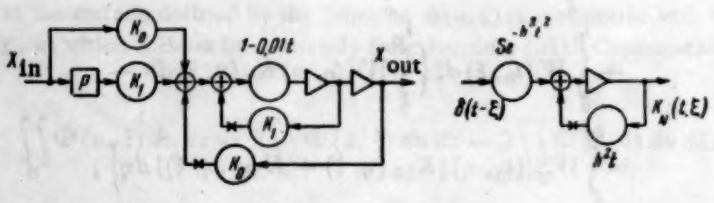

Fig. 7.

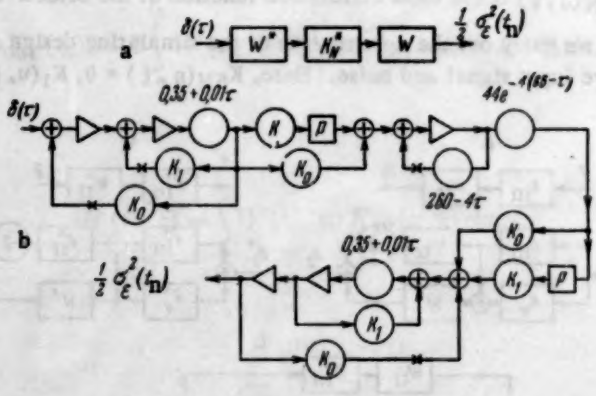

Fig. 8.

The circuit investigated seems to be the most general. For the case of a follower system, it is sufficient to set $W_{tr}(t, \xi) = \delta(t-\xi)$, i.e., to include in the closed-loop circuit the systems W_{tr} and W^*_{tr}. For the case of a stabilizing system $W_{tr}(t, \xi) = 0$, $K_{in} = 0$, and the systems W_{tr}, W^*_{tr} and K_{in} must be linked in an open-loop

circuit. In the case of a stationary input signal, the systems simulating the correlation functions K_{1n} and K_1 will be systems with constant parameters since for a stationary process $K(u, \xi) = K(u, -\xi)$, which corresponds to the impulsive response function of a system with constant parameters.

The table below provides a comparison of the two methods of investigating systems with variable parameters in the general, nonstationary, case.

Method	Number of times model is used in determining one value of dispersion	Number of variants investigated	Total number of model usages	Subsidiary operations
Use of original system to determine integral $I(t_n, \xi)$ and the dispersion [3]	$\underline{k}$ usages to determine $\underline{k}$ points of the curve $I(t_n, \xi)$	n	kn	Introduction of the functions $K_{1n}(\xi, t)$ and $I(t_n, \xi)$ from external devices
Use of the inverse system	One	n	n	None

3. Simulating the Correlation Function of a Random Process by a Linear System

A random process may be considered as an infinite collection of random variables depending on the time $\underline{t}$. Since experimental conditions permit only a finite number of observations to be made of the possible values of the random function, the practical use of an experimentally derived function as the correlation function only approximates to some degree or other the desired values. It thus becomes clear that it is unreasonable to strive in a simulating device for an accurate reproduction of the form of the given correlation function, but is sufficient merely to provide a good enough approximation. In particular, the function

$$K(t_1, t_2) = \sum_{i=1}^{n} q_i(t_1)\, q_i(t_2), \tag{38}$$

satisfying an n'th order linear differential equation with variable coefficients, may provide, depending on the number of terms used, an approximation to the correlation function which is as good as desired. However, in the majority of practical cases, it suffices to limit oneself to one or two terms of Polynomial (38). If, for example,

$$K(t_1, t_2) = q_1(t_1)\, q_1(t_2) \tag{39}$$

must be the impulsive response function of some linear system, then

$$x_{\text{out}}(t_1) = \int_0^{t_1} K(t_1, u)\, x_{\text{in}}(u)\, du. \tag{40}$$

Substituting (39) in (40), differentiating with respect to t_1 and eliminating the intermediate variable, we shall have

$$\frac{dx_{\text{out}}}{dt_1} - \frac{q_1'(t_1)}{q_1(t_1)} x_{\text{out}} = K(t_1, t_1)\, x_{\text{in}}. \tag{41}$$

Substituting $x_{\text{in}} = \delta(t_1 - t_2)$ in (40) and (41), we finally obtain

$$\frac{d}{dt_1} K(t_1, t_2) - \frac{q_1'(t_1)}{q_1(t_1)} K(t_1, t_2) = K(t_1, t_1)\, \delta(t_1 - t_2). \tag{42}$$

Equation (42) also determines a linear system with variable parameters which simulates the correlation function for values $t_1 \geq t_2$. For stationary processes $K(t_1, t_2) = K(t_1 - t_2)$. It is easy to show that, in this case, the corresponding differential equation will have constant coefficients.

Example

In a second-order stabilizing system described by the equation

$$a^2(t)\frac{d^2x_{out}}{dt^2} + K_1\frac{dx_{out}}{dt} + K_0x_{out} = K_0x_{in} + K_1\frac{dx_{in}}{dt},$$

it is required to find, by simulation, the optimal value of the coefficient K_1 corresponding to the minimum dispersion of the output signal $\sigma_\varepsilon^2(t_n)$ at the moment of observation $t = t_n$.

The input signal is a nonstationary random process with the correlation function

$$K_N = S\exp\left[-\frac{h^2}{2}(t^2 + \xi^2)\right].$$

The given data are characterized by the following table:

$a_2(t)$	K	S, volt^2 · sec.	h, $\frac{1}{\text{sec.}}$	t_n, sec.
$\frac{1}{1-0.01t}$	0.9	44	2	65

According to (42), the equation of the system which simulates the correlation function takes the form

$$\frac{d}{dt}K_N(t, \xi) + h^2tK_N(t, \xi) = Se^{-h^2t^2}\delta(t - \xi).$$

The block schematics of both original systems are given in Fig. 7. In accordance with Section 3 of this paper the inverse circuit for simulating the stabilizing system must have the form shown in Fig. 8a. By carrying out the construction of this circuit in accordance with the rules studied earlier, we finally obtain the simulating circuit shown in Fig. 8b. By varying the value of coefficient K_1 and observing the output signal one can determine the optimal value of K_1 corresponding to minimum dispersion.

Simulation of the circuit by a type IPT-5 model gave an optimal value of $K_1 = 1.65$. A numerical solution of the same problem gave a value of K_1 equal to 1.62.

SUMMARY

The use of inverse simulating devices extends the possibilities of using statistical methods for the analysis and synthesis of automatic control systems containing variable parameters. A great practical advantage of the method of inverse systems consists in the possibility it gives of complete mechanizing the bulk of the process of determining the dispersion of the error, and its applicability in cases where it is necessary to use, as an element of the simulating device, an actual linear regulator with constant parameters, the equations for which may not be previously known. The accuracy of the results obtained depends basically on the accuracy of the simulating devices used.

Received May 7, 1957

LITERATURE CITED

[1] V. S. Pugachev, Theory of Random Functions and their Use in Problems of Automatic Control [in Russian] (Gostekhizdat, 1957).

[2] D. A. Venttsel' Computation of Variable Trajectory Elements (F. E. Dzerzhinskii Military-Technical Academy Press, 1928).*

[3] J. H. Lanning and R. H. Battin, "An application of analog computers to the statistical analysis of time-variable networks," Trans. IRE vol. CT-2 (March 1955).

[4] L. A. Zadeh, "The determination of the impulsive response of variable networks," Journ. Appl. Phys. vol. 21 (1950).

*In Russian.

THE INFLUENCE OF FLUCTUATIONS ON THE OPERATION OF AN AUTOMATIC RANGE-FINDER

I. N. Amiantov and V. I. Tikhonov

(Moscow)

Errors of distance measurement arising from fluctuating disturbances and the problem of stability are considered for a system of automatic tracking using a linear approximation of range.

1. Short Description of Automatic Range-Finder Operation.

Figure 1 provides the block schematic for a system for the automatic tracking of a target by radar range, a system called, for brevity, an automatic range-finder.

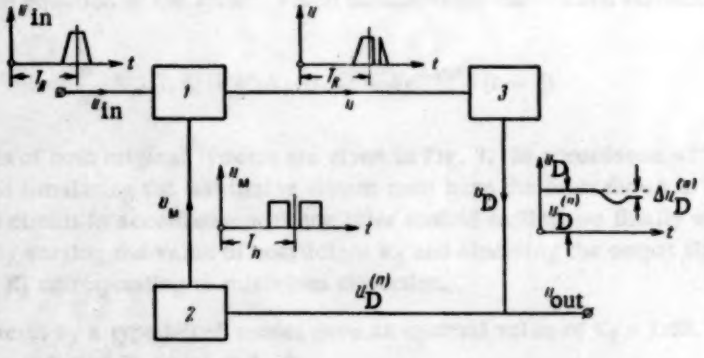

Fig. 1. Block schematic of the automatic range-finder. 1 is the time detector, 2 is the time modulator and 3 is the differential detector.

The input voltage u_{in} is the sum of the effective signal and the noise: $u_{in}(t) = u(t) + \xi(t)$ (only the signal u is shown in Fig. 1). The effective signals are pulses reflected from the target, assumed to be stationary, and thus have a fixed repetition period T_0. The moment the reflected pulse appears, measured from the emission of the scanning pulse, is denoted by T_R.

The time modulator develops a pair of rectangular selector pulses, the moment of appearance of which, during the n'th repetition period, is shifted with respect to the scanning pulse origination T_n, by a quantity which depends on the dc voltage $u_D^{(n)}$ existing at the output of the differential detector during that period. The task of the automatic range-finder is the accurate placement of the selector pulses on the reflected pulses. The error signal, depending on the difference $\Delta T_n = T_R - T_n$, is obtained at the output of the time detector in the form of a pair of pulses of different areas.

The time detector consists of two coincidence tubes, each of which fires only upon simultaneous action of one of the selector pulses and the input signal. The difference of the areas of the pulses at the output of the

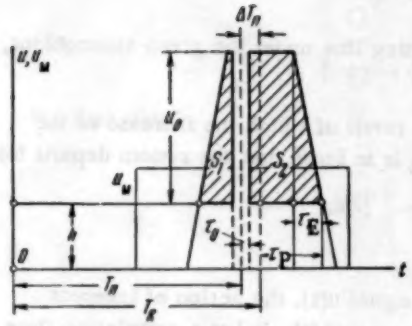

Fig. 2. Mutual orientation of the reflected signal and the selector pulses.

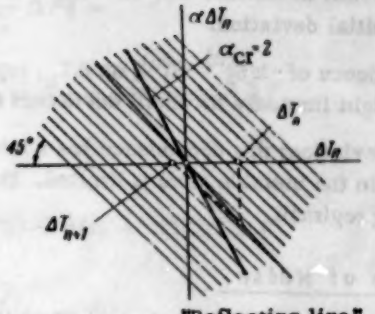

Fig. 3. Graphic determination of ΔT_{n+1} from ΔT_n.

time detector, depending on ΔT_n, is measured by the differential detector and converted to a dc voltage $u_D^{(n+1)}$ which controls the moment at which the selector pulses appear. This dc voltage may also be used as the system's output signal.

The following assumptions are made in constructing the proposed automatic range-finder model.

1. The form of the pulses reflected from the target is approximated by a trapezoid, but the selector pulses were assumed rectangular, with a definite height. The feeding to one grid of a coincidence tube of a selector pulse sets up a completely determinate condition for the conduction of the tube: the input signal voltage, acting on the other grid, must exceed a certain threshold value $\underline{h}$; to cut off the tube, this voltage must become less than $\underline{h}$. The presence of such a threshold is connected with the assumption of the rectangular form of the selector pulses.

2. The differential detector reacts to the difference of areas of the pulses from the time detector S_2 and S_1 (Fig. 2), i.e.,

$$\Delta u_D^{(n)} = k_1 [S_2^{(n)} - S_1^{(n)}], \tag{1}$$

where $\Delta u_D^{(n)}$ is the voltage increase at the differential detector output and k_1 is some proportionality coefficient. This assumption means that the differential detector does not have a firing threshold.

3. The shift δT_n of the selector pulses with respect to the scanning pulse in the n'th repetition period is proportional to the increase in voltage at the input to the time modulator

$$\delta T_n = k_2 \Delta u_D^{(n)}, \tag{2}$$

where k_2 is some proportionality factor.

It is easily seen that the equation of the closed-loop range tracking system can be written as

$$\Delta T_{n+1} = \Delta T_n - k [S_2^{(n)} - S_1^{(n)}], \; k = k_1 k_2. \tag{3}$$

In the absence of noise we have, for a small displacement ΔT_n,

$$S_2^{(n)} - S_1^{(n)} = 2u_0 \Delta T_n$$

and, consequently,

$$\Delta T_{n+1} = \Delta T_n - 2ku_0 \Delta T_n = \Delta T_n - \alpha \Delta T_n, \; \alpha = 2ku_0. \tag{4}$$

This equation may be interpreted graphically, as shown in Fig. 3. The quantity $\Delta T_{n+1} - \Delta T_n$ is connected with ΔT_n via the "reflecting line," the tangent of whose slope equals $-\alpha$. For $0 < \alpha < 1$ there occurs

an aperiodic damping of the initial deviation ΔT_0 with increasing n. For $1 < \alpha < 2$, there occurs an oscillatory damping of the initial deviation. For $\alpha > \alpha_{cr} = 2$ the system is unstable, since with increasing n there occurs an increase in the initial deviation.

The dependence of $-k(S_2^{(n)} - S_1^{(n)})$ on ΔT_n, represented by the reflecting line under the given assumptions, is actually a straight line only for small deviations ΔT_n.

For large deviations this dependence has a nonlinear character, as a result of which the increase of the initial deviation in the unstable state is limited. However, the error ΔT_∞ is so large that the system departs from the auto-tracking regimen.

2. Influence of Noise.

At the input of the system let there be, in addition to the effective signal u(t), the action of inherent fluctuations from the receiver output, appearing as a stationary random process, $\xi(t)$. It has a correlation time τ_C of the order of the pulse length T_P:

$$\tau_C \approx \frac{1}{\Delta f} \approx T_P, \tag{5}$$

where Δf is the energy bandwidth of the receiver for intermediate frequencies at the level 0.5.

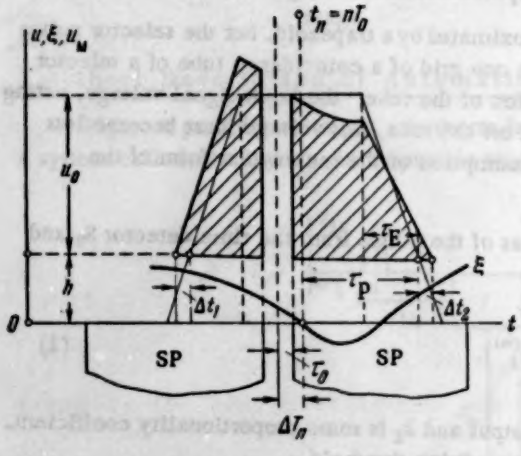

Fig. 4. Influence of fluctuations on the functioning of the time detector. SP is a selector pulse.

The fluctuations $\xi(t)$ may have an arbitrary character (with a normal, or some other, probability density). However, the intensity of the fluctuations $\xi(t)$, characterized by the dispersion σ^2, is considered to be not too large, so that the deviation ΔT_n will be small, and therefore the possibility of a false firing of the coincidence tubes can be neglected.

It was assumed above that the differential detector measures the difference in areas $S_2^{(n)} - S_1^{(n)}$ of the pulses at the time detector output. With the presence of not very large fluctuations, this difference will be a random variable, due to two causes: 1) "creeping" fluctuations at the vertices and faces of the pulses during the time when the coincidence tubes are firing; 2) "tremors" of the moment of firing of the coincidence tubes due to the superimposition of fluctuations on the pulse edges (Fig. 4).

Let us first study the first cause. Let $t_n - \tau_p$, $t_n + \tau_p$ be the firing times (the first – conducting, the second – cutting off) of the coincidence tubes, without taking into account the variations of these times under the action of fluctuations. The time interval τ_p is determined by the pulse front voltage reaching the threshold h. In the given case, the difference of areas will equal (Fig. 4).

$$\Delta S_1^{(n)} = S_2^{(n)} - S_1^{(n)} = 2u_0 \Delta T_n + \Phi(\Delta T_n), \tag{6}$$

where

$$\Phi(\Delta T_n) = \int_{t_n - \Delta T_n + \tau_0}^{t_n + \tau_p} \xi(x)\,dx - \int_{t_n - \tau_p}^{t_n - \Delta T_n - \tau_0} \xi(x)\,dx.$$

For a small deviation, $\Delta T_n \ll \tau_C$, $\Phi(\Delta T_n)$ may be expanded in a Taylor series about zero, and limited just to the linear terms

$$\Phi(\Delta T_n) \approx \Phi(0) + \frac{\partial \Phi}{\partial \Delta T_n} \Delta T_n =$$

$$= \int_{\tau_0}^{\tau_p} [\xi(t_n + x) - \xi(t_n - x)]\, dx + [\xi(t_n + \tau_0) + \xi(t_n - \tau_0)]\, \Delta T_n.$$

We then obtain

$$\Delta S_1^{(n)} = 2u_0 \Delta T_n + [\xi(t_n + \tau_0) + \xi(t_n - \tau_0)]\, \Delta T_n + \int_{\tau_0}^{\tau_p} [\xi(t_n + x) - \xi(t_n - x)]\, dx. \tag{7}$$

We shall ignore incorrect firings (which is approximately permissible for $2\sigma < h$) and consider a tremor of the moment of firing of a coincidence tube due to fluctuations. Such a study (even in a first approximation) requires consideration of the joint probability density of the fluctuations themselves, $\xi(t)$, and their derivative $d\xi(t)/dt$ [1]. However, we shall effect a simplification. Let Δt be the instantaneous value of the shift (tremor) in the moment of firing. The variation of $\xi(t)$ in the interval Δt is proportional to $\Delta t/\tau_C$.

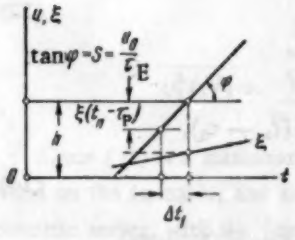

Fig. 5. Approximate determination of the instability of the moment of firing.

Since $\sigma_{\Delta t} = \sqrt{\overline{\Delta t^2}} < \tau_C$, the function $\xi(t)$ can be approximately considered as constant on the segment Δt^*. We thus obtain a simple relationship for the quantity Δt, the meaning of which is clarified by Fig. 5:

$$\Delta t_1 = \frac{\xi(t_n - \tau_p)}{s}, \quad \Delta t_2 = \frac{\xi(t_n + \tau_p)}{s}, \tag{8}$$

where $s = u_0/\tau_E$ is the steepness of the leading pulse edge.

The difference of areas attributable to the shift of the firing moment equals

$$\Delta S_2^{(n)} = \frac{1}{2s} [\xi^2(t_n + \tau_p) - \xi^2(t_n - \tau_p)]. \tag{9}$$

The total difference will equal

$$\Delta S^{(n)} = \Delta S_1^{(n)} + \Delta S_2^{(n)}.$$

On the basis of Equation (3) we obtain the following equation for the closed circuit:

$$\Delta T_{n+1} - \Delta T_n = -2ku_0 \Delta T_n - k[\xi(t_n + \tau_0) - \xi(t_n - \tau_0)\, \Delta T_n + k \int_{\tau_0}^{\tau_p} [\xi(t_n - x) - \xi(t_n + x)\, dx + \frac{k\tau_E}{2u_0} [\xi^2(t_n - \tau_p) - \xi^2(t_n + \tau_p)]. \tag{10}$$

Turning to a graphical interpretation of Equation (10) in accordance with Fig. 3, we can state that the fluctuations occasion a variation of the slope of the "reflecting line" (second term on the right side) and a shift of the "reflecting line" along the axis of ordinates (third and fourth terms). The variations of the slope and shift of the "reflecting line" are different for different n.

In the general case, the deviation ΔT_n is a nonstationary random function of the discrete times $t_n = nT_\theta$, where, as will be shown below, the mean value of $\overline{\Delta T_n} = 0$. Such a character of ΔT_n requires that a special way

*Here, and in what follows, a superscript bar denotes a statistical average.

be found for determining the stability, instability and errors of this automatic range-finding system.

It will be considered that the system is stable if there is a finite limit to the sequence $\overline{\Delta T_n^2}$:

$$\sigma_{\Delta T}^2 = \lim_{n \to \infty} \overline{\Delta T_n^2}. \tag{11}$$

The system is unstable if, on the contrary, the sequence $\overline{\Delta T_n^2}$ does not have a dinite limit for $n \to \infty$.

As a quantitative measure of the error in a stable system, we take the quantity

$$\sigma_{\Delta T} = \sqrt{\lim_{n \to \infty} \overline{\Delta T_n^2}}. \tag{12}$$

3. Statistical Characteristics.

Since the deviation $y = \Delta T_n$ is a step-function of the discrete times $t_n = nT_0$, Equation (10) is a stochastic first-order linear difference equation with variable coefficients and a forcing function [2]. We rewrite it as

$$\Delta y + (\alpha + \beta\zeta)\, y = a\eta_1 + b\eta_2, \tag{13}$$

where

$$\alpha = 2ku_0, \quad \beta = a = k, \quad b = \frac{k\tau_E}{2u_0}, \quad \zeta(n) = \xi(t_n + \tau_0) + \xi(t_n - \tau_0),$$

$$\eta_1(n) = \int_{\tau_0}^{\tau_p} [\xi(t_n - x) - \xi(t_n + x)]\, dx, \qquad \eta_2(n) = \xi^2(t_n - \tau_p) - \xi^2(t_n + \tau_p). \tag{14}$$

The solution of this equation is made up of the forced component y_1 and the inherent component y_2. In a stable system, the inherent component is damped for $n \to \infty$. Therefore we consider initially a single forced solution, $y_1(N)$:

$$y_1(N) = y_1(NT_0) = \sum_{k=0}^{N-} [a\eta_1(k) + b\eta_2(k)] \times$$
$$\times \prod_{n=k+1}^{N-1} [1 - \alpha - \beta\zeta(n)] = \sum_{m=1}^{N} \Lambda_m, \tag{15}$$

where

$$\Lambda_m = [a\eta_1(N-m) + b\eta_2(N-m)] \prod_{l=1}^{m-1} [1 - \alpha - \beta\zeta(N-l)],$$
$$m = N - k, \quad l = N - n. \tag{16}$$

We note that Λ_m consists of factors with respect to moments of time separated by at least the interval T_0. Since $\tau_C \approx \tau_P \ll T_0$, the individual factors are statistically independent. Therefore, in averaging over the set of actual values of $\xi(t)$, the mean value of the product is equal to the product of the mean values of the factors, i.e.,

$$\overline{y_1(N)} = \sum_{m=1}^{N} \overline{\Lambda_m} = \sum_{m=1}^{N} \overline{[a\eta_1(N-m) + b\eta_2(N-m)]} \times \tag{17}$$
(cont'd)

$$\times \prod_{l=1}^{m-1} \overline{[1-\alpha-\beta\zeta(N-l)]}. \tag{17}$$

If $\bar{\xi} = 0$, then $\overline{\eta_1(N-m)} = \overline{\eta_2(N-m)} = 0$ for any N−m and, consequently, $\overline{y_1(N)} = 0$.

For the dispersion we obtain

$$\overline{y_1^2(N)} = \sum_{i=1}^{N}\sum_{j=1}^{N} \overline{\Lambda_i \Lambda_j} = \sum_{m=1}^{N} \overline{\Lambda_m^2}. \tag{18}$$

Since, for $i \neq j$,

$$\overline{\Lambda_i \Lambda_j} = \overline{[a\eta_1(N-i) + b\eta_2(N-i)][a\eta_1(N-j) + b\eta_2(N-j)]} \times$$
$$\times \overline{\prod_{\mu=1}^{i-1} [1-\alpha-\beta\zeta(N-\mu)] \prod_{\nu=1}^{j-1} [1-\alpha-\beta\zeta(N-\nu)}} = 0,$$

then,

$$\overline{y_1^2(N)} = \sum_{m=1}^{N} \overline{[a\eta_1(N-m) + b\eta_2(N-m)]^2} \prod_{l=1}^{m-1} \overline{[1-\alpha-\beta\zeta(N-l)]^2}. \tag{19}$$

Since $\xi(t)$ is a stationary process, the quantities $\overline{[a\eta_1(\lambda) + b\eta_2(\lambda)]}$ and $\overline{[1-\alpha-\beta\zeta(\lambda)]^2}$ do not depend on the index λ, and therefore the right member of Expression (19) appears as the sum of N terms of a geometric series, with the first term $c = \overline{[a\eta_1(\lambda) + b\eta_2(\lambda)]^2}$ and ratio $q = \overline{[1-\alpha-\beta\zeta(\lambda)]^2}$.

If $q < 1$, then a limit exists as $N \to \infty$:

$$\lim_{N\to\infty} \overline{y_1^2(N)} = \frac{c}{1-q}. \tag{20}$$

It is possible to show that for $q < 1$ the inherent component of the solution y_2 is damped. Therefore, in accordance with the previously assumed definition of the error, we have

$$\sigma_{\Delta T} = \sqrt{\frac{c}{1-q}}. \tag{21}$$

The regions of stability and instability are determined, respectively, by the expressions $q \leq 1$ and $q > 1$.

We now express the error in terms of the characteristics of the original process, $\xi(t)$, which will be considered, by way of an example, to be normal, with the correlation function:

$$\overline{\xi(t_1)\xi(t_2)} = \sigma^2 R(|t_1 - t_2|).$$

In the given case

$$q = (1-\alpha)^2 - 2(1-\alpha)\beta\bar{\zeta} + \beta^2\overline{\zeta^2} = (1-\alpha)^2 +$$
$$+ \beta^2[2\bar{\xi}^2 + 2\overline{\xi(\lambda+\tau_0)\xi(\lambda-\tau_0)}] =$$
$$= (1-\alpha)^2 + 2\beta^2\sigma^2[1 + R(2\tau_0)] \quad (\bar{\zeta} = 0),$$

$$c = a^2\overline{\eta_{l1}^2(\lambda)} + b^2\overline{\eta_{l2}^2(\lambda)} + 2ab\overline{\eta_{l1}(\lambda)\eta_{l2}(\lambda)} =$$

$$= a^2\int_{\tau_0}^{\tau_p}\int_{\tau_0}^{\tau_p}\overline{[\xi(\lambda - x_1) - \xi(\lambda + x_1)][\xi(\lambda - x_2) - \xi(\lambda + x_2)]}\,dx_1dx_2 +$$

$$+ b^2[\overline{\xi^4(\lambda - \tau_p)} + \overline{\xi^4(\lambda + \tau_p)} - 2\overline{\xi^2(\lambda - \tau_p)\xi^2(\lambda + \tau_p)}] +$$

$$+ 2ab\int_{\tau_0}^{\tau_p}\overline{[\xi^2(\lambda - \tau_p) - \xi^2(\lambda + \tau_p)][\xi(\lambda - x) - \xi(\lambda + x)]}\,dx =$$

$$= 2a^2\sigma^2\int_{\tau_0}^{\tau_p}\int_{\tau_0}^{\tau_p}[R(|x_1 - x_2|) - R(|x_1 + x_2|)]\,dx_1dx_2 + 4b^2\sigma^4[1 - R^2(2\tau_p)].$$

The last equality was written on the basis that, for a normal distribution with zero mean, we have the values

$$\overline{\xi^4} = 3\sigma^4, \quad \overline{\xi^2(t_1)\xi^2(t_2)} = \sigma^4[1 + 2R^2(|t_1 - t_2|)], \quad \overline{\xi^2(t_1)\xi(t_2)} = 0.$$

Substituting the values for $\underline{c}$ and $\underline{q}$ in Formula (21), we obtain

$$\sigma^2_{\Delta T} = \frac{\sigma^2}{\sigma_0^2 - \sigma^2}[1 + R(2\tau_0)]^{-1}\left\{\int_{\tau_0}^{\tau_p}\int_{\tau_0}^{\tau_p}[R(|x_1 - x_2|) - R(|x_1 + x_2|)]\,dx_1\,dx_2 + \frac{2\sigma^2\tau_E^2}{u_0^2}[1 - R^2(2\tau_p)]\right\}, \tag{22}$$

where

$$\sigma_0 = \frac{1}{\beta}\sqrt{\frac{\alpha(2-\alpha)}{2[1 + R(2\tau_0)]}}. \tag{23}$$

The first term within the curly brackets in (22) characterizes the influence of creeping on the vertices and edges of the pulses, and the second term characterizes the shift of the moment of firing.

As will be shown below, the stability condition $q < 1$ is equivalent to the condition that $\sigma^2 < \sigma_0^2$. Therefore, in the stable regime, the quantity $\sigma_{\Delta T}$ is real. For $\sigma = 0$, $\sigma_{\Delta T} = 0$, and for $\sigma = \sigma_0$, $\sigma_{\Delta T} = \infty$. For small σ we obtain the approximate formula

$$\sigma^2_{\Delta T} \approx \left(\frac{\sigma}{\sigma_0}\right)^2[1 + R(2\tau_0)]^{-1}\int_{\tau_0}^{\tau_p}\int_{\tau_0}^{\tau_p}[R(|x_1 - x_2|) - R(|x_1 + x_2|)]\,dx_1\,dx_2. \tag{24}$$

In accordance with the assumptions made with respect to the smallness of the deviation ΔT_n, for Formulas (23) and (24) to be correct the dispersion σ^2 must be sufficiently small so that the inequality $\sigma_{\Delta T} \ll \tau_C$ holds.

Numerical estimates can be made from Formulas (23) and (24) if some concrete form of the correlation coefficient $R(\tau)$ is given (cf. the example given below).

4. On the Stability of the System.

The limits of stability are determined from the equation

$$q = (1 - \alpha)^2 + 2\beta^2\sigma^2[1 + R(2\tau_0)] = 1.$$

This equation has the solution

$$\sigma^2 = \sigma_0^2 = \frac{\alpha(2-\alpha)}{2\beta^2[1 + R(2\tau_0)]}.$$

The quantity σ_0 characterizes the limits of stability: for $\sigma < \sigma_0$, the system is stable; for $\sigma > \sigma_0$ the system is unstable.

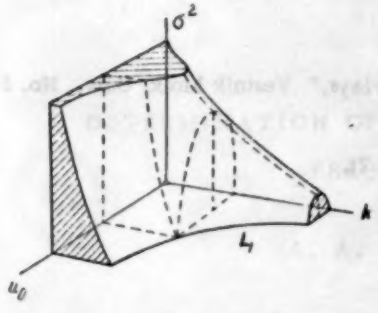

Fig. 6. Region of stability with fluctuations present.

Substituting the values of α and β from (14), we obtain the final formula for σ_0^2:

$$\sigma_0^2 = \frac{2}{1+R(2\tau_0)}\frac{u_0}{k}(1-ku_0). \qquad (25)$$

In a three-dimensional space with the coordinates $\underline{k}$, u_0 and σ^2, Equation (25) determines a certain surface, represented in Fig. 6. The intersection of this surface with the plane $k = \text{const}$ gives a parabola, and with the plane $u_0 = \text{const}$, a hyperbola.

The points lying inside the surface are in the region of stability, and those outside of it are in the region of instability. The line L_1 on the u_0, k plane, the equation for which is $u_0 = 1/k$, is the boundary of ordinary stability ($\sigma = 0$, $\alpha = 2$). For a fixed $\underline{k}$, the dependence of σ_0^2 on u_0 has a maximum at the point $u_0 = 1/2k$.

Example

Let $R(\tau) = \exp\left(-\frac{|\tau|}{\tau_C}\right)$.

Then, carrying out the integration in Formula (22) and assuming that $\tau_0 \ll \tau_C$, $\tau_0 \ll \tau_p$, we obtain

$$\sigma_{\Delta T}^2 = \frac{\sigma^2}{\sigma_0^2-\sigma^2}\frac{1}{2}\tau_C\left[2\frac{\tau_p}{\tau_C} - 2 + 2e^{-\frac{\tau_p}{\tau_C}} - \right.$$
$$\left. - \left(1-e^{-\frac{\tau_p}{\tau_C}}\right)^2 + \frac{2\sigma^2}{u_0^2}\left(\frac{\tau_E}{\tau_C}\right)^2\left(1-e^{-\frac{4\tau_p}{\tau_C}}\right)\right]. \qquad (26)$$

Let the following relationships hold: $\tau_p = 2\tau_E$, $\tau_C = T_p = 2\tau_p$, $u_0 = h$, $\sigma = u_0/2$, $\sigma/\sigma_0 = 0.6$. We can convince ourselves, from estimates, that the effect of creep on the vertices and edges of the pulses is approximately two times as large as the effect of the shift of the moment of firing of the coincidence tubes, and that the sum of the two effects leads to an error

$$\sigma_{\Delta T} \approx 0.2\,T_p. \qquad (27)$$

If $T_p = 1$ microsecond, then the error in measuring distance to the target equals $\sigma_R = \sigma_{\Delta T} v/2 \approx 30$ meters, where $\underline{v}$ is the velocity of light. We note that Equation (27) is justified by considering that we are dealing with small deviations, $\Delta T_n \ll \tau_C$.

SUMMARY

In this paper we considered the functioning of the simplest model of an automatic range-finder with the presence of sufficiently small fluctuations and a stationary target. Of course, there are desirable generalizations in the following directions: 1) rendering the model of the automatic range-finder more precise and more complex, 2) considering the nature of target motion, 3) removing the assumptions on the smallness of the fluctuations and, in particular, considering incorrect firing of the coincidence tubes.

Such investigations are necessary steps towards the making of comparative estimates of noise stability of

automatic tracking devices by angular coordinates and distance with different forms of noise.

Received March 29, 1957

LITERATURE CITED

[1] V. I. Tikhonov, "The action of small fluctuations on electronic relays," Vestnik Mosk. Univ., No. 5 (1956).

[2] A. O. Gel'fond, Calculus of Finite Differences (Gostekhizdat, 1952).

DETERMINATION OF SYSTEM PARAMETERS FROM EXPERIMENTAL FREQUENCY CHARACTERISTICS*

A. A. Kardashov and L. V. Karniushin

(Lvov)

A method is given for determining the parameters of linear links and automatic control systems from their approximate experimental amplitude-phase characteristics (a.p.c.). By interpolation, approximate values are found for the values of the coefficients in the analytic expression for the a.p.c., and then corrections to the coefficients thus found are computed by the method of least squares.

The method to be given is applicable to transfer functions with arbitrary polynomials in numerator and denominator, and gives sufficiently accurate results when calculations are done by slide rule.

Examples clarify the computational steps.

In the literature on the theory of automatic control [1-3], there are investigated only the simplest cases of approximate determination of the parameters of automatic control system (a.c.s.) links from empirically-determined dynamic characteristics. In recent years, a series of new works, detailing further development of methods for solving this problem, have been published ([4-6] and others).

The present paper attempts to give a universal and sufficiently accurate method of finding the values of the coefficients of the transfer function, or of individual parameters, in linear models of real links and a.c.s., using approximations to their empirically determined a.p.c.

STATEMENT OF THE PROBLEM

To determine the desired parameters of links or of link circuits in automatic control systems, one may start either from given amplitude-phase characteristics or from experimentally-determined amplitude-phase characteristics, obtained under conditions close to the actual ones and smoothed by well-known statistical means.

An approximate structure of the amplitude-phase characteristic may, in the majority of cases, be determined beforehand on the basis of known physical laws to which the functioning of the links (link circuits) of the automatic control system** are subject. In case these laws are not sufficiently well known, the necessity arises of determining an acceptable structure for the analytic expression of the amplitude-phase characteristic. This necessity may also arisen when the link equations have been simplified as a preliminary step.

---

*The basic statement of this work was made on April 11, 1955, at the Fourteenth Conference of the Lvov Polytechnic Institute on the results of research work carried out in the year 1954.

**The experimentally-determined characteristic in the time domain can also be used, it being a simple matter to construct the amplitude-phase characteristic from this.

If the physical relationships and initial conditions allow only the structure of the numerator of the link's transfer function to be determined, then the degree $\underline{n}$ of the denominator may be found from the experimental amplitude-phase characteristic, using the argument principle:

$$n = l + m' - m'', \tag{1}$$

where l is the number of quadrants traversed by the amplitude-phase characteristic vector when the frequency ω varies from 0 to ∞, m' is the number of roots of the numerator with negative real parts and m" is the number of roots of the numerator with positive real parts. A root of zero in the numerator leads to a counterclockwise rotation of the amplitude-phase characteristic vector by the angle $\varphi = \frac{\pi}{2} m'''$, where m''' is the multiplicity of the zero root.

In the general case, the structure of the initial linear differential equation will have the form

$$\begin{aligned}(a_n p^n + a_{n-1} p^{n-1} + \cdots + a_1 p + 1)\, u_{out} = \\ = (b_m p^m + b_{m-1} p^{m-1} + \cdots + b_1 p + k)\, u_{in},\end{aligned} \tag{2}$$

where $m < n$, u_{in} and u_{out} are the input and output coordinates, a_s, b_r ($s = 1, 2, \ldots, n$; $r = 1, 2, \ldots, m$) and $\underline{k}$ are constant coefficients, and $p = d/dt$ is the operator for differentiation with respect to time.

To Equation (2) there corresponds the amplitude-phase characteristic

$$W(j\omega) = \frac{K(j\omega)}{D(j\omega)} = \frac{u_n(\omega) + jv_n(\omega)}{u_d(\omega) + jv_d(\omega)} = U(\omega) + jV(\omega), \tag{3}$$

where

$$u_n(\omega) = k - b_2\omega^2 + b_4\omega^4 - b_6\omega^6 + \cdots, \quad v_n(\omega) = b_1\omega - b_3\omega^3 + b_5\omega^5 - b_7\omega^7 + \cdots,$$
$$u_d(\omega) = 1 - a_2\omega^2 + a_4\omega^4 - a_6\omega^6 + \cdots, \quad v_d(\omega) = a_1\omega - a_3\omega^3 + a_5\omega^5 - a_7\omega^7 \cdots.$$

The problem reduces to finding those numerical values of the coefficients a_s, b_r and $\underline{k}$ and, consequently, the desired link parameters, for which Function (3) will coincide as closely as possible with the experimental amplitude-phase characteristics.

Connected with the linearization process, and also with the realization that, in practice, it is not possible to take into account all the physical phenomena bearing on the transient responses of automatic control system links, it must be borne in mind that the function, determined from analytic Expression (3), with its given structure, may not coincide with the experimental amplitude-phase characteristic even with selected values of the coefficients a_s, b_r and $\underline{k}$. It follows from this that the problem of determining these coefficients may be solved by simple interpolation only in individual cases, and that, therefore, in the solution of the problem under consideration, use must be made of a method giving the best, in some sense or other, approximation to the function.

For a link with a static characteristic, the coefficient $\underline{k}$ is the gain coefficient, which is most simply determined from the initial portion of the amplitude-phase characteristic:

$$k = W(j\omega)\,|_{\omega=0} = U(0) \tag{4}$$

or from the characteristic in the time domain

$$k = \frac{u_{out}(\infty)}{u_{in}(\infty)}. \tag{5}$$

For a link with an astatic characteristic, i.e., when $D(p) = a_n p^n + a_{n-1} p^{n-1} + \ldots + a_1 p$, the coefficient $\underline{k}$ may be found by the same method, to be given below, as the other coefficients.

If the value of $\underline{k}$ is found by a preliminary step, then the solution of the problem entails setting up and solving n + m linear algebraic equations in the n + m desired coefficients a_s and b_r (n + m + 1 equations for an astatic system). These equations can be set up using known principles of function approximation [7].

DESCRIPTION OF THE METHOD

One may present as follows the nub of the method for determining the numerical values for the desired coefficients a_s and b_r: initially, rough values of these coefficients are determined using the method, detailed below, of simple interpolation from the experimental (given) amplitude-phase characteristic, expressed in linear-fractional form (3), and thereafter, if necessary, the approximation to the amplitude-phase characteristic is brought into better correspondence with the experimental curve at intermediate points by improving the coefficients already found by means of least-squared computations.

Method of Interpolation

In the interpolation method given here, the interpolation points are chosen at arbitrary points, not at the intersections of the amplitude-phase characteristic with the axes of the phase plane, as is the case in the method given in [5]. Since the interpolation is performed only as a preliminary step in the determination of the desired coefficients, the choice of interpolation points does not exert much influence on the accuracy of the final result. Still, it is advisable that the chosen points lie within the relevant frequency band.

To find numerical values of the n + m coefficients a_s and b_r it suffices to choose N points on the experimental amplitude-phase characteristic, where $N = \frac{1}{2}(n + m)$ for n + m even, and $N = \frac{1}{2}(n + m + 1)$ for odd n + m.

Starting from the condition

$$W(j\omega) - W_e(j\omega) = 0, \tag{6}$$

where $W_e(j\omega) = U_e(\omega) + jV_e(\omega)$ is the experimental amplitude-phase characteristic, and taking (3) into account, we obtain the following system of equations for the N interpolation points:

$$\frac{u_n(\omega_i) + jv_n(\omega_i)}{u_d(\omega_i) + jv_d(\omega_i)} - U_e(\omega_i) - jV_e(\omega_i) = 0 \quad (i = 1, 2, \ldots, N). \tag{7}$$

After multiplication by the common denominator, and separation of real and imaginary parts, System (7) takes the form:

$$\begin{aligned} u_d(\omega_i)U_e(\omega_i) - v_d(\omega_i)V_e(\omega_i) - u_n(\omega_i) &= 0, \\ u_d(\omega_i)V_e(\omega_i) + v_d(\omega_i)U_e(\omega_i) - v_n(\omega_i) &= 0 \quad (i = 1, 2, \ldots, N). \end{aligned} \tag{8}$$

Equations (8) are linear, and there are 2N = n + m of them, i.e., there are as many equations as there are desired coefficients.* The degree of the equations of System (8) with respect to a_s and b_r may easily be reduced by one. For this, we first eliminate $v_d(\omega_i)$ from the first $\underline{n}$ equations, and then eliminate $u_d(\omega_i)$, obtaining the following two systems of equations:

$$u_d(\omega_i)[U_e^2(\omega_i) + V_e^2(\omega_i)] - v_n(\omega_i)V_e(\omega_i) - u_n(\omega_i)U_e(\omega_i) = 0 \quad (i = 1, 2, \ldots, n), \tag{9}$$

$$v_d(\omega_i)[U_e^2(\omega_i) + V_e^2(\omega_i)] - v_n(\omega_i)U_e(\omega_i) + u_n(\omega_i)V_e(\omega_i) = 0 \quad (i = 1, 2, \ldots, n), \tag{10}$$

the solutions of which give the dependence of the sought quantities, $a_1, a_3, a_5, \ldots$, and also $a_2, a_4, a_6, \ldots$ on the quantities $b_1, b_2, b_3, \ldots$. We then substitute these relationships in the remaining $\underline{m}$ equations of System (8),

* When n + m is an odd number, it is necessary to choose just one of the two equations of System (8) for some one of the chosen points.

obtaining a system of equations with respect to the unknowns $b_1, b_2, b_3, \ldots$, the solutions of which will be the numbers $b_1^0, b_2^0, b_3^0, \ldots$ By means of these, one easily determines the numerical values of $a_1^0, a_2^0, a_3^0, \ldots, a_n^0$.

After the numerical values of the desired coefficients are found, it is possible to construct the computed amplitude-phase characteristic for comparison with the experimental.

To the extent that the method of simple interpolation uses a limited number of interpolation points, coincidence of the experimental and computed amplitude-phase characteristics may be expected only at the chosen points, and significant discrepancies may be expected at the intermediate points.

Therefore, in those cases when the coefficients found by the method of simple interpolation do not provide a sufficiently accurate mirroring of the dynamic properties of the links, it is necessary to change over from the interpolation method to a method for approximating the experimental amplitude-phase characteristic by an expression for this characteristic which corresponds to the given differential equation.

Computed Corrections

To obtain improved coincidence of the experimental, $W_e(j\omega)$, and computed, $W(j\omega)$, amplitude-phase characteristics, not only at the interpolation points but also at intermediate points, it is necessary to add corrections, $\Delta a_1, \Delta a_2, \ldots, \Delta a_n, \Delta b_1, \Delta b_2, \ldots \Delta b_m$, to the numerical values of the coefficients as found by the method of simple interpolation. These corrections are most expeditiously found by the method of least squares [7, 8], i.e., from the condition:

$$\sum_{i=1}^{l} \left| \frac{K(j\omega_i)}{D(j\omega_i)} - W_e(j\omega_i) \right|^2 = \min \quad \left(l > \frac{n+m}{2} \right), \tag{11}$$

where l is comprised, not only of the previously used points of the experimental amplitude-phase characteristic, but also of some intermediate points.

Condition (11) can be put in the following form:

$$\sum_{i=1}^{l} \{[U(\omega_i) - U_e(\omega_i)]^2 + [V(\omega_i) - V_e(\omega_i)]^2\} = \min. \tag{12}$$

If we assume that the desired corrections are small, we can linearize the functions $U(\omega_i)$ and $V(\omega_i)$, expanding them in Taylor series and restricting ourselves to terms of the first power in the quantities $\Delta a_1, \Delta a_2, \ldots, \Delta a_n, \Delta b_1, \Delta b_2, \ldots, \Delta b_m$. Then, instead of Expression (12), we obtain

$$\sum_{i=1}^{l} \left\{ \left[\sum_{r=1}^{m} \left(\frac{\partial U(\omega_i)}{\partial b_r} \right)_0 \Delta b_r + \sum_{s=1}^{n} \left(\frac{\partial U(\omega_i)}{\partial a_s} \right)_0 \Delta a_s - \Delta U(\omega_i) \right]^2 + \right.$$
$$\left. + \left[\sum_{r=1}^{m} \left(\frac{\partial V(\omega_i)}{\partial b_r} \right)_0 \Delta b_r + \sum_{s=1}^{n} \left(\frac{\partial V(\omega_i)}{\partial a_s} \right)_0 \Delta a_s - \Delta V(\omega_i) \right]^2 \right\} = \min, \tag{13}$$

where

$$\Delta U(\omega_i) = U_e(\omega_i) - U_0(\omega_i), \quad \Delta V(\omega_i) = V_e(\omega_i) - V_0(\omega_i),$$

From known rules for minimizing functions, Condition (13) transforms to the system of equations:

$$\sum_{i=1}^{l} \left\{ \left[\sum_{r=1}^{m} \left(\frac{\partial U(\omega_i)}{\partial b_r} \right)_0 \Delta b_r + \sum_{s=1}^{n} \left(\frac{\partial U(\omega_i)}{\partial a_s} \right)_0 \Delta a_s - \Delta U(\omega_i) \right] \left(\frac{\partial U(\omega_i)}{\partial b_g} \right)_0 + \right.$$
$$\left. + \left[\sum_{r=1}^{m} \left(\frac{\partial V(\omega_i)}{\partial b_r} \right)_0 \Delta b_r + \sum_{s=1}^{n} \left(\frac{\partial V(\omega_i)}{\partial a_s} \right)_0 \Delta a_s - \Delta V(\omega_i) \right] \left(\frac{\partial V(\omega_i)}{\partial a_g} \right)_0 \right\} = 0, \tag{14}$$
$$(g = 1, 2, \ldots, m), \quad \text{(cont'd)}$$

$$\sum_{i=1}^{l}\left\{\left[\sum_{r=1}^{m}\left(\frac{\partial U(\omega_i)}{\partial b_r}\right)_0\Delta b_r+\sum_{s=1}^{n}\left(\frac{\partial U(\omega_i)}{\partial a_s}\right)_0\Delta a_s-\Delta U(\omega_i)\right]\left(\frac{\partial U(\omega_i)}{\partial a_h}\right)_0+\right.$$

$$(h=1,2,\ldots,n \qquad (14)$$

$$\left.+\left[\sum_{r=1}^{m}\left(\frac{\partial V(\omega_i)}{\partial b_r}\right)_0\Delta b_r+\sum_{s=1}^{n}\left(\frac{\partial V(\omega_i)}{\partial a_s}\right)_0\Delta a_s-\Delta V(\omega_i)\right]\left(\frac{\partial V(\omega_i)}{\partial a_h}\right)_0\right\}=0.$$

Using the fact that, for example,

$$\frac{\partial W(j\omega_i)}{\partial b_1}=\frac{\partial U(\omega_i)}{\partial b_1}+j\frac{\partial V(\omega_i)}{\partial b_1}, \qquad (15)$$

we may write System (14) in the form

$$\sum_{i=1}^{l}\mathrm{Re}\left\{\left[\sum_{r=1}^{m}\left(\frac{\partial W(j\omega_i)}{\partial b_r}\right)_0\Delta b_r+\sum_{s=1}^{n}\left(\frac{\partial W(j\omega_i)}{\partial a_s}\right)_0\Delta a_s-\Delta W(j\omega_i)\right]\left(\frac{\partial\overline{W}(j\omega_i)}{\partial b_g}\right)_0\right\}=0;$$

$$(g=1,2,\ldots,m),$$

$$\sum_{i=1}^{l}\mathrm{Re}\left\{\left[\sum_{r=1}^{m}\left(\frac{\partial W(j\omega_i)}{\partial b_r}\right)_0\Delta b_r+\sum_{s=1}^{n}\left(\frac{\partial W(j\omega_i)}{\partial a_s}\right)_0\Delta a_s-\Delta W(j\omega_i)\right]\left(\frac{\partial\overline{W}(j\omega_i)}{\partial a_h}\right)_0\right\}=0. \qquad (16)$$

$$(h=1,2,\ldots,n).$$

Making use of (3), we find

$$\left(\frac{\partial W(j\omega_i)}{\partial b_r}\right)_0=\frac{(j\omega_i)^r}{D_0(j\omega_i)}=B_0(\omega_i)\,e^{j\varphi_0(\omega_i)}(j\omega_i)^r,$$

$$\left(\frac{\partial W(j\omega_i)}{\partial a_s}\right)_0=-\frac{K_0(j\omega_i)}{[D_0(j\omega_i)]^2}(j\omega_i)^s=A_0(\omega_i)\,e^{j\alpha_0(\omega_i)}\,(j\omega_i)^s. \qquad (17)$$

We substitute the values of the derivatives from (17) in the system of Equations (16), and also represent $\Delta W(j\omega_1)$ in the form

$$\Delta W(j\omega_i)=C_0(\omega_i)\,e^{j\beta_0(\omega_i)},$$

obtaining

$$\sum_{i=1}^{l}\mathrm{Re}\left\{\left[B_0(\omega_i)\,e^{j\varphi_0(\omega_i)}\sum_{r=1}^{m}(j\omega_i)^r\Delta b_r+A_0(\omega_i)\,e^{j\alpha_0(\omega_i)}\sum_{s=1}^{n}(j\omega_i)^s\Delta a_s-\right.\right.$$

$$\left.\left.-C_0(\omega_i)\,e^{j\beta_0(\omega_i)}\right]B_0(\omega_i)\,e^{-j\varphi_0(\omega_i)}(-j\omega_i)^g\right\}=0 \qquad (g=1,2,\ldots,m), \qquad (18)$$

$$\sum_{i=1}^{l}\mathrm{Re}\left\{\left[B_0(\omega_i)\,e^{j\varphi_0(\omega_i)}\sum_{r=1}^{m}(j\omega_i)^r\Delta b_r+A_0(\omega_i)\,e^{j\alpha_0(\omega_i)}\sum_{s=1}^{n}(j\omega_i)^s\Delta a_s-\right.\right.$$

$$\left.\left.-C_0(\omega_i)\,e^{j\beta_0(\omega_i)}\right]A_0(\omega_i)\,e^{-j\alpha_0(\omega_i)}(-j\omega_i)^h\right\}=0 \qquad (h=1,2,\ldots,n).$$

We multiply out the parentheses and brackets and, for simplicity of writing, we omit the notation for the ranges of summation and for the indices of the coefficients, finally obtaining the system of n + m normal equations in the desired corrections:

$$\sum B^2\omega^2\Delta b_1 - \sum B^2\omega^4\Delta b_3 + \sum B^2\omega^6\Delta b_5 - \cdots + \sum AB\cos(\alpha-\varphi)\,\omega^2\Delta a_1 -$$
$$-\sum AB\sin(\alpha-\varphi)\,\omega^3\Delta a_2 - \sum AB\cos(\alpha-\varphi)\,\omega^4\Delta a_3 + \sum AB\sin(\alpha-\varphi)\,\omega^5\Delta a_4 +$$
$$+\sum AB\cos(\alpha-\varphi)\,\omega^6\Delta a_5 - \cdots = \sum CB\sin(\beta-\varphi)\,\omega,$$
$$\sum B^2\omega^4\Delta b_2 - \sum B^2\omega^6\Delta b_4 + \sum B^2\omega^8\Delta b_6 - \cdots + \sum AB\sin(\alpha-\varphi)\,\omega^3\Delta a_1 +$$
$$+\sum AB\cos(\alpha-\varphi)\,\omega^4\Delta a_2 - \sum AB\sin(\alpha-\varphi)\,\omega^5\Delta a_3 - \sum AB\cos(\alpha-\varphi)\,\omega^6\Delta a_4 +$$
$$+\sum AB\sin(\alpha-\varphi)\,\omega^7\Delta a_5 + \cdots = -\sum CB\cos(\beta-\varphi)\,\omega^2,$$
$$-\sum B^2\omega^4\Delta b_1 + \sum B^2\omega^6\Delta b_3 - \sum B^2\omega^8\Delta b_5 + \cdots - \sum AB\cos(\alpha-\varphi)\,\omega^4\Delta a_1 +$$
$$+\sum AB\sin(\alpha-\varphi)\,\omega^5\Delta a_2 + \sum AB\cos(\alpha-\varphi)\,\omega^6\Delta a_3 - \sum AB\sin(\alpha-\varphi)\,\omega^7\Delta a_4 -$$
$$-\sum AB\cos(\alpha-\varphi)\,\omega^8\Delta a_5 + \cdots = -\sum CB\sin(\beta-\varphi)\,\omega^3,$$
$$-\sum B^2\omega^6\Delta b_2 + \sum B^2\omega^8\Delta b_4 - \sum B^2\omega^{10}\Delta b_6 + \cdots - \sum AB\sin(\alpha-\varphi)\,\omega^5\Delta a_1 -$$
$$-\sum AB\cos(\alpha-\varphi)\,\omega^6\Delta a_2 + \sum AB\sin(\alpha-\varphi)\,\omega^7\Delta a_3 + \sum AB\cos(\alpha-\varphi)\,\omega^8\Delta a_4 -$$
$$-\sum AB\sin(\alpha-\varphi)\,\omega^9\Delta a_5 - \cdots = \sum CB\cos(\beta-\varphi)\,\omega^4,$$
$$\sum B^2\omega^6\Delta b_1 - \sum B^2\omega^8\Delta b_3 + \sum B^2\omega^{10}\Delta b_5 - \cdots + \sum AB\cos(\alpha-\varphi)\,\omega^6\Delta a_1 -$$
$$-\sum AB\sin(\alpha-\varphi)\,\omega^7\Delta a_2 - \sum AB\cos(\alpha-\varphi)\,\omega^8\Delta a_3 + \sum AB\sin(\alpha-\varphi)\,\omega^9\Delta a_4 +$$
$$+\sum AB\cos(\alpha-\varphi)\,\omega^{10}\Delta a_5 - \cdots = \sum CB\sin(\beta-\varphi)\,\omega^5,$$
$$\cdots\cdots\cdots\cdots\cdots\cdots\cdots\cdots\cdots\cdots\cdots\cdots\cdots\cdots\cdots\cdots \qquad (19)$$
$$\sum AB\cos(\alpha-\varphi)\,\omega^2\Delta b_1 + \sum AB\sin(\alpha-\varphi)\,\omega^3\Delta b_2 - \sum AB\cos(\alpha-\varphi)\,\omega^4\Delta b_3 -$$
$$-\sum AB\sin(\alpha-\varphi)\,\omega^5\Delta b_4 + \sum AB\cos(\alpha-\varphi)\,\omega^6\Delta b_5 + \cdots + \sum A^2\omega^2\Delta a_1 -$$
$$-\sum A^2\omega^4\Delta a_3 + \sum A^2\omega^6\Delta a_5 - \cdots = \sum CA\sin(\beta-\alpha)\,\omega,$$
$$-\sum AB\sin(\alpha-\varphi)\,\omega^3\Delta b_1 + \sum AB\cos(\alpha-\varphi)\,\omega^4\Delta b_2 + \sum AB\sin(\alpha-\varphi)\,\omega^5\Delta b_3 -$$
$$-\sum AB\cos(\alpha-\varphi)\,\omega^6\Delta b_4 - \sum AB\sin(\alpha-\varphi)\,\omega^7\Delta b_5 + \cdots + \sum A^2\omega^4\Delta a_2 -$$
$$-\sum A^2\omega^6\Delta a_4 + \sum A^2\omega^8\Delta a_6 - \cdots = -\sum CA\cos(\beta-\alpha)\,\omega^2,$$
$$-\sum AB\cos(\alpha-\varphi)\,\omega^4\Delta b_1 - \sum AB\sin(\alpha-\varphi)\,\omega^5\Delta b_2 + \sum AB\cos(\alpha-\varphi)\,\omega^6\Delta b_3 +$$
$$+\sum AB\sin(\alpha-\varphi)\,\omega^7\Delta b_4 - \sum AB\cos(\alpha-\varphi)\,\omega^8\Delta b_5 - \cdots - \sum A^2\omega^4\Delta a_1 +$$
$$+\sum A^2\omega^6\Delta a_3 - \sum A^2\omega^8\Delta a_5 + \cdots = -\sum CA\sin(\beta-\alpha)\,\omega^3,$$
$$\sum AB\sin(\alpha-\varphi)\,\omega^5\Delta b_1 - \sum AB\cos(\alpha-\varphi)\,\omega^6\Delta b_2 - \sum AB\sin(\alpha-\varphi)\,\omega^7\Delta b_3 +$$
$$+\sum AB\cos(\alpha-\varphi)\,\omega^8\Delta b_4 + \sum AB\sin(\alpha-\varphi)\,\omega^9\Delta b_5 - \cdots - \sum A^2\omega^6\Delta a_2 +$$
$$+\sum A^2\omega^8\Delta a_4 - \sum A^2\omega^{10}\Delta a_6 + \cdots = \sum CA\cos(\beta-\alpha)\,\omega^4,$$
$$\sum AB\cos(\alpha-\varphi)\,\omega^6\Delta b_1 + \sum AB\sin(\alpha-\varphi)\,\omega^7\Delta b_2 - \sum AB\cos(\alpha-\varphi)\,\omega^8\Delta b_3 -$$
$$-\sum AB\sin(\alpha-\varphi)\,\omega^9\Delta b_4 + \sum AB\cos(\alpha-\varphi)\,\omega^{10}\Delta b_5 + \cdots + \sum A^2\omega^6\Delta a_1 -$$
$$-\sum A^2\omega^8\Delta a_3 + \sum A^2\omega^{10}\Delta a_5 - \cdots = \sum CA\sin(\beta-\alpha)\,\omega^5,$$
$$\cdots\cdots\cdots\cdots\cdots\cdots\cdots\cdots\cdots\cdots\cdots\cdots\cdots\cdots\cdots\cdots$$

Insofar as System (19) was set up on the basis of certain assumptions, since the functions $U(\omega_i)$ and $V(\omega_i)$ were linearized in order to obtain (19) from (12), the process of finding the corrections (if required by accuracy conditions on the coefficients of the differential equation) may be repeated, taking into account the corrections already found.

Computation of the coefficients of the equations in System (19) by means of a slide rule [9] is quite simply accomplished.

To render clearer the manner in which the method presented here is applied in practice, and also to evaluate the results thereby obtained, examples are given in the Appendix of the evaluation of the coefficients of the differential equations for certain links in systems, the transfer functions for which are so constituted that the interpolation method expounded in [5] is inapplicable.

SUMMARY

The method presented here for determining the parameters of linear links and automatic control systems from the experimental amplitude-phase characteristic appears more universal, and more accurate, in comparison with other methods of solving this problem.

As is clear from the examples given in the Appendix, in those cases when the desired parameters are determined with sufficient accuracy using simple interpolation from the experimental amplitude-phase characteristic, the interpolation method expounded in this article is preferable to the method given in [5]: the method proposed here allows solutions to be found for a broader class of approximating transfer functions and, moreover, does so without significantly complicating the necessary computation.

A significant increase in the amount of computational work is required only in those cases in which the accuracy conditions on the approximate function require that corrections be computed for the desired coefficients. However, even this work, in the majority of cases, does not introduce significant toil if the computing scheme given in this article is employed.

In the simplest cases,* the method given here may be inferior to other methods by virtue of the amount of computational work required.

The method may prove to be useful for verifying the admissibility of simplifications of the equations for objects and elements of automatic control systems, and for determining the equations and parameters of automatic control systems from their given dynamic characteristics.

APPENDIX

Example 1

We find the coefficients of the differential equation of a link consisting of electronic and electromagnetic amplifiers (EA-EMA), using an oscillographic determination of the transient response (curve a on Fig. 1).

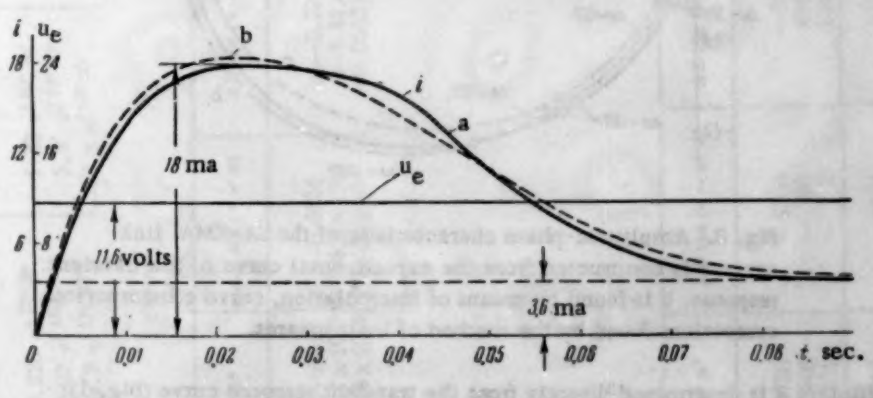

Fig. 1. Transient response of the EA-EMA link: a) is the experimental curve, b) is the computed curve.

The circuit diagram is given in Fig. 2.*

*The tests were carried out on an actual paper-board-making machine of the Zhidachevski paper-board combine.

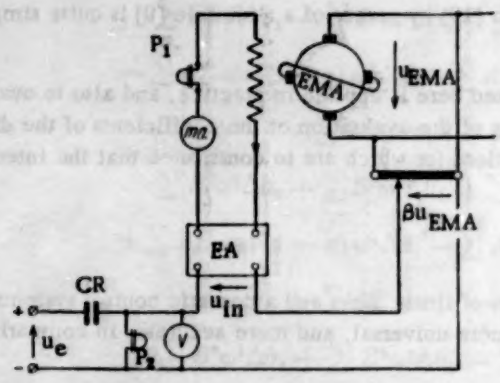

Fig. 2. EMA is the electromagnetic amplifier, EA is the electronic amplifier, CR are contacts of a relay, P_1 and P_2 are oscillograph pickups, ma is a milliammeter.

The differential equation for the link under consideration has the form

$$\left(\frac{T_d T_q}{1+\beta k_{EA} k_{EMA}} p^2 + \frac{T_d + T_q}{1+\beta k_{EA} k_{EMA}} p + 1\right) i = (T_q p + 1) \frac{k_{EA}}{1+\beta k_{EA} k_{EMA}} u_e$$

where T_d is the time constant of the longitudinal circuit of EMA, T_q is the time constant of the transverse circuit of EMA, β is the feedback rigidity coefficient, k_{EA} is the transfer coefficient of the electronic amplifier (equal, in the steady state, to i/u_e), k_{EMA} is the transfer coefficient of the electromagnetic amplifier (equal, in the steady state, to u_{EMA}/i).

The approximating differential equation has the form:

$$(a_2 p^2 + a_1 p + 1)\, i = (b_1 p + k)\, u_e.$$

Such a structure for the equation accords completely with the character of the amplitude-phase characteristic, constructed from the experimental curve of the transient response (Fig. 3, curve a).

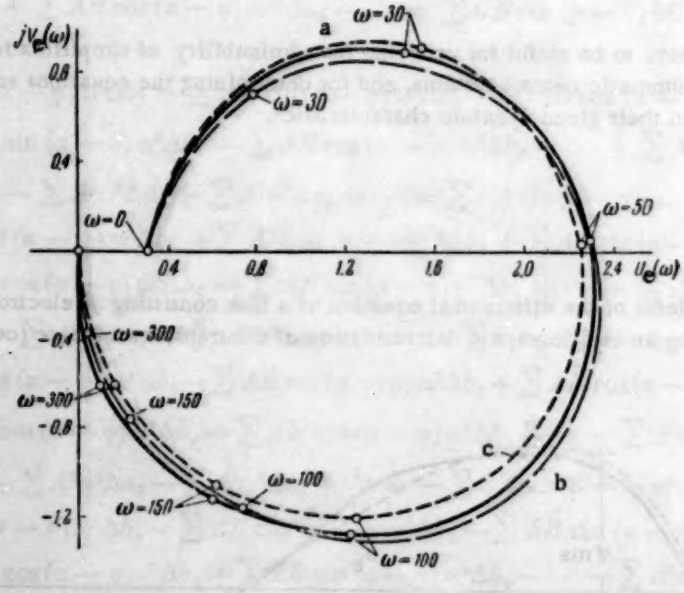

Fig. 3. Amplitude-phase characteristic of the EA-EMA link: curve a is constructed from the experimental curve of the transient response, b is found by means of interpolation, curve c incorporates corrections found by the method of least squares.

The coefficient k is determined directly from the transient response curve (Fig. 1):

$$k = \frac{i(\infty)}{u_e} = 0.31 \text{ ma/volt}.$$

TABLE 1

No. of point	D	K	$\frac{1}{D}$	$-\frac{K}{D^3}$	$\frac{K}{D}$	ΔW	B^2
1	$0.820\ e^{i\ 79°\ 20'}$	$1.83\ e^{i\ 80°\ 15'}$	$1.22\ e^{-i\ 79°\ 20'}$	$2.72\ e^{i\ 101°\ 35'}$	$2.23\ e^{i\ 0°\ 55'}$	0	1,49
2	$7.07\ e^{i\ 160°}$	$5.40\ e^{i\ 86°\ 50'}$	$0.141\ e^{-i\ 160°}$	$0.108\ e^{-i\ 53°\ 10'}$	$0.764\ e^{-i\ 73°\ 10'}$	$0.535\ e^{-i\ 46°\ 40'}$	19.9×10^{-3}
3	$29.9\ e^{i\ 170°\ 42'}$	$10.8\ e^{i\ 88°\ 25'}$	$0.0334\ e^{-i\ 170°42'}$	$0.0121\ e^{-i\ 170°42'}$	$0.361\ e^{-i\ 82°\ 17'}$	$0.261\ e^{-i\ 81°\ 30'}$	1.12×10^{-3}

No. of point	A^2	$AB\sin(\alpha-\varphi)$	$AB\cos(\alpha-\varphi)$	$CB\sin(\beta-\varphi)$	$CA\sin(\beta-\alpha)$	$CA\cos(\beta-\alpha)$	ω	ω^2	ω^3	ω^4
1	7.40	−0.0531	−3.32	0	0	0	50	25×10^2	125×10^3	625×10^4
2	11.7×10^{-3}	14.6×10^{-3}	-4.41×10^{-3}	69.3×10^{-3}	6.54×10^{-3}	57.4×10^{-3}	150	225×10^2	3380×10^3	50600×10^4
3	0.146×10^{-3}	0.401×10^{-3}	-0.0542×10^{-3}	8.72×10^{-3}	0.466×10^{-3}	3.12×10^{-3}	300	9×10^4	27×10^6	81×10^8

TABLE 2

No. of point	$B^2\omega^2$	$AB\cos(\alpha-\varphi)\omega^2$	$AB\sin(\alpha-\varphi)\omega^2$	$A^2\omega^2$	$A^2\omega^4$	$CB\sin(\beta-\varphi)\omega$	$CA\sin(\beta-\alpha)\omega$	$CA\cos(\beta-\alpha)\omega^2$
1	3730	−8300	−6650	18500	4620×10^4	0	0	0
2	448	− 99	49400	260	592×10^4	10.4	0.98	1290
3	101	− 5	10800	10	118×10^4	2.62	−0.14	281
Σ	4279	−8404	53550	18770	5330×10^4	13,02	0.84	1571

To determine the remaining coefficients of the differential equation, we choose two points on the amplitude-phase characteristic, $\omega = 50$ and $\omega = 300$, and set up, in accord with (9) and (10), the system of equations:

$$(1 - 25\times10^2 a_2)\,5.30 = 0.0535\times50\,b_1 + 2.30\times0.31,$$

$$5.30\times50\,a_1 = 2.30\times50\,b_1 - 0.0535\times0.31,$$

$$(1 - 9\times10^4 a_2)\,0.087 + 0.616\times300\,a_1 - 0.31 = 0.$$

Solving the given system, we get: $a_2^0 = 0.000339$, $a_1^0 = 0.0161$, $b_1^0 = 0.036$.

The amplitude-phase characteristic corresponding to these coefficients is shown on Fig. 3 (curve b).

In order to obtain a better correspondence between the experimental and computed amplitude-phase characteristics at points with equal ω, it is necessary to determine corrections Δa_2, Δa_1 and Δb_1. For this, we choose three points on the experimental amplitude-phase characteristic: $\omega = 50$, $\omega = 150$ and $\omega = 300$. The computations which follow, using (19), are given in Tables 1 and 2.

The system of normal equations is set up from the data of Tables 1 and 2:

$$4280\,\Delta b_1 - 8400\,\Delta a_1 - 53{,}600\,\Delta a_2 = 13, \quad -8400\,\Delta b_1 + 18{,}800\,\Delta a_1 = 0.84,$$

$$-53{,}600\,\Delta b_1 + 5330\times10^4\,\Delta a_2 = -1570.$$

Solving this system, we find that $\Delta a_2 = -0.000004$, $\Delta a_1 = 0.0113$ and $\Delta b_1 = 0.0254$.

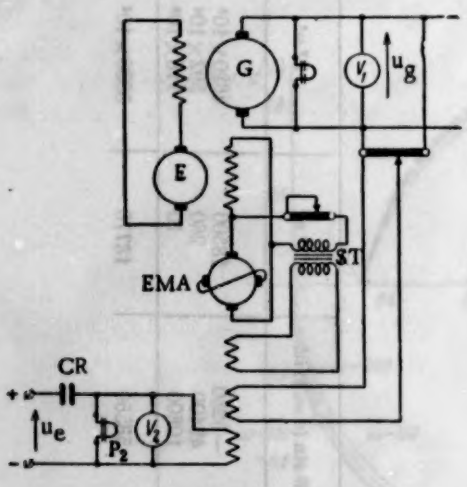

Fig. 4. G is the generator, E is the exciter, EMA is the electromagnetic amplifier, ST is the stabilizing transformer, CR are relay contacts, P_1 and P_2 are oscillograph pickups, V_1 and V_2 are voltmeters.

Carrying out a second approximating procedure, taking into account the corrections already found, we obtain $\Delta a_2' = 0.672 \times 10^{-5}$, $\Delta a_1' = 0.294 \times 10^{-3}$ and $\Delta b_1' = 0.206 \times 10^{-2}$. Hence, the desired coefficients of the differential equation are: $a_2 = 0.000342$, $a_1 = 0.0277$ and $b_1 = 0.0635$. The differential equation itself takes the form:

$$(0.000342\,p^2 + 0.0277\,p + 1)\,i = (0.0635 + 0.31)\,u_e.$$

The solution of this for a step-function excitation, $u_e = 11.6$ volts, will be

$$i = 3.6 + 56\,e^{-40.5t}\cos(35.9\,t + 1.64).$$

The corresponding amplitude-phase characteristic and transient response curve are shown on Fig. 3 (curve c) and Fig. 1 (curve b).

Since the corrections found during the second approximation procedure are significantly less (in absolute magnitude) than the coefficients of the differential equation found by the interpolation method, and also less than the corrections found in the first approximation procedure, it might not have been necessary to find them.

From the coefficients of the differential equation thus found, it is easy to determine the individual parameters of the EA-EMA link.

To do this, we set up the system of equations:

$$\frac{T_d T_q}{1+\beta k_{EA} k_{EMA}} = 0.000342, \quad \frac{T_d + T_q}{1+\beta k_{EA} k_{EMA}} = 0.0277,$$

$$\frac{T_q k_{EA}}{1+\beta k_{EA} k_{EMA}} = 0.0635, \quad \frac{k_{EA}}{1+\beta k_{EA} k_{EMA}} = 0.31,$$

the solution of which is* $T_d = 0.0131$ sec., $T_q = 0.205$ sec., $k_{EA} = 2.44$ ma/volt, $k_{EMA} = 15.5$ volts/ma.

Example 2

We consider a system for automatic control of a voltage generator, the system circuit being given in Fig. 4.

We will determine the coefficients of the differential equation for this system by means of the transient response curve (Fig. 5, curve a) taken off by oscillograph.

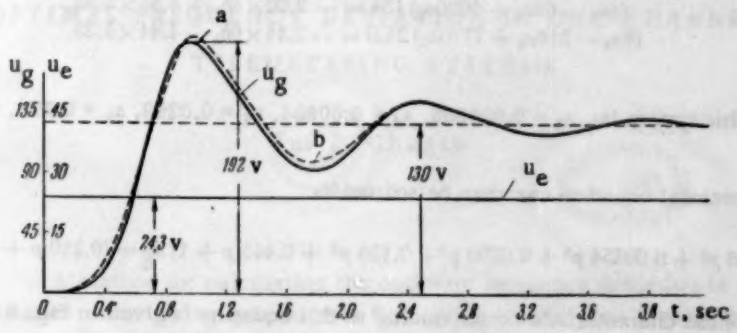

Fig. 5. Transient response in system for automatic control of a voltage generator: a is the experimental curve, b is the computed curve.

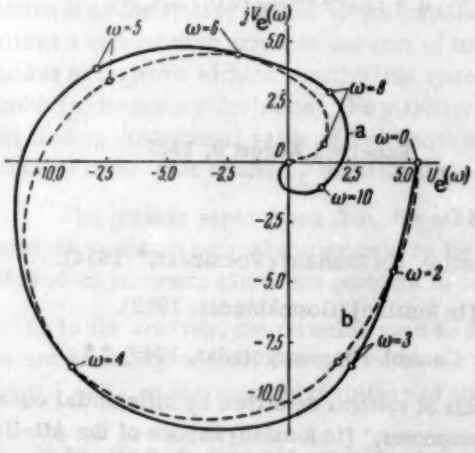

Fig. 6. Amplitude-phase characteristic of the system for automatic control of a voltage generator: a is the transient response curve constructed from empirical data, b is the curve found by interpolation.

The generator G and the exciter E may be considered as aperiodic first-order links, the electromagnetic amplifier as an aperiodic second-order link, and the stabilizing transformer ST may be characterized by a transfer function of the form

$$\frac{T_1 p}{T_2 p + 1}.$$

We consider the differential equation of the system

$$(a_5 p^5 + a_4 p^4 + a_3 p^3 + a_2 p^2 + a_1 p + 1) u_g = (b_1 p + k) u_e, \qquad (A)$$

The term $b_1 p$ on the right side of the equation stems from the presence of the stabilizing transformer in the system.

From the character of the amplitude-phase characteristic, constructed from the empirical curve of the transient response (Fig. 6, curve a), it follows from (1) that, for the given right member, the left side of Equation (A) must be, not fifth-order, but sixth-order. Since the coordinate values of the amplitude-phase characteristic are relatively small in absolute value in the fifth and sixth quadrants, the system may be described with sufficient accuracy by differential Equation (A).

The gain coefficient k is determined from the transient response curve:

$$k = \frac{u_{g(\infty)}}{u_e} = 5.35.$$

*The feedback rigidity coefficient, $\beta = 0.182$, was previously found experimentally.

To determine the remaining coefficients of the differential equation, we choose three points, $\omega = 2$, $\omega = 4$ and $\omega = 6$, on the experimental amplitude-phase characteristic, and set up the following system of equations, making use of (9) and (10):

$$(1 - 4a_2 + 16a_4)\,39{,}2 = -4.55\times 2b_1 + 4{,}30\times 5.35,$$
$$(1 - 16a_2 + 256a_4)\,154 = -8.55\times 4b_1 - 9{,}00\times 5.35,$$
$$(1 - 360a_2 + 1300a_4)\,24.0 = 4.411\times 6b_1 - 2.11\times 5.35,$$
$$(2a_1 - 8a_3 + 32a_5)\,39.2 = 4.30\times 2b_1 + 4.55\times 5.35,$$
$$(4a_1 - 64a_3 + 1020a_5)\,154 = -9{,}00\times 4b_1 + 8.55\times 5.35,$$
$$(6a_1 - 216a_3 + 7770a_5)\,24.0 = -2.11\times 6b_1 - 4.41\times 5.35.$$

The solution of this system is: $a_5 = 0.000336$, $a_4 = 0.00254$, $a_3 = 0.0293$, $a_2 = 0.126$, $a_1 = 0.445$ and $b_1 = 0.210$.

The desired differential equation can then be written as

$$(0.000336\,p^5 + 0.00254\,p^4 + 0.0293\,p^3 + 0.126\,p^2 + 0.445\,p + 1)\,u_g = (0{,}210\,p + 5.35)\,u_e. \qquad (B)$$

The amplitude-phase characteristic corresponding to this equation is given in Fig. 6 (curve b).

Since there is satisfactory correspondence between the experimental and computed amplitude-phase characteristics, it is not necessary to carry out the computation of the corrections.

Integrating Equation (B) with a step-function excitation, $u_e = 24.3$ volts, we get the equation for the transient response

$$u_g = 5.35 - 3.31\,e^{-3.35\,t} + 5.70\,e^{-0.836\,t}\cos(4.07\,t - 4.31) + 1.16\,e^{-1.27t}\cos(7.07t - 1.37),$$

which is constructed on Fig. 5 (curve b).

Received August 9, 1957

LITERATURE CITED

[1] A. A. Voronov, Elements of the Theory of Automatic Control [in Russian] (Voenizdat,* 1954).

[2] M. A. Aizerman, Theory of Automatic Motor Control [in Russian] (Gostekhizdat, 1952).

[3] R. Oldenburger and G. Sartorius, Dynamics of Automatic Control (Gosenergoizdat, 1949).**

[4] Ia. Z. Tsypkin, "Determination of the dynamic parameters of systems described by differential equations of no higher than second order, from oscillograms of the transient responses," [in Russian] Reports of the All-Union Correspondence Institute of Power Engineering (extracted in 6 Elektrotekhnika, 1955).

[5] G. L. Rabkin, B. A. Mitrofanov and Iu. O. Shterenberg, "On the determination of the numerical value of transfer function coefficients for linearized links and systems from the experimental frequency characteristics," Automation and Remote Control (USSR) 16, 5 (1955).

[6] M. P. Simoiu, "Determination of the coefficients of the transfer functions of linearized links and automatic control systems," Automation and Remote Control (USSR) 18, 6 (1957).***

[7] V. L. Goncharov, Theory of Interpolation and Function Approximation [in Russian] (Gostekhizdat, 1954).

[8] A. N. Krylov, Lectures on Approximate Calculations, [in Russian] (Gostekhteoretizdat, 1954).

[9] F. A. Reznikov, "Operations with complex numbers by means of slide rules," Elektrichestvo 4 (1956).

* Military Publishing House.
** Russian translation.
*** See English translation.

OPTIMAL FREQUENCY DEVIATION IN ONE-CHANNEL TELEMETERING SYSTEMS

Iu. I. Chugin

(Moscow)

A method for calculating the optimum frequency deviation in one-channel telemetering systems with fluctuating interference is presented, based on analysis of the noise energy spectrum.

1. Introduction

One of the principal indications of the quality of a telemetering system is its accuracy of measurement. Errors in the transmission of information may arise either due to instability of coefficients in the transmitting element of the system or due to the influence of noise. It is well known that the use of frequency modulation allows a reduction in errors at the cost of increasing receiver band-width. However it is impossible by such means to improve without limiting the system's stability under noise or interference. At a certain value of band-width (or frequency deviation), the stability under interference deteriorates. Until now, no theoretic means existed for finding the optimal value of the frequency deviation as a function of the parameters of the signal and of the channel noise, thus rendering difficult the computation and construction of such systems.

The present paper shows that, for telemetering systems with idealized characteristics of the receiver, it is possible to obtain an analytic expression for the magnitude of the optimal deviation. The methods of the theory of random processes allow this problem to be solved.

In the analysis, the criterion used to measure the interference stability of a telemetering system is the mean-square error engendered, determined by the ratio of the effective noise voltage at the receiver output, in the band from 0 to F_f, to the maximum voltage of the output signal.

2. Frequency Spectrum at the Frequency Receiver's Output

We consider the receiving devices of a frequency receiver (Fig. 1), consisting of an input filter Φ_1 which passes the band $f_0 \pm \Delta f$, limiter 1, frequency discriminator 2 and ideal output filter Φ_2 for the receiving band from 0 to F_f, i. e., the receiver consists of two linear systems (filters Φ_1 and Φ_2) and two nonlinear ones (limiter and discriminator). Ordinarily, for telemetering systems, $F_f \ll \pm \Delta f$.

It will be assumed that the nonlinear systems possess no inertia, that the amplitude limiter is ideal, and the frequency discriminator is such that its output voltage is directly proportional to the deviation of the frequency from the central value, ω_0:

$$u_{out} = (\omega - \omega_0). \tag{1}$$

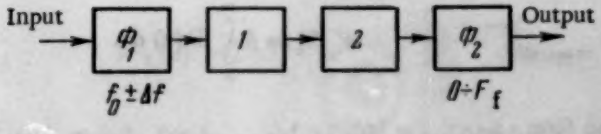

Fig. 1. Block schematic of the frequency receiver.

In order to determine the error at the receiver output, it is necessary to find the noise power in the band 0 to F_f of the output filter, for which, in turn, it is necessary to know the energy spectrum of the noise at the output of the frequency discriminator. The energy spectrum can be obtained from the Fourier transform of the auto-correlation function of the discriminator output voltage.

In [1, 2] were obtained general expressions for the correlation function at the putput of the discriminator when the elements of the receiving devices had the characteristics given above, and when the signal frequency $\omega_s = \omega_0$.

If the frequency characteristic $C(\omega)$ of the filter input is Gaussian,

$$C(\omega) = C_0 \exp\left[-\frac{\pi}{2}\frac{(\omega-\omega_0)^2}{(2\Delta\omega)^2}\right], \tag{2}$$

where $\Delta\omega = 2\pi\Delta f$ and $2\Delta f$ is the receiver band-width, the expression for the correlation function for the noise $B(\tau)$ may be written in the following way [2]:

$$B(\tau) = B_1(\tau) + B_2(\tau). \tag{3}$$

Here,

$$B_1(\tau) = \alpha\left[2\alpha\tau^2 + e^{-\frac{z}{\rho}}\left(1 - 2\alpha\tau^2\frac{z}{\rho}\right)E_i\left(\frac{z}{\rho}\right)\right], \tag{4}$$

$$B_2(\tau) = \alpha\left\{2\alpha\tau^2\left(-\frac{2e^{-z}}{1-\rho} + \frac{1+\rho}{1-\rho}e^{-\frac{2z}{1+\rho}}\right) + e^{-\frac{z}{\rho}}\left(1 - 2\alpha\tau^2\frac{z}{\rho}\right)\left[E_i\left(\frac{1-\rho}{1+\rho}\frac{z}{\rho}\right) - 2E_i\left(\frac{1-\rho}{\rho}z\right)\right]\right\}, \tag{5}$$

$z = (U_s/U_n)^2$ is the ratio of signal power to mean noise power at the output of filter Φ_1 (at the limiter's input), ρ is the correlation coefficient of the noise at the output of filter Φ_1, $E_i(x)$ is the integral exponential function (tabulated in [3]), $\rho = \rho(\tau) = e^{-\alpha\tau^2}$, $\alpha = \pi(2\Delta f)^2$.

The energy spectrum of the noise, W(f), is determined from the well-known relationship

$$W(f) = 4\int_0^\infty B(\tau)\cos 2\pi f\tau d\tau. \tag{6}$$

Figure 2 gives the curves for the noise energy spectrum at the discriminator output for Gaussian frequency characteristic of the filters and with $\omega_s = \omega_0$ [2, 4]. The spectrum was computed from Formula (6) using numerical integration. With a deviation of the frequency ($\omega_s \neq \omega_0$), the intensity of the noise energy spectrum, in the region $f/\Delta f < 1$ is lowered [5], and the interference stability of the system increases. Below we shall investigate the worst case, when $\omega_s = \omega_0$. For telemetering systems where $F_f \ll \Delta f$ one can obtain analytic expressions for the noise energy spectrum and power at the receiver output. Figure 2,b shows an enlarged view of the curve of the spectrum W(f) for $z = 5$. It is clear from the figure that for $z = 5$ (and $z > 5$), the spectrum, determined by Formula (6), is conveniently represented in the form

$$W(f) = W(0) + W(f)^*, \tag{7}$$

where

$$W(0) = 4\int_0^\infty B(\tau)\,d\tau.$$

We write (6) in the form

$$W(f) = W_1(f) + W_2(f), \tag{8}$$

where

$$W_1(f) = W_1(0) + W_1(f)^* = 4\int_0^\infty B_1(\tau)\cos 2\pi f\tau d\tau, \tag{9}$$

$$W_2(f) = W_2(0) + W_2(f)^* = 4\int_0^\infty B_2(\tau)\cos 2\pi f\tau d\tau. \tag{10}$$

Then,

$$W(0) = W_1(0) + W_2(0), \quad W(f)^* = W_1(f)^* + W_2(f)^*. \tag{11}$$

Determining the spectrum $W_1(f)$ from Formula (9), we obtain for $z \geq 5$ (Cf. Appendix I)

$$W_1(f) = \frac{2\pi^3\Delta f}{z}\left(\frac{f}{\Delta f}\right)^2 \sum_{n=1}^{3} \frac{(n-1)!}{\sqrt{n}\, z^{n-1}} \exp\left[-\frac{1}{n}\frac{\pi}{4}\left(\frac{f}{\Delta f}\right)^2\right]. \tag{12}$$

It is obvious from (12) that $W_1(0) = 0$; hence $W(0) = W_2(0)$.

Comparing the two spectra from (11), $W_1(f)^*$ and $W_2(f)^*$, one may show that $W_2(f)^* \ll W_1(f)^*$. To find these spectra, we multiply the functions $B_1(\tau)$ and $B_2(\tau)$ by $(\cos 2\pi f\tau - 1)$, and integrate the resulting expressions. For function $B_2(\tau)$, only numerical integration is possible. The computations confirm that the spectrum obtained from function $B_1(\tau)$ has significantly greater intensity than that obtained from $B_2(\tau)$. Consideration of Fig. 3 leads to the same conclusion, the figure showing the curves for $B_1(\tau)$ and $B_2(\tau)$ constructed with different scales along the y axis. The ratio of the scales equal e^z/z, and becomes huge for $z \geq 5$. Therefore, the integral of function $B_1(\tau)$ will be much larger than the integral of $B_2(\tau)$, i.e.,

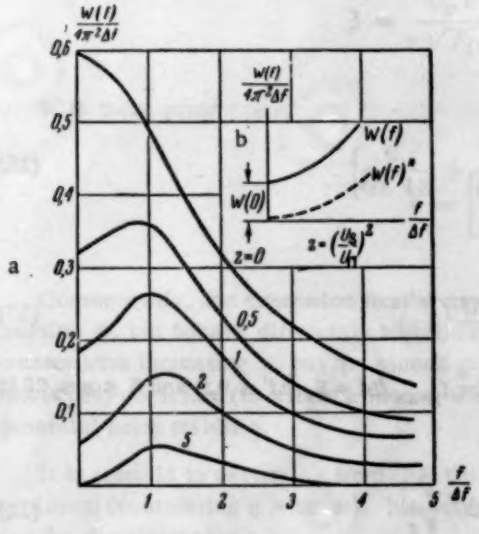

Fig. 2.

$$W(f)^* = W_1(f)^* + W_2(f)^* \approx W_1(f)^*. \tag{13}$$

Since $W_1(0) = 0$, $W_1(f)^* = W_1(f)$, and the spectrum of (7) becomes equal to

$$W(f) = W_2(0) + W_1(f),$$

where $W_1(f)$ is determined from Formula (12).

The analytic expression for the spectrum

$$W_2(0) = 4\int_0^\infty B_2(\tau)\, d\tau \tag{14}$$

for $5 \leq z \leq 0$, has the form (Cf. Appendix II):

$$W_2(0) = 29\Delta f \frac{e^{-z}}{\sqrt{z}}. \tag{15}$$

For telemetering systems, $F_f/\Delta f \leq 0.2$. For $f_{max}/\Delta f = F_f/\Delta f \leq 0.2$ and $n \geq 1$

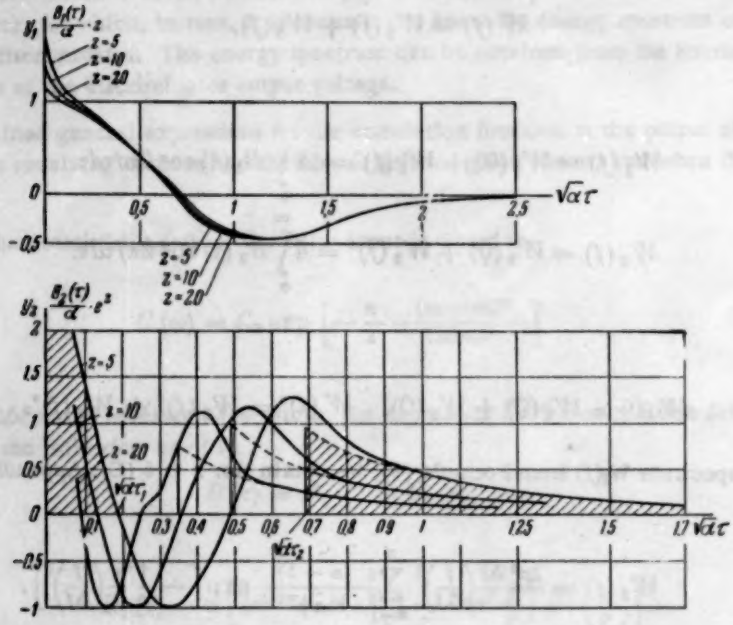

Fig. 3. Correlation functions $B_1(\tau)$ and $B_2(\tau)$ at the discriminator output.

$$\exp\left[-\frac{\pi}{4n}\left(\frac{f_{max}}{\Delta f}\right)^2\right] \approx 1,$$

and in the range $0 \leq f \leq f_{max}$. Formula (12) takes the form:

$$W_1(f) = \frac{2\pi^2\Delta f}{z}\left(\frac{f}{\Delta f}\right)^2\left\{1 + \frac{1}{2\sqrt{2}z} + \frac{2}{3\sqrt{3}z^2}\right\}. \tag{16}$$

For $z \geq 5$

$$W_1(f) \approx \frac{2\pi^2\Delta f}{z}\left(\frac{f}{\Delta f}\right)^2 = \frac{19.74\Delta f}{z}\left(\frac{f}{\Delta f}\right)^2. \tag{17}$$

The total noise energy spectrum at the discriminator output for $f_{max}/\Delta f = F_f/\Delta f \leq 0.2$ and $5 \leq z \leq 20$ is, according to (17) and (15),

$$W(f) = \frac{19.74\,\Delta f}{z}\left(\frac{f}{\Delta f}\right)^2 + 29\Delta f\,\frac{e^{-z}}{\sqrt{z}}. \tag{18}$$

The noise power at the output of the low-frequency ideal filter Φ_2, with a receiver band-width of 0 to F_f, equals

$$W_0 = \int_0^{F_f} W(f)\,df = 6.58\,\frac{(\Delta f)^3}{z}\left(\frac{F_f}{\Delta f}\right)^3 + 29\,(\Delta f)^2\,\frac{e^{-z}}{\sqrt{z}}\left(\frac{F_f}{\Delta f}\right), \tag{19}$$

and the effective noise voltage is

$$\sqrt{W_0} = \left[6.58\,\frac{\Delta f^3}{z}\left(\frac{F_f}{\Delta f}\right)^3 + 29\Delta f^2\,\frac{e^{-z}}{\sqrt{z}}\left(\frac{F_f}{\Delta f}\right)\right]^{1/2}. \tag{20}$$

3. Optimal Frequency Deviation

By definition, the magnitude of the mean square error at the output of the frequency receiver equals

$$\delta = \frac{\sqrt{W_0}}{2U_{\max}}, \tag{21}$$

where U_{max} is the maximum dc voltage of the signal at the receiver output equal, according to Formula (1), to $\omega_{D\,max}$, where $\omega_{D\,max}$ is the maximum frequency deviation.

To determine the error, we express the quantity z in terms of the signal voltage and the specific noise voltage, σ:

$$z = \left(\frac{U_s}{U_n}\right)^2 = \frac{U_c^2}{2\sigma^2\Delta f}. \tag{22}$$

Substituting the magnitudes of $\sqrt{W_0}$ and U_{max} in (21), and replacing z by its expression in terms of σ from (22), we get

$$\delta = \left[0.083\left(\frac{\sigma}{U_s}\right)^2\frac{F_f^2}{\Delta f^2} + 0.26\left(\frac{\sigma}{U_s}\right)\frac{F_f}{\Delta f^{1/2}}e^{-0.5\frac{U_s^2}{\sigma^2\Delta f}}\right]^{1/2}\frac{\Delta f}{f_{D\max}}. \tag{23}$$

Formula (23) can be transformed by the introduction of the generalized parameters

$$\beta = \frac{U_s}{\sigma\sqrt{F_f}}, \quad \eta = \frac{\Delta f}{f_{D\max}} \text{ and } \gamma = \frac{f_{D\max}}{F_f}.$$

With these parameters,

$$\delta = \left[\frac{0.083}{\beta^2\gamma^2\eta^2} + \frac{0.26}{\beta\gamma^{1/2}\eta^{1/2}}e^{-0.5\frac{\beta^2}{\gamma\eta}}\right]^{1/2}\eta. \tag{24}$$

Consequently, the expression for the mean square error δ consists of two terms. Both terms decrease with increasing β, but behave differently with increasing γ, i.e., with increasing frequency deviation. The first term decreases with increasing γ, but the second grows. For large β, the second term is much less than the first, and Formula (24) coincides (to within a factor) with the formula obtained for the mean square error from the theory of potential noise stability.

It is possible to determine from (24) the magnitude of the frequency deviation for which the error will be a minimum (considering η = const). We equate the derivative with respect to γ to zero, thus obtaining the condition for determining γ_{opt}:

$$e^{-\frac{\beta^2}{2\gamma_{opt}\eta}}\left(\frac{\beta^2}{\gamma_{opt}\eta} - 1\right) = \frac{1.28}{\beta\gamma_{opt}^{3/2}\eta^{3/2}}. \tag{25}$$

For $z = \frac{\beta^2}{2\gamma_{opt}\eta} \geq 5$, $\frac{\beta^2}{\gamma_{opt}\eta} \gg 1$, and Equation (25) will take the following form:

$$e^{-\frac{\beta^2}{2\gamma_{opt}\eta}} = \frac{1.28}{\beta^2\gamma_{opt}^{3/2}\eta^{3/2}}. \tag{26}$$

From the transcendental equation thus obtained, we can find $\gamma_{opt} = \varphi(\beta, \eta)$, i.e., we can determine the dependence of the optimal frequency deviation on the signal voltage U_s, the specific noise voltage σ, and the filter output band-width F_f, determining the system's rapidity of action.

As is clear from the results obtained above, Formula (26) is correct for

$$5 \leqslant z_{opt} = \frac{\beta^2}{2\gamma_{opt}\eta} \leqslant 20 \text{ and } \frac{F_f}{\Delta f_{opt}} = \frac{1}{\gamma_{opt}\eta} \leqslant 0.2.$$

We see from (26) that $8 \leq \beta \leq 250$. This condition determines the limit of applicability of Formula (26). Knowing γ_{opt}, one can determine the least error possible with given values of β and η. Substituting (26) in (24), we obtain

$$\delta_{min} = \left[\frac{0.083}{\beta^2\gamma_{opt}^2\eta^2} + \frac{0.33}{\beta^4\gamma_{opt}\eta}\right]^{1/2}\eta. \qquad (27)$$

It is obvious from (27) that, for given β and γ_{opt}, δ_{min} is minimum for $\Delta f / f_{D\,max} = 1$, i.e., when the maximum frequency deviation equals half the receiving band-width at the filter input.

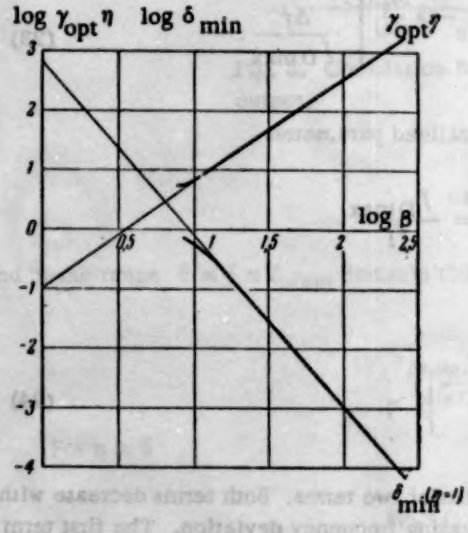

Fig. 4.

Figure 4 gives the dependence of $\gamma_{opt}\eta$ and δ_{min} (for $\eta = 1$) on β, computed from Formulas (26) and (27).

It follows from the curves that, for example, for $\beta = 10$, $\gamma_{opt}\eta = 6.3$, and for $F_f = 0.5$ cps, the deviation $f_{D\,max} = 3.15$ cps, but the error $\delta_{min} = 0.56\%$; for $\beta = 50$, $\gamma_{opt}\eta = 100$, and for $F_f = 0.5$ cps, the deviation $f_{D\,max} = 50$ cps but the error $\delta_{min} = 0.7 \times 10^{-2}\%$.

It is clear from Fig. 4 that these relations are almost linear when plotted on a logarithmic scale. For $8 \leq \beta \leq 250$ (the range of practical variation of this parameter) these dependences are very well approximated by the functions

$$\log(\gamma_{opt}\eta) = -1.0 + 1.8 \log \beta, \log(\delta_{min})_{\eta=1} = 2.8 - 2.9 \log \beta. \qquad (28)$$

Here, δ_{min} is expressed in per cent. Dependences (28) are given in fine lines on Fig. 4.

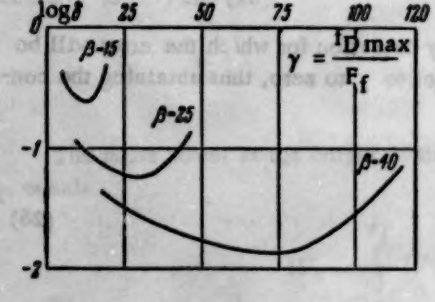

Fig. 5.

Figure 5 gives the functional dependence $\delta = \varphi(\gamma)_{\eta=1}$ for $\beta = 15, 25, 40$, all computed from Formula (24). It is clear from the Figure that, for a definite value of the frequency deviation ($\gamma = \gamma_{opt}$), the mean square error at the frequency receiver output is a minimum. With increasing β, δ_{min} is decreased, and the value of γ for which $\delta = \delta_{min}$ becomes less sharply defined.

4. Experimental Results

Experimental verification of the dependence of the error on the frequency deviation were carried out under laboratory conditions. For this, use was made of a frequency receiver with a two-way discriminator for strongly limiting signal amplitude. The mean square error was measured by a special instrument developed at IATAN Laboratory 4. An unmodulated 2 kilocycle signal was applied to the receiver input, as well as fluctuating noise from noise generator LIG-24-48.

Figure 6 gives the dependence of the error on the frequency deviation, as obtained experimentally (1) and by computation (2).

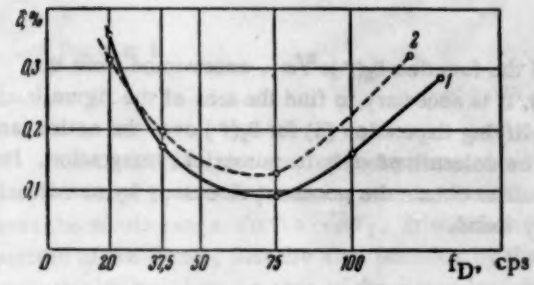

Fig. 6.

It was assumed for this that $U_s/\sigma = 36$, $F_f = 4$ cps, $f_{D\,max} = \Delta f$.

It is clear from Fig. 6 that there is good coincidence between the experimental and computed values for the optimal frequency deviation, for the minimum error, and the character of the dependence of the error on the frequency deviation.

SUMMARY

1. For a telemetering system there is an optimal value of frequency deviation for which a minimum error is obtained from the action of fluctuating noise.

2. The optimal frequency deviation is determined by the value of the generalized transmission parameter, $\beta = U_s/\sigma\sqrt{F_f}$. For $8 \leq \beta \leq 250$, the optimal frequency deviation ($\gamma_{opt} = f_{D\,max}/F_f$) and the minimum error, δ_{min}, are determined from Formulas (28).

The author wishes to express his thanks to G. A. Shastov for a series of good counsels, given to aid in the performance of this work.

APPENDIX I

Energy Spectrum $W_1(f)$.

To find the spectrum $W_1(f)$ from (9), we simplify the expression for $B_1(\tau)$ from (4).

It is well-known that for large x

$$E_i(x) = \frac{e^x}{x}\left[\sum_{k=0}^{n}\frac{k!}{x^k} + r_n(x)\right], \quad |r_n(x)| \leqslant \frac{(n+1)!}{|x|^{n+1}}. \tag{I. 1}$$

For large x and a fixed, but not too large, n, $r_n(x)$ will be small in comparison to the other terms in the square brackets. For $x \geq 5$,

$$E_i(x) \approx \frac{e^x}{x}\left(1 + \frac{1}{x} + \frac{2}{x^2} + \frac{6}{x^3}\right). \tag{I. 2}$$

If $E_1(z/\rho)$ is determined from Formula (I. 2), Expression (4) may be transformed to the form

$$B_1(\tau) = \alpha\left\{\frac{\rho}{z}(1-2\alpha\tau^2) + \frac{\rho^2}{z^2}(1-2\times 2\alpha\tau^2) + \frac{2\rho^3}{z^3}(1-3\times 2\alpha\tau^2)\right\} = \alpha\sum_{n=1}^{3}\frac{\rho^n\,(n-1)!}{z^n}(1-n\,2\alpha\tau^2). \tag{I. 3}$$

Figure 3,a gives the curves of $B_1(\tau)z/\alpha$ for $z = 5$, 10 and 20 (for positive τ). We determine $W_1(f)$ by substituting $B_1(\tau)$ in (9). Integrating twice by parts for each term in the sum, and substituting the value $\alpha = \pi(2\Delta f)^2$, we obtain

$$W_1(f) = \frac{2\pi^2\Delta f}{z}\left(\frac{f}{\Delta f}\right)^2\left\{e^{-\frac{\pi}{4}\left(\frac{f}{\Delta f}\right)^2} + \frac{1}{2\sqrt{2}\,z}e^{-\frac{1}{2}\frac{\pi}{4}\left(\frac{f}{\Delta f}\right)^2} + \frac{2}{3\sqrt{3}\,z}e^{-\frac{1}{3}\frac{\pi}{4}\left(\frac{f}{\Delta f}\right)^2}\right\} = \frac{2\pi^2\Delta f}{z}\left(\frac{f}{\Delta f}\right)^2\sum_{n=1}^{3}\frac{(n-1)!}{n\sqrt{n}\,z^{n-1}}e^{-\frac{1}{n}\frac{\pi}{4}\left(\frac{f}{\Delta f}\right)^2}. \tag{I. 4}$$

APPENDIX II

Energy Spectrum $W_3(0)$

For finding the spectrum $W_3(0)$, we consider the graph of the function $B_3(\tau)e^{z}/\alpha$, constructed from the exact Formula (5) (Fig. 3,b). To find $W_3(0)$ from Formula (14), it is necessary to find the area of the figure bounded by the graph of the function and by the coordinate axes. Simplifying Expression (5) for $B_3(\tau)$ over the entire range of variation of τ (from 0 to ∞) is difficult, since the area can be determined only by numerical integration. However, for $\sqrt{\alpha}\tau \to 0$ and $\sqrt{\alpha}\tau \to \infty$ (i.e., when it is difficult to obtain the necessary accuracy by numerical integration methods), an analytic expression for $B_3(\tau)$ is readily found.

We consider these cases.

The case when $\alpha\tau^2 \ll 1$. Here,

$$\rho = e^{-\alpha\tau^2} = 1 - \alpha\tau^2, \quad \frac{1-\rho}{\rho} z = \frac{\alpha\tau^2}{1-\alpha\tau^2} z \approx \alpha\tau^2 z. \tag{II. 1}$$

If, in addition, $\alpha\tau^2 z \ll 1$, then Formula (5) may be simplified. For small x

$$E_i(x) \approx C + \ln x + \sum_{n=1}^{\infty} \frac{x^n}{n!n} \quad (C = 0.577). \tag{II. 2}$$

For $x \ll 1$, $E_i(x) \approx C + \ln x + x$.

Then,

$$E_i\left(\frac{1-\rho}{1+\rho}\frac{z}{\rho}\right) - 2E_i\left(\frac{1-\rho}{\rho} z\right) \approx -C - \ln 2\alpha\tau^2 z, \tag{II. 3}$$

$$-\frac{2e^{-z}}{1-\rho} + \frac{1+\rho}{1-\rho} e^{-\frac{2z}{1+\rho}} \approx -e^{-z}(1+z). \tag{II. 4}$$

Substituting (II. 3) and (II. 4) in (5), we obtain

$$B_3(\tau)_I = \alpha e^{-z}\left\{-2\alpha\tau^2(1+z) - (1-2\alpha\tau^2 z)(C + \ln 2\alpha\tau^2 z)\right\}. \tag{II. 5}$$

The case when $\alpha\tau^2 \gg 1$. Then, $\rho \ll 1$ and, for $z \geq 5$, it may be considered that

$$\frac{1-\rho}{\rho} z \gg 1, \quad \frac{1+\rho}{1-\rho} e^{-\frac{2z}{1+\rho}} \ll \frac{2e^{-z}}{1-\rho}$$

and

$$E_i\left(\frac{1-\rho}{1+\rho}\frac{z}{\rho}\right) \ll 2E_i\left(\frac{1-\rho}{\rho} z\right). \tag{II. 6}$$

Substituting into (5) the value of $E_i\left(\frac{1-\rho}{\rho} z\right)$ determined from Formula (I. 2), and discarding small quantities, we obtain, for $z \geq 5$,

$$B_3(\tau)_{II} = \alpha e^{-z}\left\{\frac{2}{z}\left[\frac{2\alpha\tau^2\rho}{(1-\rho)^2} - \frac{\rho}{1-\rho}\right]\right\}. \tag{II. 7}$$

From Formula (II. 5), one may determine the value of $\sqrt{\alpha}\ \tau_1$ (Fig. 3,c, curve for $z = 5$) for which the function $B_3(\tau)_I\, e^{z}/\alpha$ becomes equal to zero. Setting $B_3(\tau)_I$ from (II. 5) equal to zero, we obtain, for $z \geq 5$,

$$\sqrt{\alpha}\tau_1 = \frac{0.408}{\sqrt{z}} \qquad \text{(II. 8)}$$

For $z \geq 5$

$$\alpha\tau_1^2 \leqslant 0{,}033 \ll 1. \quad \alpha\tau_1^2 z = 0.165 \ll 1. \qquad \text{(II. 9)}$$

Consequently, the area of the region from $\sqrt{\alpha}\tau = 0$ to $\sqrt{\alpha}\tau_1$ (Fig. 3,b, striped portion of the curve for $z = 5$) may be found by a definite integration of Function (II. 5). Formula (II. 7) may be employed for finding the area over the whole range $\sqrt{\alpha}\tau > \sqrt{\alpha}\tau_1$. It was found, by a numerical integration to determine the area of the central portion of the figure, that the area bounded by the portion of the graph of Function (5) from $\sqrt{\alpha}\tau_1$ to ∞ was numerically equal to the area of the figure bounded by the graph of Function (II. 7) from $\sqrt{\alpha}\tau_2$ to ∞.

From the graphs constructed for $z = 5$, 10 and 20 (Fig. 3,b), it was found that

$$\sqrt{\alpha}\tau_2 = 1.55/\sqrt{z}. \qquad \text{(II. 10)}$$

On the basis of this, we may write

$$W_2(0) = W_2(0)_{\mathrm{I}} + W_2(0)_{\mathrm{II}} = 4\int_0^{\tau_1} B_2(\tau)_{\mathrm{I}}\, d\tau + 4\int_{\tau_2}^{\infty} B_2(\tau)_{\mathrm{II}}\, d\tau. \qquad \text{(II. 11)}$$

Integrating Function (II. 5) between 0 and τ_1, and Function (II. 7) between τ_2 and ∞, we easily obtained the expressions for $W_2(0)_{\mathrm{I}}$ and $W_2(0)_{\mathrm{II}}$. Finally, we obtain

$$W_2(0)_{\mathrm{I}} = 3.74\sqrt{\alpha}\,\frac{e^{-z}}{\sqrt{z}} \qquad \text{(II. 12)}$$

and

$$W_2(0)_{\mathrm{II}} = \frac{8\alpha e^{-z}}{z}\left[\int_{\tau_2}^{\infty} \frac{2\alpha\tau^2\rho}{(1-\rho)^2}\, d\tau - \int_{\tau_2}^{\infty} \frac{\rho}{1-\rho}\, d\tau\right] = \frac{8\alpha e^{-z}}{z}\,\frac{\tau_2\rho_2}{1-\rho_2}, \qquad \text{(II. 13)}$$

since integration by parts of the first term in brackets gives

$$\int_{\tau_2}^{\infty} \frac{2\alpha\tau^2\rho}{(1-\rho)^2}\, d\tau = \frac{\tau_2\rho_2}{1-\rho_2} + \int_{\tau_2}^{\infty} \frac{\rho}{1-\rho}\, d\tau. \qquad \text{(II. 14)}$$

For $5 \leqslant z \leqslant 20$, $\xi = \frac{1}{z}\,\frac{\rho_2}{1-\rho_2} = 0.33$ to 0.39. Using (II. 10) and letting $\xi = 0.36$, we obtain

$$W_2(0)_{\mathrm{II}} = 4.46\sqrt{\alpha}\,\frac{e^{-z}}{\sqrt{z}}. \qquad \text{(II. 15)}$$

Substituting (II. 12) and (II. 15) in (II. 11), we obtain, for $5 \leq z \leq 20$,

$$W_2(0) = 8.2\sqrt{\alpha}\,\frac{e^{-z}}{\sqrt{z}} = 29\,\Delta f\,\frac{e^{-z}}{\sqrt{z}}. \qquad \text{(II. 16)}$$

It is clear from Formulas (14) and (II. 16) that, for $\Delta f = \text{const}$, the intensity of the noise energy spectrum for $f = 0$ is directly proportional to $e^{-z}/\sqrt{z}$.

Received July 12, 1957

LITERATURE CITED

[1] Threshold Signals (Sovetskoe Radio, 1952).

[2] G. A. Malolepshii, "Fluctuating noise in single-channel radio links with frequency modulation, and in multi-channel links with frequency modulation and frequency separation," Trudy TsNIIIC, 6 (1956).

[3] E. Jahnke and F. Emde, Tables of Functions with Formulae and Curves (Dover Publications).

[4] S. O. Rice, "Statistical properties of sine-wave plus random noise," Bell System Tech. J. 27, 1 (1948).

[5] D. Middleton, "The spectrum of frequency-modulated waves after reception in random noise," Quart. Appl. Math. 7, 2 (1949).

A SELECTIVE LOW-FREQUENCY RC-AMPLIFIER AS A CONTROL SYSTEM ELEMENT

Iu. G. Kochinev

(Leningrad)

The dynamic properties of a selective low-frequency RC-amplifier with a double T configuration are investigated.

1. General Considerations

Two modifications of selective low-frequency RC-amplifiers have strongly recommended themselves in use [1]: a circuit with a Wien bridge and a circuit with a double T configuration (Fig. 1, a and b). The tuning frequency, in both cases, is determined by the relationship $\omega_0 = 1/RC$. Both circuits are capable of guaranteeing high selectivity.

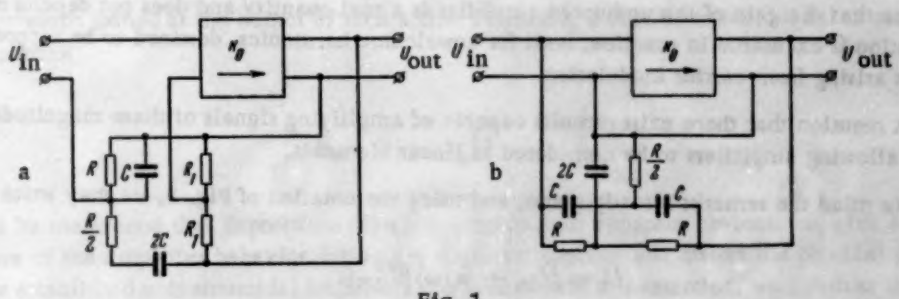

Fig. 1.

In the actual realization of these circuits, difficulties arise in summing the input and feedback signals. More simply constructed solutions are obtained by the use of double T configurations. We turn now to such a circuit, and investigate its dynamic properties.

The general questions of matching the feedback loop parameters with the amplifier have been clarified in sufficient detail in [2, 3], and will not be treated here.

The transfer coefficient of the unloaded double T equals the ratio of the steady-state output and input vectors when sinusoidal signals are passed:

$$\dot{\alpha}(\omega) = \frac{\omega^2 - \omega_0^2}{\omega^2 - 4j\omega\omega_0 - \omega_0^2}. \qquad (1)$$

In order to obtain high selectivity, it is necessary that the amplifier, without the feedback loop, have high gain and comparatively little nonlinearity and frequency distortion, all within the given frequency range. On the other hand, the input and output impedances of the feedback path must be matched with the amplifier parameters.

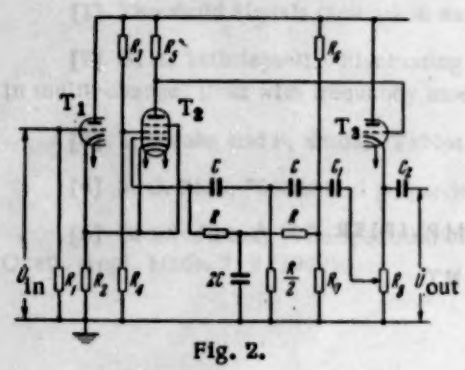

Fig. 2.

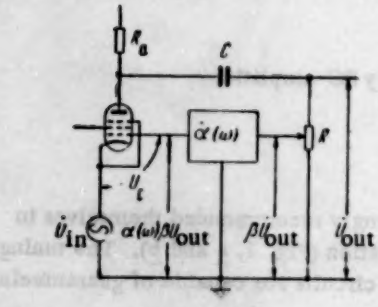

Fig. 3.

Figure 2 gives a schematic of a circuit for a selective amplifier satisfying the conditions imposed. This circuit may be considered a development of the circuit described in [4] for a double triode with cathode followers.

The high gain in the amplifier we are considering is obtained by means of a reduced potential on the anode and screen grid of the pentode, and by the use of a high ohmic load resistance (a vacuum tube functioning in the so-called "starvation" regimen). The cathode followers (T_1 and T_3) implement the impedance matching of the selective circuit and the amplifier cascade.

We now determine the transfer function of a selective RC-amplifier, constructed according to the circuit of Fig. 2. To simplify the argument, we introduce the following simplifications, which will allow us to go over to the circuit of Fig. 3:

1) the cathode followers have unit gain;

2) the cathode connections of T_1 and T_3 are of negligible influence;

3) we will conditionally assume that the double T does not load the amplifier cascade. Such an assumption is permissible since, in actuality, the selective circuit is connected to the low-impedance output of cathode follower T_3.

We assume that the gain of the unshunted amplifier is a real quantity and does not depend on frequency. Such an assumption is excusable in practice, both for unwelcome harmonics, destined to be suppressed, and for side frequencies arising from carrier modulation.

We might mention that there exist circuits capable of amplifying signals of these magnitudes without distortion, thus allowing amplifiers to be considered as linear elements.

Keeping in mind the remarks already made, and using the notation of Fig. 3, we may write

$$\dot{U}_i = \dot{U}_{in} + \dot{\alpha}(\omega)\beta\dot{U}_{out}, \tag{2}$$

$$\dot{U}_{out} = -k_0\dot{U}_i \tag{3}$$

where β is the feedback coefficient and k_0 is the open-loop amplifier gain.

Possible cases are $\beta < 1$ and $\beta > 1$; the latter case indicates that there is an amplifier in the feedback path.

From (2) and (3) we obtain the expression for the gain of the selective amplifier:

$$\dot{k}(\omega) = \frac{\dot{U}_{out}}{\dot{U}_{in}} = \frac{-k_0}{1+\dot{\alpha}(\omega)\beta k_0}. \tag{4}$$

2. Transfer Function of the Selective Amplifier

We will call the amplifier transfer function the ratio of the Laplace transforms expressing the envelope at the amplifier output and input for zero initial conditions:

$$k^-(p) = \frac{\overline{E_{out}}(p)}{\overline{E_{in}}(p)}. \tag{5}$$

The carrier transfer function will be the name given to

$$k(s) = \frac{U_{\text{out}}^{-}(s)}{U_{\text{in}}^{-}(s)}. \tag{6}$$

With these definitions, (5) is permissible only in case the carrier is not subject to phase shift and the form of the rounding at the output is independent of the initial carrier phase.

The concept of the complex transfer function may also be applied to the selective amplifier:

$$\dot{k}(\Omega) = \frac{\dot{E}_{\text{out}}}{\dot{E}_{\text{in}}}, \tag{7}$$

corresponding to the steady state, and characterizing the amplitude and phase variation at the output for sinusoidal rounding at the input.

In [5] is to be found an approximate expression for the complex transfer function of a selective amplifier for small values of the modulating frequency Ω:

$$\dot{k}(\Omega) = \frac{k_0}{1 + j\Omega\tau'}, \tag{8}$$

where

$$\tau' = \frac{k_0\beta}{2\omega_0}. \tag{9}$$

Based on (8), the selective amplifier is equivalent to a first-order inertial link with time constant τ' and gain k_0. The envelope formed at the output of such a link by passing a unit sinusoidal signal is described by the well-known equation

$$E_{\text{out}}(t) = k_0\left(1 - e^{-\frac{t}{\tau'}}\right). \tag{10}$$

It should be mentioned that Expressions (8)-(10), despite their apparent obviousness, give an insufficiently accurate picture of the amplifier behavior during the transient response and distort the physical picture of the phenomena for established unit sinusoidal impulses. To corroborate this assertion, we consider the passage of the following signal by the selective amplifier:

$$U_{\text{in}}(t) = \sin(\omega_0 t + \varphi_0). \tag{11}$$

The Laplacé transformation of (11) is well-known [6]:

$$U_{\text{in}}^{-}(s) = \frac{s\sin\varphi_0 + \omega_0\cos\varphi_0}{s^2 + \omega_0^2}. \tag{12}$$

The transfer function (carrier) for the double T and $k^{-}(s)$ are obtained from (1) and (4):

$$\alpha^{-}(s) = \frac{s^2 + \omega_0^2}{s^2 + 4\omega_0 s + \omega_0^2}, \tag{13}$$

$$k^{-}(s) = \frac{-k_0}{1 + k_0\beta}\,\frac{s^2 + 4\omega_0 s + \omega_0^2}{s^2 + \frac{4\omega_0}{1 + k_0\beta}s + \omega_0^2}. \tag{14}$$

Then, in accordance with (6), we obtain

$$U_{\text{out}}^{-}(s)=\frac{-k_0}{1+k_0\beta}\,\frac{s^3\sin\varphi_0+s^2(\omega_0\cos\varphi_0+4\omega_0\sin\varphi_0)+s(\omega_0^2\sin\varphi_0+4\omega_0^2\cos\varphi_0)+\omega_0^3\cos\varphi_0}{(s^2+\omega_0^2)\cdot\left(s^2+\frac{4\omega_0}{1+k_0\beta}s+\omega_0^2\right)}=$$

$$=-k_0\,\frac{s\sin\varphi_0+\omega_0\cos\varphi_0}{s^2+\omega_0^2}+k_0\,\frac{k_0\beta}{1+k_0\beta}\,\frac{s\sin\varphi_0+\omega_0\cos\varphi_0}{s^2+\frac{4\omega_0}{1+k_0\beta}s+\omega_0^2}. \tag{15}$$

The source, in the time domain, of the first term of (15) is the steady-state solution:

$$U_{\text{out st}}(t)=-k_0\sin(\omega_0 t+\varphi_0). \tag{16}$$

To determine the source, in the time domain, of the second term, we employ an approximate method germane to systems with little damping [6].

For the case under consideration, in the expression

$$\frac{s\sin\varphi_0+\omega_0\cos\varphi_0}{s^2+\frac{4\omega_0}{1+k_0\beta}s+\omega_0^2}=\frac{s\sin\varphi_0+\omega_0\cos\varphi_0}{s^2+\delta\omega_0 s+\omega_0^2} \tag{17}$$

as the "small parameter" of the problem we may take the quantity $\delta = 4/(1 + k_0\beta)$, characterizing, as is easily verified [4], the "damping" of the selective amplifier.

The roots of the denominator of (17), for $\delta = 0$, assume the values $s_{1,2}^0 = \pm j\omega_0$. To find the roots lying in the neighborhood of $j\omega_0$, we set $s = q + j\omega_0$ (q is a small quantity, of the order of magnitude of δ).

Then, $(q + j\omega_0)^2 + \delta\omega_0 (q + j\omega_0) + \omega_0^2 = 0$. Hence, dropping terms of the order of magnitude of δ^2, we find that $j\omega_0 (2q + \omega_0\delta) = 0$, or $q = -\omega_0\delta/2$.

Thus, improved values of the roots will be

$$s_1'=\omega_0\left(-\frac{\delta}{2}+j\right),\qquad s_2'=\omega_0\left(-\frac{\delta}{2}-j\right)\quad\text{for}\quad\frac{\delta}{2}\ll|j|.$$

Now, we decompose (17) into partial fractions:

$$\frac{s\sin\varphi_0+\omega_0\cos\varphi_0}{s^2+\delta\omega_0 s+\omega_0^2}=\frac{a_1}{s-s_1'}+\frac{a_2}{s-s_2'}$$

and, finding the inverse transformations in the time domain, we get

$$L^{-1}\left\{\frac{a_1}{s-s_1'}+\frac{a_2}{s-s_2'}\right\}=a_1e^{s_1't}+a_2e^{s_2't}=e^{-\frac{\delta\omega_0}{2}t}\sin(\omega_0 t+\varphi_0).$$

Thus the source, in the time domain, of $U_{\text{out}}^{-}(s)$ takes the following form:

$$U_{\text{out}}(t)=-k_0\sin(\omega_0 t+\varphi_0)\left(1-\frac{k_0\beta}{1+k_0\beta}e^{-\frac{t}{\tau}}\right), \tag{18}$$

where $\tau=\dfrac{1+k_0\beta}{2\omega_0}$.

It is clear from a comparison of (18) and (11) that only the envelope which is unconnected with the initial phase of the carrier, is subject to variation. It is possible to leave out of consideration the phase inversion of the carrier, which is a property of all amplifiers with nonreactive anode loading.

The "independence" of the transmission of the carrier and the envelope allows the concept of the transfer function to be applied to the latter [Cf. (5)]. Its values are found by applying the Laplace transform to the expressions for the envelope at the input and the output:

$$E_{\text{in}}(t) = 1, \quad E_{\text{out}}(t) = k_0\left(1 - \frac{k_0\beta}{1+k_0\beta}e^{-\frac{t}{\tau}}\right), \tag{19}$$

$$\bar{E}_{\text{in}}(p) = \frac{1}{p}, \quad \bar{E}_{\text{out}}(p) = k_0\left(\frac{1}{p} - \frac{k_0\beta}{1+k_0\beta}\frac{1}{p+\tau}\right) = k_0\frac{1+p\frac{\tau}{1+k_0\beta}}{p(1+p\tau)}. \tag{20}$$

We obtain the results

$$\bar{k}(p) = \frac{\bar{E}_{\text{out}}(p)}{\bar{E}_{\text{in}}(p)} = k_0\frac{1+p\frac{\tau}{1+k_0\beta}}{1+p\tau}. \tag{21}$$

The qualitative differences between Expressions (21) and (8) are quite evident. The establishment of an envelope (21) with unit sinusoidal impulse is described by Equation (19), where the final value of the output signal, corresponding to the moment of switching, equals

$$E_{\text{out}}(t_0) = k_0\left(1 - \frac{k_0\beta}{1+k_0\beta}\right) = \frac{k_0}{1+k_0\beta}. \tag{22}$$

At the same time (21) and (8) should not be considered as in contradiction to one another. Their identity for $k_0\beta \gg 1$ is obvious. Expression (21) should be considered as the more accurate and correct reflection of the physical side of the process.

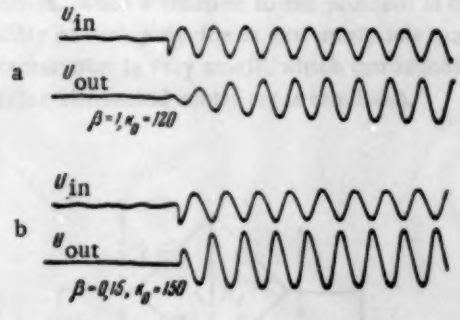

Fig. 4.

Figure 4 shows the oscillograms of the process occurring when a sinusoidal voltage was applied to the input of a selective amplifier built according to the circuit of Fig. 2, using tubes 6N2P (tubes T_1 and T_3) and 6Zh1P (tube T_2). The values of resistance and capacitance used in the circuit were as follows: R = 680 kilohms, R_1 = 1 megohm, R_2 = 10 kilohms, R_3 = 1.6 megohms, R_4 = 180 kilohms, $R_5 = R_6$ = 2.2 megohms, R_7 = 20 kilohms, R_8 = 270 kilohms, C = 5000 μμf, $C_1 = C_2$ = 0.1 μf.

The upper curve corresponds to the input signal, the lower curve to the output signal. The form of the oscillograms, read off with two values of feedback (β_a = 1.0 and β_b = 0.15), is in good agreement with (21).

In conclusion, a remark of a practical character should be made. It is more correct to consider k_0, not as the open-loop amplifier gain, but as the gain at the tuning frequency. For large values of gain, these two quantities can differ considerably.

Received January 28, 1957

LITERATURE CITED

[1] A. M. Bonch-Bruevich, Application of Vacuum Tubes in Experimental Physics (Gostekhizdat, 1955).

[2] R. Ia. Berkman and Iu. I. Spektor, Selective Amplifiers with Double T Configurations, Ext. 4 (Izd. AN SSSR, Kiev, 1955).

[3] Iu. G. Kochinev, "Computations for a frequency-selective low-frequency amplifier," Elektrichestvo 4 (1954).

[4] V. I. Syshkevich (ed.), Vacuum Tube Amplifiers, Part II, (Sovetskoe Radio, 1951).

[5] L. S. Gol'dfarb and N. M. Aleksandrovskii, "Certain questions in computing correcting links in ac servo systems," Automation and Remote Control (USSR) 16, 1 (1955).

[6] M. I. Kontorovich, Operational Calculus and Nonstationary Phenomena in Electric Circuits (Gostekhizdat, 1955).

PHASE DETECTOR FOR MULTIPLE FREQUENCIES

R. Ia. Berkman

(Lvov)

In a host of circuits, the output quantity is a voltage whose frequency is an even multiple of the frequency of the exciting voltage. The most widely used circuits of that type today are magnetic amplifiers and magnetic probes of the "second harmonic" type, wherein the output quantity is a voltage of doubled frequency.

The rectification of second harmonics by means of phase detectors of the usual type involves complicating the circuit, since a frequency doubler is necessary. Differential amplitude voltmeters, frequently employed for the same purpose, have poor zero stability, narrow limits of linearity and provide low output power.

A new circuit for a phase detector, due to M. A. Rozenblat [1], is based on the use of nonlinear carborundum resistors with symmetric voltampere characteristics. This circuit is simple and possesses high zero stability. It is not free, however, of certain drawbacks, connected with the facts that carborundum resistors work reliably only with high controlling voltages and pass only comparatively small currents. The controlling power thereby obtained is considerable. Therefore, in those cases when devices of high efficiency are called for and significant rectification of current is required, the circuits mentioned are hardly suitable.

It should also be mentioned that carborundum resistors of the necessary dimensions are not manufactured industrially at present.

It is stated in [2] that instead of carborundum resistors, one may use reverse-connected semiconducting rectifiers. Such a solution to the problem is impossible to accept as satisfactory since, in the first place, the zero stability of such a device is extremely low and, in the second place, the curvilinear portion of the rectifying characteristic is very small, which introduces difficulties in the computation of the circuit (a large number of series-connected rectifiers is required).

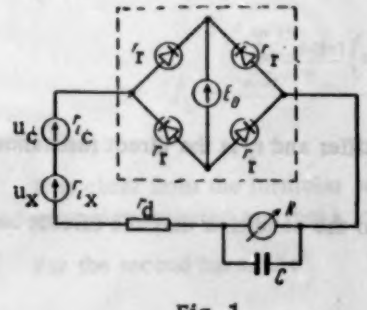

Fig. 1.

We have developed a new circuit for a phase detector for multiple frequencies, similar to the type of detector with nonlinear symmetric resistances (Fig. 1). It is based on the use of nonlinear elements with symmetric voltampere characteristics, taking the form of a bridge circuit with four rectifiers, so connected as to cut off all voltage (in Fig. 1, the bridge is enclosed in dotted lines). With this connection, the nonlinear element possesses a great deal of symmetry, since opening of the link occurs for one and the same value, $u > U_0$, independently of the direction of the applied voltage (Fig. 2). The influence of other sources of asymmetry – variation in the direct resistance of the rectifiers – can be decreased by connecting additional resistance in the circuit.

The phase detector built on the circuit of Fig. 1 may be designed easily for variations, within wide limits, of the magnitude of the putput resistance, sensitivity and linearity with respect to the measured voltage, by means of a limited number of rectifiers, by varying the cutting-off voltage and the auxiliary resistance. It is essential for this that, if auxiliary resistances are introduced, the power in the rectifying circuit exceed slightly the power dissipated by the rectifiers.

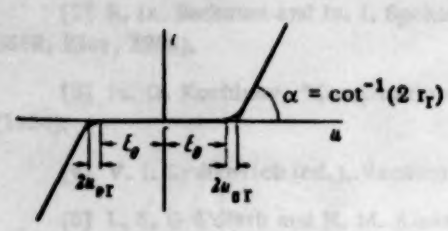

Fig. 2.

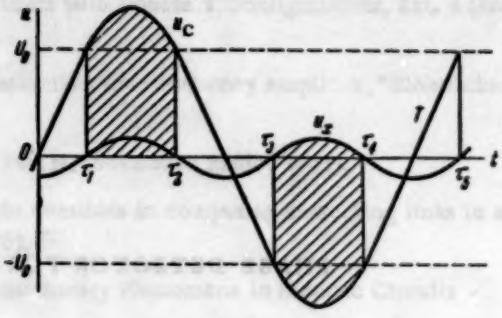

Fig. 3.

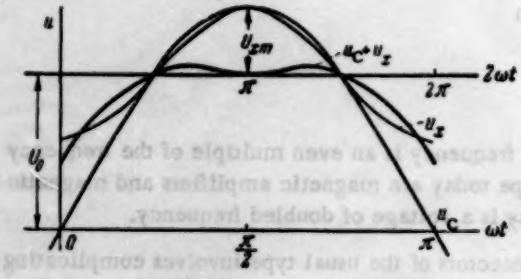

Fig. 4.

Figure 3 clarifies the principles according to which our circuit works. During the intervals of time τ_2 to τ_3 and τ_4 to τ_5, the circuit is cut off, since $u < U_0$. During the intervals τ_1 to τ_2 and τ_3 to τ_4, the circuit conducts and, for a definite current i, the principle of superposition may be used. The average value of the commutating current during the times (τ_1 to τ_2) + (τ_3 to τ_4) equals zero.

Thus, the circuit functions as an interruptor with doubled frequency, where the "closed" time is controlled by the magnitude of the closing voltage U_0 (for a given u_C).

For the analysis, we assume a piecewise linear voltampere characteristic approximating that of the rectifier. Detector behavior is investigated during the steady state. We may write the initial relationships:

commutating voltage

$$u_C = U_{Cm} \sin \omega t;$$

measured voltage

$$u_x = \sum_{n=1}^{\infty} U_{m(2n)} \sin (2n\omega t - \varphi_{2n}) + U_{m(2n+1)} \sin [(2n+1)\omega t - \varphi_{2n+1}];$$

closing voltage

$$U_0 = E_N (1 + \delta_e) + 2U_{0r};$$

total resistance to ac in the circuit

$$r = 2r_r + r_{ix} + r_{iC} + r_d,$$

$$RC \gg \frac{2\pi}{\omega}.$$

We have used the notation: U_{0r} is the initial voltage across the rectifier and r_r is the direct resistance of the rectifier.

We choose a nominal value for the closing voltage E_N, starting from the condition that the circuit be in the open and closed states for equal intervals of time. This corresponds to

$$E_N = \frac{1}{\sqrt{2}} U_{Cm} - 2U_{0r}, \quad U_N = \frac{U_{Cm}}{\sqrt{2}}. \tag{1}$$

The quantity δ_e characterizes the deviation of E_0 from its nominal value; $\delta_e \gtrless 0$, $\delta_e \ll 1$.

The rectified current in load resistor R is determined from the equation

$$I_L = \frac{1}{T}\left(\int_{\tau_1}^{\tau_2} i\,dt + \int_{\tau_3}^{\tau_4} i\,dt\right) =$$

$$= \frac{\omega}{2\pi r}\left[\int_{\tau_1}^{\tau_2}(u_c + u_x - U_0 - I_L R)\,dt + \int_{\tau_3}^{\tau_4}(u_c + u_x + U_0 - I_L R)\,dt\right]. \quad (2)$$

We determine the moments of time τ_1 for small measured voltages, neglecting the quantities u_x and $I_L R_L$. Then

$$U_{cm}\sin\omega\tau_i \approx \pm U_N(1+\delta_e), \quad \sin\omega\tau_i = \pm\frac{1}{\sqrt{2}}(1+\delta_e).$$

Expanding arc sin $\omega\tau_1$ in a Taylor series, and limiting ourselves to the first two terms, we get

$$\omega\tau_1 = \frac{\pi}{4} + \delta_e, \quad \omega\tau_2 = \frac{5\pi}{4} - \delta_e, \quad \omega\tau_3 = \frac{3\pi}{4} + \delta_e, \quad \omega\tau_4 = \frac{7\pi}{4} - \delta_e. \quad (3)$$

Since $\tau_3 = \tau_1 + \pi/\omega$ and $\tau_4 = \tau_2 + \pi/\omega$,

$$\int_{\tau_1}^{\tau_2}(u_c - U_0)\,dt + \int_{\tau_3}^{\tau_4}(u_c + U_0)\,dt = 0,$$

$$\int_{\tau}^{\tau}\sum_{n=1}^{\infty} U_{m(2n+1)}\sin[(2n+1)\omega t - \varphi_{2n+1}]\,dt + \quad (4)$$

$$+\int_{\tau_3}^{\tau_4}\sum_{n=1}^{\infty} U_{m(2n+1)}\sin[(2n+1)\omega t - \varphi_{2n+1}]\,dt = 0,$$

i.e., the odd harmonics of the controlling voltage are not rectified. For even harmonics we obtain

$$I_L = -\frac{I_L R}{\pi r}\left(\frac{\pi}{2} - 2\delta_e\right) - \frac{1}{2\pi r}\sum_{n=1}^{\infty}\frac{U_{m(2n)}}{n}\cos(2n\omega t - \varphi_{2n})\Big|_{\tau_3}^{\tau_2}$$

or, after transformation,

$$I_L = \frac{\sum_{n=1}^{\infty}\frac{U_{m(2n)}}{n}\left(\sin\varphi_{2n}\cos 2n\delta_e \sin\frac{\pi n}{2} + \sin\varphi_{2n}\sin 2n\delta_e \sin\frac{\pi(n+1)}{2}\right)}{\pi\left[r + \frac{R}{2}\left(1 - \frac{4}{\pi}\delta_e\right)\right]}. \quad (5)$$

It is clear from the formulas we have obtained that, for the nominal value of closing voltage ($\delta_e = 0$), the only harmonics detected are those with ordinal numbers in the series $2n = 2 + 4m$ ($m = 1, 2, \ldots$).

For the second harmonic

$$I_L = \frac{U_{m2}}{\pi\left(r + \frac{R}{2}\right)}\sin\varphi_2. \quad (6)$$

In the unloaded state (for $R \to \infty$)

$$U_L \to \frac{2}{\pi} U_{m2} \sin \varphi_2. \quad (7)$$

At maximum power in the load, determined by the condition that $\partial P_L/\partial R = 0$, we have

$$R_{opt} = 2r. \quad (8)$$

Clearly, an optimal value of r does not exist, $r_{opt} \to 0$. The minimum value of r is limited by the admissible power required of the controlling voltage source.

For use of the detector in a noncompensated circuit, an important part is played by the degree of nonlinearity of its voltampere characteristic. To determine the degree of nonlinearity analytically is, in the general case, quite difficult, since it is necessary to deal, in the expansion of arc sin $\omega\tau_1$, with quantities of greater than third order smallness (Cf. [3]). Linearity appears to be best for short-circuited states and for loads which are not shunted by capacitance. In these cases, as is clear from the physical picture of detector behavior, linearity is maintained down to the value of U_{xm} for which the commutation angle (3) is disturbed. As is clear from Fig. 4, this corresponds to the condition

$$U_{xm} \ll U_{cm}\left(1 - \frac{1}{\sqrt{2}}\right) \quad \text{or} \quad u_x \ll 0{,}3u_c \quad \text{for} \quad \varphi_2 = 90°. \quad (9)$$

With the introduction of load resistance, the linearity deteriorates somewhat, as compared to the unloaded regimen.

For the practical execution of the circuit of Fig. 1, it is convenient to replace the source of closing voltage, E_0, by a resistance shunted by a sufficiently large capacitance. The value of this resistance is determined from the condition that the voltage drop across it from the rectified commutating current will equal the required value of closing voltage:

$$E_0 \approx R_0 \frac{2}{T_r} \int_{\tau_1}^{\tau_2} (u_c - U_0)\, dt,$$

from which

$$R_0 = \frac{2\pi r}{4 - \pi} \approx 7.3\, r. \quad (10)$$

A circuit for the detector employing capacitance-ohmic closing is given in Fig. 5,a. Resistor R_{ez} serves to establish zero.

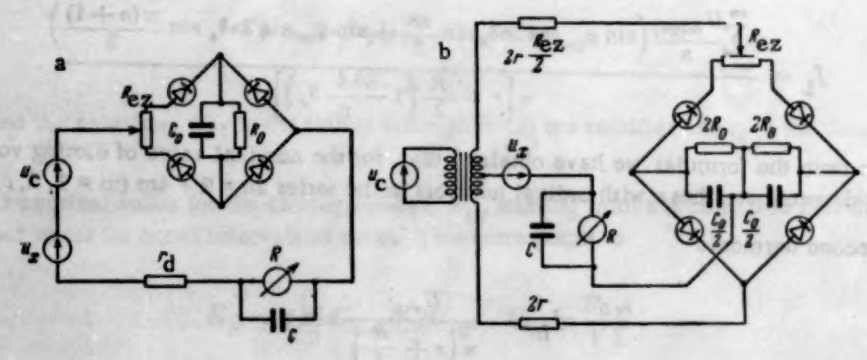

Fig. 5.

It is undesirable, in many cases, that commutating current pass through the source of rectified voltage. To avoid this condition, it is possible to use the symmetric detector circuit given in Fig. 5,b. The sensitivity

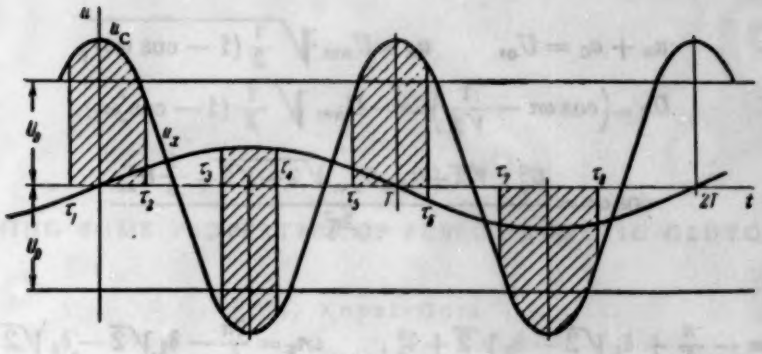

Fig. 6.

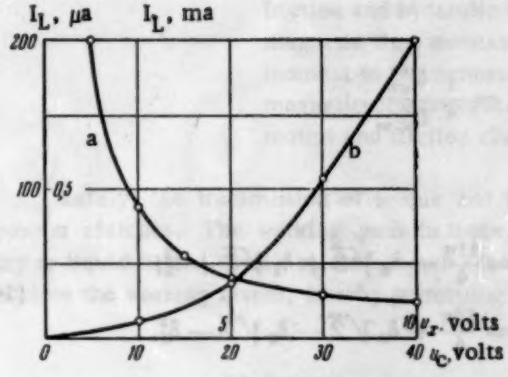

Fig. 7.

threshold of this circuit is determined by the zero drift during the time of rectifier aging, variation of commutating voltage, etc. Zero instability was experimentally determined for detectors of germanium diodes of type DG-Ts over a period of one day and, for variation of ± 20% of the commutating voltage, was between 5 and 20 millivolts of equivalent rectified voltage, depending on the type of rectifier and on the matching of characteristics.

Thus, with respect to sensitivity threshold, our detector does not differ from the usual circuit using semiconductor rectifiers. Its use seems expedient in those cases when the attainment of a minimum sensitivity threshold is not essential, for example, in devices with second harmonic preamplifiers, in intermediate and output cascades of magnetic amplifiers, etc.

In detectors of the type we have been considering, there is also rectification if the frequency of the commutating voltage exceeds that of the measured voltage. For an example, we consider the behavior of the circuit of Fig. 1 with the conditions

$$u_c = U_{cm}\cos\omega t, \quad u_x = U_{xm}\sin\frac{\omega}{2}t, \quad U_0 = U_N = \frac{U_{cm}}{\sqrt{2}}. \tag{11}$$

It is obvious from Fig. 6 that, to determine the magnitude of the rectified current, there should be carried out an integration over two periods of controlling voltage:

$$I_L = \frac{\omega}{4\pi r}\Big[\int_{\tau_1}^{\tau_2}(u_c + u_x - U_0 - I_L R)\,dt + \int_{\tau_3}^{\tau_4}(u_c + u_x + U_0 - I_L R)\,dt + \int_{\tau_5}^{\tau_6}(u_c + u_x - U_0 - I_L R)\,dt + \int_{\tau_7}^{\tau_8}(u_c + u_x + U_0 - I_L R)\,dt\Big]. \tag{12}$$

We compute the values of τ_i by means of Taylor series expansions of the functions $\sqrt{y}$ and arc sin y obtained from the previous solution, and retaining quantities up to the second order of smallness.

The moments of time $\tau_1, \tau_2, \tau_3, \tau_4$ are determined from the conditions

$$u_x + u_c = U_0, \qquad u_x = U_{xm}\sqrt{\tfrac{1}{2}(1-\cos\omega\tau)},$$

$$U_{cm}\left(\cos\omega\tau - \frac{1}{\sqrt{2}}\right) = -U_{xm}\sqrt{\tfrac{1}{2}(1-\cos\omega\tau)},$$

$$\cos\omega\tau = \frac{U_{cm}^2\sqrt{2} \pm U_{cm}U_{xm}\sqrt{2-\sqrt{2}} - \frac{1}{2}U_{xm}^2}{2U_{cm}^2},$$

where we obtain

$$\omega\tau_1 = -\frac{\pi}{4} + \delta_1\sqrt{2} - \delta_2\sqrt{2} + \delta_1^2, \qquad \omega\tau_5 = \frac{7\pi}{4} - \delta_1\sqrt{2} - \delta_2\sqrt{2} + \delta_1^2,$$
$$\omega\tau_2 = \frac{\pi}{4} + \delta_1\sqrt{2} + \delta_2\sqrt{2} - \delta_1^2, \qquad \omega\tau_6 = \frac{9\pi}{4} - \delta_1\sqrt{2} + \delta_2\sqrt{2} - \delta_1^2, \tag{13}$$

where

$$\delta_1 = \frac{\sqrt{2-\sqrt{2}}}{2}\frac{U_{xm}}{U_{cm}}, \qquad \delta_2 = \frac{1}{4}\frac{U_{xm}^2}{U_{cm}^2}.$$

Analogously for τ_3, τ_4, τ_7, τ_8, we find

$$\omega\tau_3 = \frac{3\pi}{4} + \delta_3\sqrt{2} + \delta_3\sqrt{2} + \delta_3^2, \qquad \omega\tau_7 = \frac{11\pi}{4} - \delta_3\sqrt{2} + \delta_3\sqrt{2} + \delta_3^2,$$
$$\omega\tau_4 = \frac{5\pi}{4} - \delta_3\sqrt{2} - \delta_3\sqrt{2} - \delta_3^2, \qquad \omega\tau_8 = \frac{13\pi}{4} + \delta_3\sqrt{2} - \delta_3\sqrt{2} - \delta_3^2, \tag{14}$$

where

$$\delta_3 = \frac{\sqrt{2+\sqrt{2}}}{2}\frac{U_{xm}}{U_{cm}}.$$

Transforming Equation (12), we finally obtain

$$I_L = \frac{3+\sqrt{2}}{\pi}\frac{U_{xm}^2}{rU_{cm}} \approx 2\frac{U_{xeff}}{rU_{ceff}}. \tag{15}$$

It is interesting to note that in detectors with such circuits, as opposed to detectors of other types (including detectors of carborundum resistors), the magnitude of the rectified current is inversely proportional to the commutating voltage. This might be exploited in a host of automatic devices.

Experimental curves for $I_L = f_1(u_x)$ (curve b) and $I_L = f_2(u_c)$ (curve a) are given in Fig. 7. Curve a is given for u_x = 2 volts and r = 1 kilohm, curve b is given for u_c = 30 volts and r = 1 kilohm.

Received December 1, 1956

LITERATURE CITED

[1] M. A. Rozenblat, "Basic theory and design of selective rectifiers of nonlinear symmetric resistances," Automation and Remote Control (USSR) 15, 4 (1954).

[2] M. A. Rozenblat, "Basic construction of magnetic amplifiers with low sensitivity thresholds," Automation and Remote Control (USSR) 17, 1 (1956).*

*See English translation.

CONCERNING SOME PROPERTIES OF FERROMAGNETIC CLUTCHES[1]

P. N. Kopai-Gora

(Moscow)

Ferromagnetic clutches are compared with electric motors and friction and hydraulic clutches in terms of their starting time, electromagnetic time constant, control power, and the ratio of the output moment to the moment of inertia. The said parameters of the ferromagnetic clutches are shown to be better than those of the electric motors and friction clutches.

Lately, the transmission of torque and its control is being accomplished by means of ferromagnetic powder clutches. The working space in these clutches is filled with powdered carbonyl iron together with a dry or liquid filler. Such a mixture, when acted on by a magnetic field, is able to couple the surfaces which enclose the working spaces, thereby permitting the transmission of torque between the shafts.

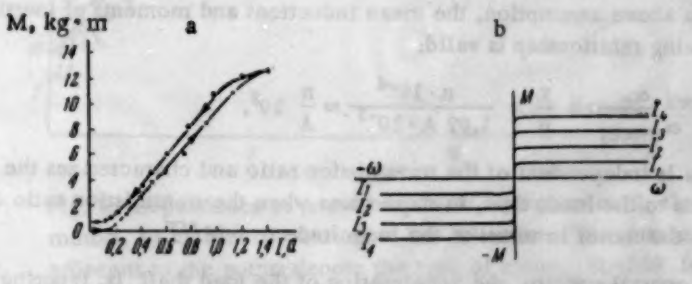

Fig. 1. Dependence of the transmitted torque on the excitation current and speed of rotation.

The dependence of the transmitted torque on the excitation (a) and angular frequency (b) for ferromagnetic clutches is shown in Fig. 1. The diagrams show that the clutch characteristics are very favorable for use in automatic control systems, since the moment is a linear function of the excitation current over a very wide range, and is independent of the speed of rotation.

The following qualitative comparison of such clutches with electric motors and friction and hydraulic clutches is carried out to establish more fully the possibilities of utilizing ferromagnetic clutches as actuating devices in automatic control systems. The comparison of the indicated devices is carried out on the basis of their starting time, control power, and the relationship $\frac{M}{\sqrt{J}} = \alpha$ (where M is the output moment, J is the moment of inertia).[2]

[1] There is no standard name for such clutches at present. They are called powder clutches, clutches with a magneto-liquid or ferromagnetic filler, etc.

[2] Motors are usually evaluated in terms of the relationship M/J, but such an evaluation does not always prove to be satisfactory since the system's properties also depend on the transmission ratio between the motor and the load.

The value of α for a motor of the SL (a) and PN (b) type, depending on the power, rpm, etc., varies between a few units and several tens, as is apparent in Fig. 2 (the numbers adjacent to the points indicate the type of electric motor).

The comparison is conducted with the following assumptions:

a) the mean induction in the gaps (B_{mean})[3] of the samples of the ferromagnetic clutches and motors being compared are equal;

b) the dimensions of the rotors of the electric motors and ferromagnetic clutches, as well as their moments of inertia, are respectively equal; the dimensions and moments of inertia of the friction discs and the ferromagnetic clutches are also equal;

c) the design coefficient of the polar arc (α') for dc electric motors is equal to the ferromagnetic clutch's coefficient of utilization of the active surface (k).

Such a comparison permits, in the design of automatic control systems, the direct choice of the actuating mechanism from the torque, and also permits an indirect comparison of mechanisms having equal power ratings if the angular speed is known.[4] The mean tangential force per unit area for ferromagnetic clutches, over the linear portion of the characteristic (for $500 < B_{mean} < 10{,}000$ gauss), and for the usual relationships between the filler and iron in the work mixture, can be approximated by the formula

$$\tau = B_{mean}\, nk \times 10^{-4}\ \text{kg/cm}^2, \tag{1}$$

where n is the number of pairs of active surfaces or the number of work layers of the mixture.

In the case of dc electric motors the mean force per unit area p can be approximated by

$$p = 1.02\, B_{mean} A\alpha' \cdot 10^{-7}\ \text{kg/cm}^2, \tag{2}$$

where A is the linear load on the electric motor.

Since, according to the above assumption, the mean inductions and moments of inertia are equal and, moreover, $\alpha' = k$, the following relationship is valid:

$$\frac{\alpha_c}{\alpha_{motor}} = \frac{\tau}{p} = \frac{n \cdot 10^{-4}}{1.02\, A \cdot 10^{-7}} \approx \frac{n}{A}\, 10^3. \tag{3}$$

Since the magnitude α is independent of the transmission ratio and characterizes the ability of the drive unit to impart an acceleration to the load, then, in those cases when the transmission ratio can be chosen, it is more convenient to evaluate the motor in terms of the magnitude $\alpha = M/\sqrt{T}$.

In fact, for high speed control systems, the acceleration of the load shaft is, ignoring friction, $\epsilon = \frac{iM_{dr}}{J_{dr}i^2 + J_l}$, where i is the transmission ratio between the motor and load, M_{dr} is the driving torque at the motor's shaft, J_{dr} and J_l are the moments of inertia of the motor and load, respectively. Differentiating this expression with respect to i and equating it to zero yields the optimum transmission ratio which provides maximum acceleration. The expression for the maximum acceleration of the load shaft will be

$$\epsilon_{max} = \frac{M_{dr}}{2\sqrt{J_{dr}}} \frac{1}{\sqrt{J_l}} = \alpha \frac{1}{2\sqrt{J_l}}.$$

Thus the bigger α is, the greater is the attainable acceleration of the system's output shaft.

[3] The mean value of the magnetic induction in the gap is understood to be that value which, when multiplied by the gage length of the polar arc, is numerically equal to the integral of the actual induction curve taken over the whole length of the polar arc.

[4] The comparison of ferromagnetic clutches with other types of actuating devices having the same power rating is complicated by the fact that, at the present time, the optimum geometrical dimensions of certain types of mechanisms have not been developed (for example, hydraulic mechanisms, ferromagnetic and friction clutches). Moreover, the power developed by the clutches can vary over a considerable range, depending on the nature of the cooling system.

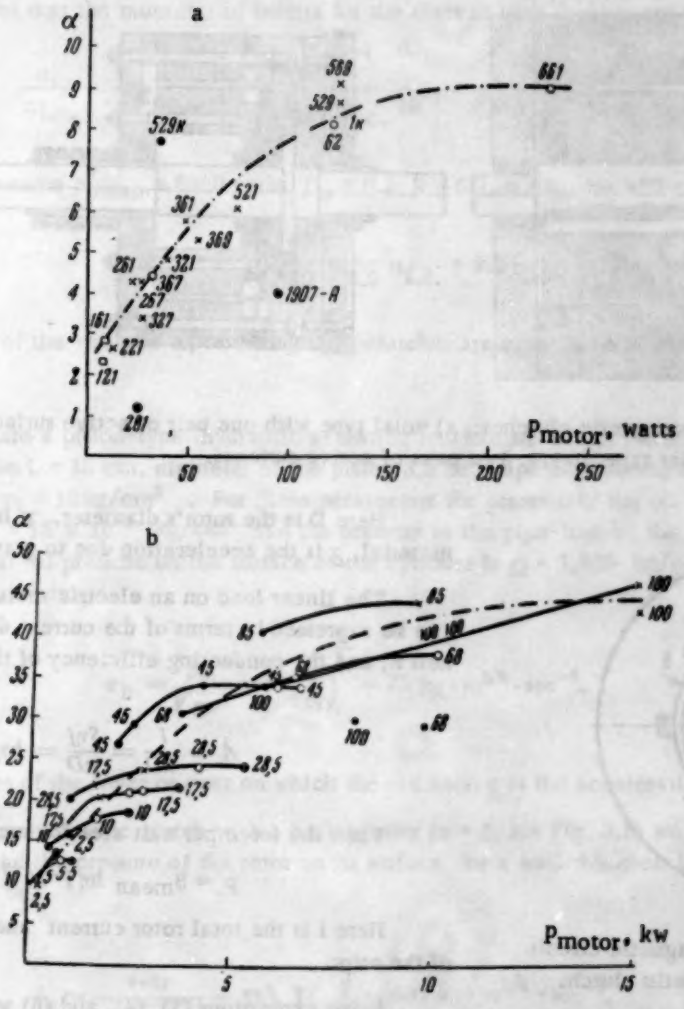

Fig. 2. Dependence of α on the power: a) for series SL electric motors, b) for electric motors of the PN series. The numbers adjacent to the points denote the type of motor. SL-569 is designated by 569. The signs used for the points in Fig. 2,a correspond to the rpm's of the motors: ●) 850, ○) 2400-3800, ×) 3000-3800, □) 4000-4500 and ⊕) 5200 rpm. In Fig. 2,b the full curves join points corresponding to one type of electric motor. The point designation corresponds to the motors' rpm's; ●) 1000, ×) 1450-1500, ○) 2000 and ⊕) 2800-2870 rpm.

where α_c and α_{motor} are the $M/\sqrt{J}$ expression for the ferromagnetic clutch and electric motor, respectively.

The linear load on conventional electric motors, depending on the power and other factors, is in the region of $100 < A < 450$ amp/cm, where the upper values of A apply to high-power electric motors.

Then, for n = 1 (for the clutch shown in Fig. 3a) $\alpha_c = (2.2-10)\,\alpha_{motor}$.

Drum-type clutches with hollow cylindrical rotors and having two pairs of active surfaces (Fig. 3b), are compared with direct current electric motors having hollow rotors.

The moment of inertia, referred to 1 cm² of the cylindrical surface of the rotor, is expressed, for both devices, by the same formula:

$$J = \frac{\gamma}{g}\frac{hD^2}{4}. \qquad (4)$$

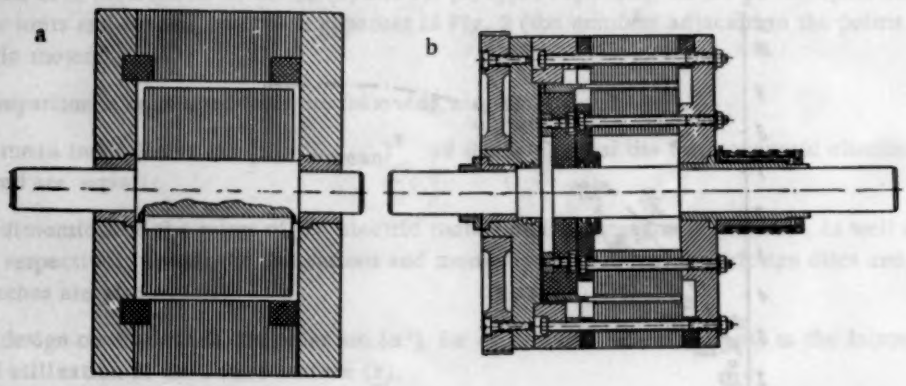

Fig. 3. Ferromagnetic clutches: a) usual type with one pair of active surfaces, b) hollow-rotor type, having two pairs of active surfaces.

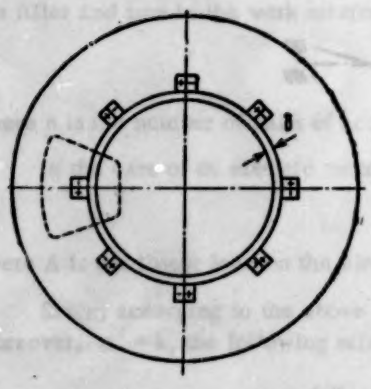

Fig. 4. Cross section of magnetic circuit for a high speed ferromagnetic clutch.

Here D is the rotor's diameter, γ is the density of the material, g is the acceleration due to gravity.

The linear load on an electric motor having a hollow rotor can be expressed in terms of the current density j, rotor thickness h, and the conducting efficiency of the rotor body, η:

$$A = \frac{I}{\pi D} = \frac{S\eta j}{\pi D} = h\eta j. \tag{5}$$

Then the force per unit area for such a motor will be

$$p \approx B_{mean}\, h\eta j \cdot 10^{-7}\ kg/cm^2. \tag{6}$$

Here I is the total rotor current and S is the cross section of the rotor.

Using expressions (1), (4), and (6) we can write

$$\frac{\alpha_c}{\alpha_{motor}} = \frac{(B_{mean}\, kn)_c\, 10^3}{(B_{mean}\, h\eta\, j)_{motor}} \sqrt{\frac{(h\gamma D^2)_{motor}}{(h\gamma D^2)_c}}. \tag{7}$$

Taking into account the equality in geometric dimensions and mean induction, and taking $j = 500\ amp/cm^2$, $k = \eta = 0.7$, $n = 2$ and $\gamma_c = \gamma_{motor}$, we obtain

$$\alpha_c = \frac{2 \times 10^3}{500\, h_{motor}}\, \alpha_{motor} = \frac{4}{h_{motor}}\, \alpha_{motor}. \tag{8}$$

If $h_{motor} = 0.2$ cm, then $\alpha_c = 20\, \alpha_{motor}$.

The performed calculations are approximate but, nevertheless, they offer convincing proof of the preeminence of ferromagnetic clutches in comparison with direct current electric motors. The indicated relationships remain valid for alternating current electric motors.

Let us now turn to a comparison of ferromagnetic and friction clutches. At the same time we will assume that disc clutches are being compared. The unit tangential force q for friction clutches is, as is well known, expressed by the formula

$$q = 0.4\, B^2_{mean}\, f_{fr}\, n_1 \times 10^{-7}\ kg/cm^2. \tag{9}$$

Here f_{fr} is the coefficient of friction, n_1 is the number of pairs of active surfaces.

Taking into account that the moments of inertia for the discs in both devices are the same, we have

$$\frac{\alpha_c}{\alpha_{f.c.}} = \frac{\tau}{q} = \frac{(B_{mean}kn)_c\ 10^{-4}}{0.4(B^2_{mean} f_{fr}\ n_1)_{f.c.}\ 10^{-7}} = \frac{kn \times 10^3}{0.4\ B_{mean} f_{fr}\ n_1}. \tag{10}$$

From here, if we assume $B_{mean} = 8000$ gauss, $f_{fr} = 0.2$, $k = 0.7$, $n = n_1$, we will obtain

$$\alpha_c = \frac{0.7 \times 10^3}{0.4 \times 8000 \times 0.2}\alpha_{f.c.} = 8.7\ \alpha_{f.c.}. \tag{11}$$

Thus, on the basis of the value of α, ferromagnetic clutches are superior to electric motors and friction clutches.

Example:[5] Let us compare a piston-type hydraulic actuating mechanism with a ferromagnetic clutch. Let the actuator's piston-travel be $L = 15$ cm, diameter of the piston 3.5 cm, pipe-line diameter $d = 1$ cm, pipe length $l = 150$ cm, oil pressure $p_1 = 10$ kg/cm^2. For these parameters the pressure of the oil in the cylinder on 1 cm^2 of the piston's surface $g_2 = 15 \times 10^{-3}$ kg/cm^2 and the pressure in the pipe-line on the cylinder surface is 1.82 kg/cm^2. The total oil pressure on the surface of the cylinder is $g_3 = 1.835$ kg/cm^2. The value of α for such an actuating device is

$$\alpha_h = \frac{p_1 r}{\sqrt{mr^2}} = p_1\left(\frac{g}{g_3}\right)^{\frac{1}{2}} = 23\ \text{kg} \cdot \text{m}^{1/2} \cdot \text{sec}^{-1}. \tag{11a}$$

Here r is the radius of the lever or gear on which the rod acts, g is the acceleration due to gravity.

For a two-layer ferromagnetic clutch with a hollow rotor ($n = 2$; see Fig. 3,b) we can take τ to be 0.7 kg/cm^2, $k = 0.7$, and the pressure of the rotor on its surface, for a wall thickness $h = 0.25$ cm, is equal to $g_4 = 0.002$ kg/cm^2. Then

$$\alpha_c = \frac{\tau n k r}{\sqrt{\frac{g_4}{g} r^2}} = \tau n k \sqrt{\frac{g}{g_4}} = 690\ \text{kg} \cdot \text{m}^{1/2} \cdot \text{sec}^{-1}. \tag{11b}$$

The calculations show that, in this particular case, the ferromagnetic clutch is, on the basis of the value of α, 30 times better than the hydraulic clutch. However, it should be noted that for other types of hydraulic actuating devices (for example, the rotating type) the magnitude g_3 can be smaller by an order of one or two, while the working pressure can be chosen to be 100 atmos and greater.

In connection with this, α for such actuating devices can take on values greater than those for ferromagnetic clutches. For the comparison of concrete types of ferromagnetic clutches and hydraulic actuating devices in terms of α one can make use of the formula obtained from dividing (11b) by (11a):

$$\alpha_c = \frac{\tau n k}{p_2}\left(\frac{g_3}{g_4}\right)^{\frac{1}{2}}\alpha_h. \tag{12}$$

Let us now consider the starting times of various devices. The starting time t_s can be approximated by the formula[6]

$$t_s = \int_0^{\omega_n} \frac{J d\omega}{\beta M_n} = \frac{J\omega_n}{\beta M_n}, \tag{13}$$

[5] The example is taken from [2].

[6] Equation (13) is a very approximate one, but its use in this case is justified to the extent that this comparison of the various actuating devices is a qualitative one.

where β is the multiplication factor of the starting moment, which here is assumed to be equal to 1.5 for all the devices, M_n and ω_n are the nominal values of the moment and the angular frequency, respectively.

If in (13) we express M_n in terms of α, we then obtain

$$t_s = \frac{J^{\frac{1}{2}}\omega_n}{\beta\alpha}. \tag{14}$$

In accordance with the above assumptions the multiplication factors of the starting moments and the moments of inertia of the devices being compared are respectively equal. If we further assume that the nominal speeds are equal, then

$$\frac{t_{s_1}}{t_{s_2}} \frac{\alpha_2}{\alpha_1} \quad \text{or} \quad t_{s_1} = \frac{\alpha_2}{\alpha_1} t_{s_2}. \tag{15}$$

Thus the starting times of the actuating devices being compared are inversely proportional to α. For ferromagnetic clutches the starting time turns out to be from 2 to 20 times smaller than for electric motors and several times smaller than for friction clutches. The starting times of hydraulic actuating devices can be, depending on their construction, smaller (for high pressure, rotating actuating devices) as well as larger (for low pressure, piston mechanisms with a long piston travel) than those of ferromagnetic clutches.

Let us compare the electromagnetic time constant of the ferromagnetic clutches to the time constants of other mechanisms.

The magnetic circuit of a ferromagnetic clutch can be achieved by means of several configurations. One construction of a magnetic circuit for a fast-acting ferromagnetic clutch, containing an iron mixture, is shown in Fig. 4. The layout of the magnetic circuit of such a clutch is very similar to a direct current electric motor with the sole difference that the air gaps between adjacent poles, which exist in electric motors to reduce leakage currents, are absent in the clutch. This permits better utilization of the stator's periphery and the choice of a large number of poles. We will show that the electromagnetic time constants of a single-layer, ferromagnetic clutch and an electric motor's field coil associated with one pair of poles, are equal if the dimensions, gaps, and inductions are equal. At the same time we will ignore the leakage currents and ampere-turns, which cause a magnetic flux to be set up in the steel, in comparison to the ampere-turns necessary to set up a magnetic flux in the gap.

Let $Z = \pi D/p$ be the pole width, where D is the rotor's diameter and p is the number of poles.

Then the inductance of the field coil on one pair of poles will be

$$L = \frac{\Phi}{I} W = \frac{B_{mean} SW}{I}. \tag{16}$$

Here I is the current in the field coil, W is the number of ampere turns, $S = Zl$ is the pole area (l is the pole length).

It is known that the magnetic induction, ampere-turns, gap size δ, and magnetic permeability μ are related through the expression

$$B_{mean} = \frac{IW\mu}{2\delta}. \tag{17}$$

The coil resistance is approximated by the formula

$$R = \rho \frac{(l+Z)2W}{q_e}, \tag{18}$$

where q_s is the wire gage, ρ is the specific resistance of the wire.

Taking Equations (16) to (18) into consideration, the electromagnetic time constant of the coil will be

$$T_{em} = \frac{L}{R} = \frac{B_{mean} S q_s}{2I\rho(l + Z)} = \frac{\mu W S q_s}{4\delta\rho(l + Z)}. \quad (19)$$

In Equations (16) to (19) all quantities, except μ and W, in accordance with the assumptions made earlier, are equal for both devices.

As a result of the equality of the magnetic inductions, and taking into account the fact that the magnetic permeability of the mixture μ_{mix} is 5 to 8 times greater than the permeability of air μ_a, we can write

$$IW_c\mu_{mix} = IW_m\mu_a. \quad (20)$$

If $J_m = J_c$, then $\frac{\mu_{mix}}{\mu_a} = \frac{W_m}{W_c} = 5\text{-}8$ and, therefore, the product μW remains constant in (18) for both devices.

In this way, the time constants of the ferromagnetic clutch's control winding and the electric motor's field coil are equal when their dimensions, gap sizes, and magnetic inductions are equal.

The control power for ferromagnetic clutches is 5-8 times smaller than the excitation power for a direct current electric motor since $\mu_a = 5\text{-}8\ \mu_{mix}$. Taking into account the fact that the excitation power comprises only 3-10% of the motor's total power, it should be noted that the power required to control a ferromagnetic clutch represents only 0.6-2% of the transmitted power.

The small controlling power required for ferromagnetic clutches permits the use of quick-response, inertialess, control units (e.g., electronic) to secure the forced operating mode of the actuating mechanism and to raise the quality of the whole system.

The above comparisons of the various devices specified equality in their dimensions, i.e., the equality of the active surface. Obviously, the ferromagnetic clutch can, with the help of great pressure, develop from 2 to 10 times more power than the electric motor. For the same power, the active area Dl in the ferromagnetic clutch can be chosen to be 2 to 10 times smaller, which results, approximately, in an equal reduction of the time constant and clutch control power.

It should be noted as well that ferromagnetic clutches can be made with a large number of poles, which also results in a significant reduction in the time constant.

The considerations presented here show that the time constant of ferromagnetic clutches will be considerably smaller than the time constant of an electric motor of the same power rating. This is confirmed by experimental results. Thus for a clutch with $M_n = 10$ kg·m the time constant turned out to be equal to 20 msec.

The above considerations are also quite applicable to the comparison of ferromagnetic clutches with friction types, which leads to the following results: for clutches having equal dimensions, gaps, and magnetic inductions, the time constants of the coils are equal, while the control power for the ferromagnetic clutches is 5 to 8 times smaller than for the friction ones.

The dynamic properties of ferromagnetic clutches are determined to a significant extent by their construction. Since in such clutches the torque is determined by the magnetic flux, designs aimed at decreasing the response time must take into account means of ensuring a quick build-up of the flux. In particular, to minimize eddy currents, the magnetic circuit should be made of a blended iron having a low magnetic resistance and a high resistance to current; the elimination of all short-circuited turns must be ensured. Thus, for example, the clutch's rotor should be a split type. Clutches with a liquid filler have a shorter response time since the motion of iron particles in a liquid medium is much more free than in a dry powder. To decrease the electromagnetic time constant it is desirable to design the clutch to have many poles, which permits a reduction in the volume of iron involved in a pair of pole pieces.

However, execution of the indicated recommendations does not always guarantee the proper fast response of the clutches. To confirm this let us turn to some experimental results. Experiments were carried out on a

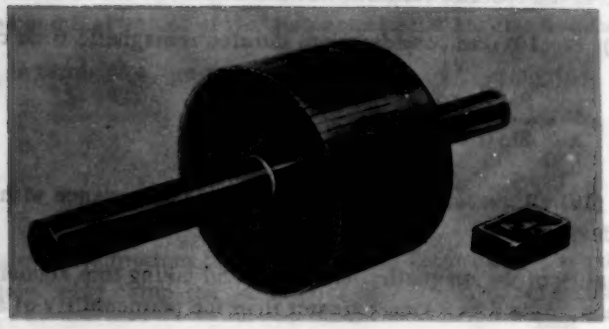

Fig. 5. Split rotor of a two-layer ferromagnetic clutch.

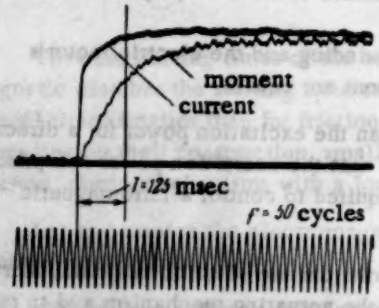

Fig. 6. T is the build-up time of the moment in a clutch with unsealed slots.

cylindrical, two-layer, ferromagnetic clutch with rotor dimension D = 150 mm and width of active area 65 mm, designed for a moment M = 10 kg·m. The rotor in the clutch was a split type, as shown in Fig. 5, and the magnetic circuit was a blended one. As experiments showed, the magnetic flux practically coincided with the electric current. One could suppose that in such a construction the moment must also coincide with the current, but experimental results have shown that the moment lags behind the current quite appreciably (see the oscillogram in Fig. 6).

The lag of the moment build-up behind the magnetic flux is explained by the motion of the iron particles, under the action of centrifugal forces, through the rotor slots, from the inside gap to the outside one. When voltage is applied to the control windings the iron particles return, under the influence of the magnetic flux, to the inside gap. This process occurs in a certain finite length of time. Moreover, the steady state value of the moment sets in after all the particles have migrated. This last is confirmed by experimental results: after the slots were sealed the build-up of the moment in the clutch practically coincided with the current, as is apparent from the oscillogram in Fig. 7.

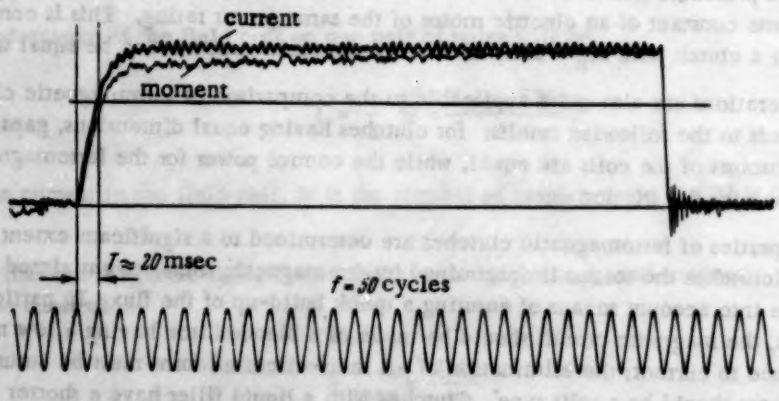

Fig. 7. T is the build-up time of the moment in a clutch with sealed slots.

The clutch was a four-pole one, with equivalent gap $2\delta = 0.6$ cm, $B_{mean} = 7000$ gauss and $k = 0.5$. The control power did not exceed 50 watts which permitted the use of an electronic control unit and guaranteed triple or quadruple forcing. The electromagnetic time constant of such a clutch turned out to be 15-20 msec which is less than for electric motors of the same power.

Ferromagnetic clutches do have some shortcomings.

Under the condition of continuous slipping the clutches generate considerably more heat per unit area than electric motors; as a result considerable effort must be put into its elimination.

Under high speeds of rotation centrifugal forces disrupt the normal operation of the clutch and, at the same time, the control power increases.

The bearings for the clutches require very careful design with seals to prevent the escape of the mixture, especially in the presence of heating.

The nonlinearity of the clutch's static characteristic and the impossibility of achieving reversal with one clutch necessitate the application of special arrangements for switching the clutches in control systems, thus providing, in particular, rectification of the characteristic and the production of a reversal.

SUMMARY

1. The properties of ferromagnetic clutches make them very suitable for use as actuating devices in fast-response automatic control systems.

2. The starting time and control power for ferromagnetic clutches are considerable smaller than for other arrangements (e.g., electric motors). On the basis of α, the ferromagnetic clutches are significantly superior to electric motors, friction clutches, and, in some cases, hydraulic actuating devices. The negligible control power required for ferromagnetic clutches permits the use of a fast-response control unit (for example, an electronic one) having a small time constant, which leads to an increase in the quality of the system.

3. The response time of ferromagnetic clutches greatly depends on their construction. The reduction of the response time requires means of ensuring a rapid build-up of the magnetic flux, as well as means of preventing the possible migration of iron particles between gaps, under the influence of centrifugal forces.

In conclusion the author expresses his gratitude to A. A. Feldbaum for his comments on the paper and his help.

Received June 14, 1957

LITERATURE CITED

[1] Iu. N. Anosov, Electromagnetic Clutches [in Russian] (Oborongiz, 1952).

[2] V. A. Trapeznikov, "Concerning forms of auxiliary energy in automatic systems," Izv. AN SSSR, OTN, No. 12 (1945).

[3] B. S. Sotskov, "Method of designing electromagnetic clutches," Automation and Remote Control (USSR) 12, 4 (1951).

[4] I. M. Postnikov, Design of Electric Motors [in Russian] (GITTL, 1952).

[5] T. A. Glazenko, "Transient processes in an electric drive system equipped with an electromagnetic clutch with a ferromagnetic filler," Elektrichestvo No. 12 (1954).

[6] V. G. Zusman and O. N. Tatur, "Electromagnetic clutches and their application in machine design," "Elektrichestvo No. 3 (1955).

[7] A. S. Pairiale and P. D. Tilton, "Characteristics of some magnetic fluid clutch servo-mechanisms," Trans. AIEE, 69, 1 (1950).

[8] I. Rabinov, Magnetic Fluid Clutch Machinery, 3. (Lloyd, 1949) p. 352. Elektrotech. Z, 71, 147 (1950).

ADDITIONS TO THE TABLE OF OPTIMAL CHARACTERISTICS GIVEN BY SOLODOVNIKOV AND MATVEEV

N. A. Smyrova

(Leningrad)

In a paper by V. V. Solodovnikov and P. S. Matveev [1], devoted to the synthesis of corrective devices for servo systems on the basis of given requirements on the dynamic accuracy in the presence of noise, there was given a table of optimal characteristics. Expressions were given in this table for the optimal impulse transient, k(t), and transfer, $\phi(s)$, functions, and also the mean-square error for different spectral densities of the random components of effective signal and noise, when certain first coefficients of error, C_0, C_1, C_2, ..., are given. The gradual accumulation of computed results allows this table of optimal characteristics to be expanded, which might be quite useful for calculations.

This paper presents computed results which supplement the table of the paper cited.

We shall consider the case when the spectral density of the noise has the form:

$$S_n(\omega) = \frac{2\alpha\beta^2(\omega^2 + a^2 + \omega_0^2)}{\omega^4 + 2(a^2 - \omega_0^2)\omega^2 + (a^2 + \omega_0^2)^2}, \tag{1}$$

The spectral density of the random component of the effective signal, $S_m(\omega)$, equals zero, and the dynamic accuracy of the reproduced effective signal is determined by given values of the error coefficients, C_0, C_1, C_2, C_3 and C_4. This last condition corresponds to an effective signal in the form of a fourth-degree polynomial in time (r = 4).

In this case, the optimal transient function has the form:

$$\begin{gathered} k(t) = A_0 + A_1 t + A_2 t^2 + A_3 t^3 + A_4 t^4 + B_1 e^{bT} + B_2 e^{-bT} + \\ + K_1 \delta(t) + D_1 \delta(t - T) \text{ for } 0 \leqslant t \leqslant T, \\ k(t) = 0 \quad \text{for} \quad t > T, \end{gathered} \tag{2}$$

where $b = \sqrt{a^2 + \omega_0^2}$.

The optimal transfer function is defined by

$$\begin{aligned} \Phi(s) = {} & \frac{A_0}{s}(1 - e^{-sT}) - \frac{A_1}{s^2}[e^{-sT}(Ts + 1) - 1] - \\ & - \frac{A_2}{s^3}[e^{-sT}(T^2s^2 + 2Ts + 2) - 2] - \\ & - \frac{A_3}{s^4}[e^{-sT}(T^3s^3 + 3T^2s^2 + 6Ts + 6) - 6] - \\ & - \frac{A_4}{s^5}[e^{-sT}(T^4s^4 + 4T^3s^3 + 12T^2s^2 + 24Ts + 24) - 24] + \\ & + \frac{B_1}{s - b}[1 - e^{-(s-b)T}] + \frac{B_2}{s + b}[1 - e^{-(s+b)T}] + K_1 + D_1 e^{-sT}. \end{aligned} \tag{3}$$

The coefficients A_0, A_1, A_2, A_3, A_4, B_1, B_2, K_1 and D_1, entering into Formulas (2) and (3), are the solutions of the following system of nine equations:

$$-2ab^5A_0+2b^6(a^2-\omega_0^2)A_1+4ab^4(3\omega_0^2-a^2)A_2+12b^3(b^4-8a^2\omega_0^2)A_3-$$
$$-48a(5\omega_0^4-10a^2\omega_0^2+a^4)A_4-b^9B_1+b^9B_2+2b^{10}K_1=0, \tag{4}$$

$$2\omega_0^2b^5A_0-4a\omega_0^2b^6A_1+4\omega_0^2b^4(3a^2-\omega_0^2)A_2-$$
$$-48a\omega_0^2b^3(a^2-\omega_0^2)A_3+48\omega_0^2(5a^4-10a^2\omega_0^2+\omega_0^4)A_4+$$
$$+b^9(b-a)B_1+b^9(b+a)B_2=0, \tag{5}$$

$$-2ab^5A_0-2b^6(a^2-\omega_0^2+ab^3T)A_1-$$
$$-2b^4[ab^4T^2+2b^3T(a^2-\omega_0^2)-2a(3\omega_0^2-a^2)]A_2-$$
$$-2b^3[ab^5T^3+3b^4T^2(a^2-\omega_0^2)-6ab^2T(3\omega_0^2-a^2)+6(b^4-8a^2\omega_0^2)]A_3-$$
$$-2[ab^6T^4+4b^5T^3(a^2-\omega_0^2)-12ab^4T^2(3\omega_0^2-a^2)+$$
$$+24b^3T(b^4-8a^2\omega_0^2)+24a(5\omega_0^4-10a^2\omega_0^2+a^4)]A_4+$$
$$+b^9e^{bT}B_1-b^9e^{-bT}B_2+2b^{10}D_1=0, \tag{6}$$

$$2\omega_0^2b^5A_0+2\omega_0^2b^6(b^2T+2a)A_1+$$
$$+2\omega_0^2b^4[b^4T^2+4ab^3T+2(3a^2-\omega_0^2)]A_2+$$
$$+2\omega_0^2b^3[b^5T^3+6ab^4T^2+6b^2T(3a^2-\omega_0^2)+24a(a^2-\omega_0^2)]A_3+$$
$$+2\omega_0^2[b^5T^4+8ab^5T^3+12b^4T^2(3a^2-\omega_0^2)+$$
$$+96ab^3T(a^2-\omega_0^2)+24(5a^4-10a^2\omega_0^2+\omega_0^4)]A_4+$$
$$+b^9(b+a)e^{bT}B_1+b^9(b-a)e^{-bT}B_2=0, \tag{7}$$

$$TA_0+\frac{T^2}{2}A_1+\frac{T^3}{3}A_2+\frac{T^4}{4}A_3+\frac{T^5}{5}A_4+$$
$$+\frac{e^{bT}-1}{b}B_1-\frac{e^{-bT}-1}{b}B_2+K_1+D_1=1-C_0, \tag{8}$$

$$\frac{T^2}{2}A_0+\frac{T^3}{3}A_1+\frac{T^4}{4}A_2+\frac{T^5}{5}A_3+\frac{T^6}{6}A_4+$$
$$+\frac{e^{bT}(bT-1)+1}{b^2}B_1-\frac{e^{-bT}(bT+1)-1}{b^2}B_2+TD_1=C_1, \tag{9}$$

$$\frac{T^3}{3}A_0+\frac{T^4}{4}A_1+\frac{T^5}{5}A_2+\frac{T^6}{6}A_3+\frac{T^7}{7}A_4+$$
$$+\frac{e^{bT}(b^2T^2-2bT+2)-2}{b^3}B_1-\frac{e^{-bT}(b^2T^2+2bT+2)-2}{b^3}B_2+T^2D_1=-C_2, \tag{10}$$

$$\frac{T^4}{4}A_0+\frac{T^5}{5}A_1+\frac{T^6}{6}A_2+\frac{T^7}{7}A_3+\frac{T^8}{8}A_4+$$
$$+\frac{e^{bT}(b^3T^3-3b^2T^2+6bT-6)-6}{b^4}B_1-$$
$$-\frac{e^{-bT}(b^3T^3+3b^2T^2+6bT+6)+6}{b^4}B_2+T^3D_1=C_3, \tag{11}$$

$$\frac{T^5}{5}A_0+\frac{T^6}{6}A_1+\frac{T^7}{7}A_2+\frac{T^8}{8}A_3+\frac{T^9}{9}A_4+$$
$$+\frac{e^{bT}(b^4T^4-4b^3T^3+12b^2T^2-24bT+24)-24}{b^5}B_1-$$
$$-\frac{e^{-bT}(b^4T^4+4b^3T^3+12b^2T^2+24bT+24-24)}{b^5}B_2+T^4D_1=-C_4 \tag{12}$$

The mean-square value of the noise at the output of the optimal system is determined by the expression

$$\frac{\varepsilon^2}{\beta^2} = \frac{2a}{b^2}\left\{\left[A_0 - \frac{2}{b^4}(3\omega_0^2 - a^2)A_2 - \frac{24}{b^8}(5\omega_0^4 - 10a^2\omega_0^2 + a^4)A_4\right](1 - C_0) + \right.$$
$$\left. + \left[A_1 - \frac{6}{b^4}(3\omega_0^2 - a^2)A_3\right]C_1 - \left[A_2 - \frac{12}{b^4}(3\omega_0^2 - a^2)A_4\right]C_2 + A_3C_3 - A_4C_4\right\}. \qquad (13)$$

Using the optimal characteristics provided by (2)-(13), corresponding to the case when r = 4, we can transfer our attention from them to the cases when r = 3, 2 or 1, i.e., to the cases when the effective input signal is expressed by a polynomial of the third, second or first degree in time.

To do this, it is sufficient to carry out the following:

1) for r = 3, in Formulas (2)-(13) set $A_4 = 0$, and discard Equation (12) from the system (4) through (12);

2) for r = 2, in Formulas (2)-(13) set $A_4 = A_3 = 0$, and discard Equations (11) and (12) from the system (4) through (12);

3) for r = 1, in Formulas (2)-(13) set $A_4 = A_3 = A_2 = 0$, and discard Equations (10), (11) and (12) from the system (4) through (12).

It is easily verified that the cases r = 1 and r = 2 give the same results as are to be found in the referenced paper [1] (Cf. items VII and VIII).

Thus, Formulas (2)-(13) supplement the table of paper [1], and provide the possibility of computing optimal system characteristics when the effective signal is expressed as a third-degree or fourth-degree polynomial in time, and the noise spectral density has the form given in (1). Moreover, the example considered here shows that, for setting up a table of optimal characteristics, it suffices to provide complete data only for the effective signal with the most complex form (in the given case, with r = 4), and to state, for the remaining cases, which of the coefficients are to be set equal to zero, and which of the equations are to be discarded.

Received July 19, 1957

LITERATURE CITED

[1] V. V. Solodovnikov and P. S. Matveev, "Synthesis of correcting devices for servo systems in the presence of noise under given requirements on dynamic accuracy," Automation and Remote Control (USSR) 16, 3 (1955).

LIST OF EXISTING LITERATURE ON MAGNETIC AMPLIFIERS AND CONTACTLESS MAGNETIC COMPONENTS

1. General

M. A. Boiarchenkov, "Seminar on magnetic amplifiers and contactless magnetic components," Automation and Remote Control (USSR) 17, 12, 1129 (1956).*

N. P. Vasil'eva, "Commission for magnetic amplifiers and contactless, magnetic components, "Automation and Remote Control (USSR) 17, 5, 488 (1956).*

N. I. Chicherin, "Seminar on magnetic amplifiers and contactless components," Automation and Remote Control (USSR) 17, 5, 488 (1956).*

Report of the Interdepartmental Conference on the Technology of Manufacturing Magnetic Amplifiers (April 10-12, 1956) [in Russian] (Leningrad, 1956).

"Conference on the technology of manufacturing magnetic amplifiers," Vestnik Elektropromyshlennosti No. 8 79-80 (1956).

2. Magnetic materials

1. Magnetic materials and magnetic measurements.

O. I. Aven, "Magnetic alloys for magnetic amplifier cores and their characteristics when magnetized simultaneously by direct and alternating fields," Automation and Remote Control (USSR) 17, 4, 347-352 (1956). 7 fig., 5 tables.*

E. I. Gurvich. The Dependence of the Magnetic Properties of Magnetically-Soft Alloys on the Frequency of Magnetic Polarity-Reversal and Thickness of Lamination (Candidate's Dissertation) [in Russian] (MEI, 1956).

E. I. Gurvich, "Measurement of the properties of magnetically-soft materials by a bridge method," Electrichestvo No. 1, 64-68 (1956). 4 illust. Bibl. 2.

V. I. Evseev, "Ferrites," Electrichestvo No. 9, 23-31 (1956). 17 illust.

B. E. Kubyshin "Measurement of the dynamic magnetic characteristics of ferromagnetic materials and the isolation of losses in them," Proceedings of the Institute of Electrical Engineering [in Russian] (AN Ukr. SSR, 1955) Issue 12, pp. 43-69.

"Magnetic measurements and investigations," Trudy VNIIM [in Russian] (Mashgiz, 1956) Issue 29, p. 89.

R. M. Bozorth, "The physics of magnetic materials," Electrical Engineering, 75, 2, 134-140, (1956). 12 fig., 15 Bibliogr.

F. Foniok, J. Rusz, "Permaloje – ich technologia i zastosowanie," Przeglad. Elektrotechn. 31, No. 10-11, 603-607 (1955).

G. H. Dion, "Les caracteristiques magnetiques des aciers. Leurs rapports avec la structure. Application á une methode de controle non destructif," Mécanique (France) No. 11 (1955). Referet. Zhur. Elektrotekh. 2, 2680 (1957).

Th. D. Gordy. Magnetic Characteristics of Round Wound Cores. (Doct. diss. Rensselaer Polytechn. Inst.) 1955. Diss. Abstrs, 15, 11, 2146 (1955). Referat. Zhur. Elektrotekh. 2, 2691 (1957).

H. Hesselbach, "Eisen Silizium-Elektrobleche. Entwicklung und Forschritte," Techn. Messen (Germany) 240, 23-24 (1956) 9 Bibliogr. Referat. Zhur. Elektrotekh. 2, 2691 (1957).

Murakami Kikuti, "The measurement of the magnetizing characteristic of a magnetic amplifier core using a vibration rectifier," Dziki Gakkai Dzassi (J. Inst. Electr. Engrs. Japan) 75, 7, 746-752 (1955).

*See English translation.

H. W. Lord, "A delta B-indicator," Electrical Engineering, 75, 11, 1012-1013, (1956) 1 fig., 1 Bibliogr.

"Magnetic materials," Ekspress-inf. VINITI Issue 9, March, 1957. (VT-37). – Electronics, 29, 10, 204-207 (1956). 5 fig.

Z. Rabiez, "Przystawka do badania petli histerezy ferroelektrykow za pomoca oscylografu," Przeglad Telekomun. 28, 12, 421-422 (1955).

Procédé de fabrication d'un noyau magnétique à cycle d'hystérésis sensiblement rectangulaire N. V. Philips' Gloeilampenfabrieken. Frants. Pat. kl. N 01 d, No. 1, 116, 334, May 7, 1956.

Procédé permettant d'obtenir un noyau magnétique doué d'un cycle d'hystérésis pratiquement rectangulaire N. V. Philips' Gloeilampenfabrieken. Frants. pat. kl. N 01 d, No. 1.115.324, December 11, 1953. Pays-Bas. Published April 23rd, 1956.

2. Core production techniques

"Rationalization of an impregnation process in the production of magnetic amplifiers." (Proposed by K. S. Marchenko). Sb. rats. predlozh M-vo Elektrotekhn. prom-sti SSSR, Issue 7 (65), 9-10 (1956). Referat. Zhur. Elektrotekh. 1, 1192, (1957).

L. I. Ozerian, "Production of large wound cores using magnetically-soft alloy ribbon," Trudy NII MSP, Issue 2 (20), 60-76 (1956). 11 fig., 8 Bibl.

3. General Considerations in the Theory and Design of Nonlinear Magnetic Circuits

L. A. Bessonov. Self-Modulation and Certain Dynamic Effects in Electrical Circuits Containing Steel (Doctorate Dissertation) [in Russian] (VEEI, Moscow, 1956).

L. A. Bessonov, "Calculation of ferroresonant systems containing saturable reactors and magnetic amplifiers," Collection of Articles on Automation and Electrical Engineering [in Russian] (IAT AN SSSR, Moscow, 1956) p. 221-230. 5 fig., 2 Bibl.

S. A. Ginzburg, "The general theory of networks containing nonlinear magnetic components," Automation and Remote Control (USSR) 17, 9, 799-810 (1956). 10 fig., 8 Bibl.*

I. Ia. Lekhtman, "Graphonalytical method of calculating the characteristics of magnetic circuits under the simultaneous action of direct and alternating fields (Continuation)," Automation and Remote Control (USSR) 17, 3, 264-273, (1956). 10 fig., 1 Bibl.*

4. Magnetic Amplifiers

1. Monographs, books and bibliographies.

M. A. Rozenblat, Magnetic amplifiers [in Russian] [Soviet Radio, 1956]. 333 fig., 260 Bibl.

I. I. Solov'ev, Automation of Power Systems [in Russian] (GEI, 1956) p. 207-210.

G. V. Subbotina, "Collection of national and foreign literature on magnetic amplifiers for 1951-1954, 1955," Automation and Remote Control (USSR) 17, 5, 471-487; 9, 858-864 (1956).*

M. Gabler, J. Haškovec and E. Tománek, Magnetické zesilovače (SNTL, praha) 1956. 252 pages, 291 fig., 3 tables, 20 Bibl.

2. Reviews

O. N. Aven and S. M. Domanitskii, "Magnetic amplifiers," Physics at School (USSR) 5, 12-14 (1946). 4 fig.

*See English translation.

N. P. Vasil'eva, "Magnetic amplifiers and their application in the automation of agricultural electrical systems," Automation of Production Processes in Agriculture [in Russian] (AN SSSR, Moscow 1956) p. 395-400. 6 fig. 1 table.

N. P. Vasil'eva, "Magnetic amplifiers," Promyshlenno-ekonomicheskaia Gazeta 41 (May 4, 1956).

Adolfo G. Abrines, "Servosistemas y su applicatión al tipo naval," Rev. Cálculo Automát. Y Cibernet. (Spain) 4, 9, 1-42 (1955); Referat. Zhur. Elektrotekh. No. 11 (1956).

G. M. Attura, "Consider using hybrid amplifiers," Control Engineering 3, 5, 77-82 (1956) 14 fig.

F. Bergtold, "Magnetverstärker—Steuerungselemente von wachsender Bedeutung," Ind.-Anz. 78, 7, 89-90 (1956). Referat. Zhur. Elektrotekh. 12, 22053 (1956).

H. C. Bourne and R. M. Saunders, "Magnetic amplifiers serve to teach power modulators," Electrical Engineering 75, 943-947 (1956). 14 fib. 3 Bibl.

S. J. Campbell, "Magnetiska förstärkare för industrins behov." Kraft och Ljus 29, 1, 9-13 (1956). Referat. Zhur. Elektrotekh. 11, 1956.

S. J. Campbell "Magnetic amplifiers in industrial control systems. I. II.," Electr. Manufact., 56, 5, 145-149, (1955). 14 fig. No. 12.

M. Guénod and J. Wahl, Le transducteur et quelques-unes de ses applications industrielles" Indicateur industr. 36, 637, 5 (1955).

"Cypak-systems - a new concept in industrial control," - Westinghouse Engineer, 15, 4, 114-119 (1955). Referat. Zhur. Elektrotekh. 3, 4773, (1956).

W. F. Eagan, "Applying magnetic amplifiers," Allis Chalmers Electr. Rev. 21, 3, 20-29, (1956). 15 fib., 3 Bibl.

M. Fujisawa, J. Inagaki, E. Hayashi and M. Toshimitu, "Industrial applications of magnetic amplifiers," Toshiba Rev. (Japan) 10, 10, 879-895 (1955).

D. C. Harris, "Some introductory notes on the magnetic amplifier ," Electr. Contractor and Retailer, 54, 635, 36-39 (1956). 11 fig. Referat. Zhur. Elektrotekh. 12, 22058 (1956).

Kobaiasi, "Magnetic amplifier circuits," Deisi koge, Electronician (Japan) 4, 2, 50-51 (1955).

Kobaiasi, "Principles of operation and examples of application of magnetic amplifiers," Deisi koge, Electronician (Japan) 4, 7, 34-38 (1955).

T. Konopiński, Zasady działania szeregowych układów wzmachiaczy magnetycznych, Przegl. Telekomun. 28, 2, 53-58 (1955).

T. Konopiński, Zastosowanie wzmachiazcy magnetycznych do wzmacniania pradów i napviec stalych oraz przebiegow wolnozmiennych, "Przegl. telekomun. (Poland) 28, 18, 398-405 (1955).

U. Krabbe, "Magnetic amplifiers invade heavy-duty systems," Control Engineering, 2, 9, 90-96 (Sept. 1955) 10 fig.

"Les transducteurs," Usine Nouvelle 30, 33-34 (1956) 9 fig.

"Magnetic amplifiers," Automation, 3, 8, 92-93 (1956).

"Magnetic amplifiers," Electrical Engineering, 75, 1, 27 (1956); Progress in Engineering during 1955. Reviewed by AIEE Techn. Committees.

K. Mangel, "Principles of magnetic amplifiers," Elevator World, 4, 8, 7-9 (1956) 8 figs.

A. J. Nathan, "The development and use of magnetic amplifiers," Electr. Inds. Export, 56, 1, 29-31 (1956), 6 fig.

W. Sorokine, Les amplificateurs magnétiques, Electronique industr. (France) 5, 162-166 (1955).

H. F. Storm, "Thesis projects in magnetic amplifiers," Electrical Engineering 75, 10, 942-943 (1956) 2 fig., 1 Bibl.

Transduktoren zum Steuern und Regeln, Brennstoff-Chemie 36, 3-4 (1955). Techn. Umschau, 16.

3. Theory of the operation of a magnetic amplifier

R. Kh. Bal'ian, "Push-Pull magnetic amplifier with a constant current output," Automation and Remote Control (USSR) 17, 2, 160--171 (1956) 11 fig., 3 tables, Bibl.;* Referat. Zhur. Elektrotekh. 12, 22056 (1956).

N. P. Vasil'eva and M. A. Boiarchenkov, "Effect of overall feedback on a multi-stage magnetic amplifier," Automation and Remote Control (USSR) 17, 10, 930-935 (1956) 4 figs., 2 Bibl.*

A. A. Golovan, Magnetic Amplifier Circuits Utilizing Modulation Currents (Dissertation) [in Russian] (MEI, 1956).

A. B. Gorodetskii, "Comparison of some typical magnetic amplifier circuits incorporating internal feedback loops," Automation and Remote Control (USSR) 17, 2, 147-159 (1956) 12 fig.;* Referat. Zhur. Elektrotekh. 12, 22062 (1956).

L. A. Grigorian, "Design of parametric, measuring units for a voltage regulator with a magnetic amplifier," Collection of Scientific Papers of the Polytechnic Institute of Erevan [in Russian] Issue 2, 12,57-71 (1956) 10 fig. 8 bibl.

A. I. Dem'ianchik, "Fast-response magnetic amplifiers for tracking systems with ac motors," Automation and Remote Control USSR) 17, 3, 250-263 (1956),* 18 fig. 1 table, 5 Bibl.; Referat. Zhur. Elektrotekh. 12, 22060 (1956).

A. G. Zdrok, G. P. Smirnov, "The operation of a saturable reactor with a semiconductor rectifier and an inductive load," Elektrichestvo 10, 44-47 (1956) 5 fig. 2 Bibl.

I. B. Negnevitskii, D. A. Lipman, "Concerning the theory of an "ideal" choke-coupled magnetic amplifier, "Elektrichestvo 1, 8-16, (1956) 12 fig., 6 Bibl.

A. M. Pshenichnikov, "The application of magnetic null-circuits in telemetering and registering devices," Elektrichestvo 1, 55-60 (1956) 8 fig., 4 Bibl.; Referat. Zhur. Elekrotekh. 2, 4019 (1957).

M. A. Rozenblat, "Principles of designing magnetic amplifiers with a low sensitivity threshold, "Automation and Remote Control (USSR) 17. 1, 66-77 (1956) 8 fig. 2 tables 11 Bibl.*

M. A. Rozenblat, "Theory and design of a modulator operating on the principle of frequency doubling," Radiotekhnika 11, 8, 36-51 (1956) 10 fig. 10 Bibl.

G. V. Subbotina, "A magnetic amplifier with a shunt load and its application in relay protection systems," Automation and Remote Control (USSR) 17, 6, 540-548 (1956) 8 fig., 6 Bibl.*

N. M. Tishchenko, "Characteristics of magnetic amplifiers having a feedback loop," Automation and Remote Control (USSR) 17, 6, 532-539 (1956) 9 fig., 6 Bibl.*

B. V. Shamrai, The Analysis of Operation of Push-pull Magnetic Amplifiers with Mixers in the Static Mode of Operation and Methods of their Design (Dissertation) [in Russian] (Leningrad Institute of Electrical Engineering, Leningrad, 1956).

J. Auricoste, "Servo-amplificateur magnétique à temps de réponse minimum," Automatisme 4, 147-148 (April 1956) 4 fig., 1 table.

Rene Boite, Publs assoc. ing. fac. polytech. Mons 1, 1-18 (1956) 7 Bibl.; Referat. Zhur. Elektrotekh. 2, 3847 (1957).

M. B. Chague, Bulletin de la Societe francaise des Electriciens 6, 61, 14-56 (January 1956) 58 fig.

H. W. Collins, "High-frequency operation of self-saturating magnetic amplifiers," Commun. and Electronics, 20, 500-505 (September 1955) 8 fig. 10 Bibl;. Trans. AIEE, 74, pt. I (1955).

H. W. Collins, "Magnetic amplifier control of switching transistors," Electrical Engineering 75, 9, 812 (1956) 2 fig. 2 Bibl.

*See English translation.

P. A. V. Deinse, "Magnetische versterkers van het amoorspoel-type," Electro-techniek 33, 24, 272-275 (1955).

W. A. Geyger, "Self-balancing magnetic servo amplifiers," Electronics 29, 3, 196-199 (1956) 4 fig. 12 Bibl.

W. A. Geyger, "Magnetic switch transient analyzer," Electronics, 29, 1, 150-151 (1956); Referat. Zhur. Elektrotekh. 1, 1251 (1957).

Kikuti, "The analysis of the ideal half-wave circuit of a magnetic amplifier," Dziki Gakkai Dzassi, J. Inst. Electr. Engrs. (Japan) 75, 6, 617-621 (1955).

U. Krabbe, "The residual time-constant of self-saturating (auto-excited) transductors," Proc. IEE, 103, pt C, 3, 71-80 (1956) 24 fig. 6 Bibl.; Referat. Zhur. Elektrotekh. 12, 22059 (1956).

A. D. Krall and E. T. Hooper, "The operation of the self-balancing magnetic amplifier," Commun. and Electronics, 23, 79-84 (March 1956) 10 fig. 6 Bibl.

G. E. Lynn and J. F. Ringelman, "A signal-discriminating magnetic amplifier," Commun. and Electronics, 23, 97-102 (March 1956) 10 fig., 5 Bibl.

A. G. Milnes and T. S. A. Law, "AC controlled transductors," Proc. IEE C 103, 3, 81-94 (1956) 17 fig., 7 Bibl.; Referat. Zhur. Elektrotekh. 12, 22063 (1956).

Iamaguti Sakurai, "The effect of a rectifier's characteristic on the behavior of a self-saturating magnetic amplifier," Dziki Gakkai Dzassi, J. Inst. Electr . Engs. (Japan) 75, 11, 1361-1368 (1955).

K. I. Selin, "The polyunit saturable reactor," Power Apparatus and Systems 26, 863-867 (1956) 3 fig.; Ekspress-inf., ETP Issue 12 (1957).

K. I. Selin and A. Kusco, "Experimental characteristic of the 3-phase polyunit saturable reactor," Power Apparatus and Systems, 26, 868-871 (1956) 5 fig.; Ekspress-inf., ETP 57 (March 1957).

J. Ch. Travis, "The effect of eddy current on the behavior of magnetic amplifiers," Dissertation Abstracts 15, 10, 1817-1818 (1955).

H. H. Woodson, "Full-wave bridge magnetic amplifiers with inductive loads," Commun. and Electronics, 23, 7-9 (March 1956) 5 fig. 4 Bibl.

D. D. Kotel'nikov and E. I. Klypalo, "Magnetic Amplifier," Class $21a^2$ 18/08, No. 103357 (452411) 745 of June 25, 1955, Biull. izobr. 5, (1956).

Amplificateur magnétique autoéquilibreur et à faible puissance (Industrial Development Co. Establishment). French patent N 03f, N 1. 115. 480, April 25, 1956.

G. Barth, "Ritchungsempfindlicher Magnetverstärker," (Siemens and Halske Akt. Ges.) Patent FRG, $21a^2$, 18/08, No. 936049, December 1, 1955; Referat. Zhur. Elektrotekh. 1, 1235P (1957).

G. Barth, "Richtungsempfindlicher Magnetverstärker," (Siemens und Halske Akt. Ges.) Patent FRG, $21a^2$, 18/08, No. 933872 October 20, 1955.

M. D. H. Belamin, "Elecktrische Steuer-und Regeleinrichtung," (Siemens-Schuckertwerke Akt.-Ges.). Patent FRG, 21c 46/50, No. 928112, May, 23 (1955). Referat. Zhur. Elektrotekh. 1, 1236P (1957).

J. A. Crawford, "Magnetic Amplifiers," US patent, cl. No. 2731521, January 17, 1956; Referat. Zhur. Elektrotekh. 1, 1234P (1957).

Elektromagnetisk forsterker (Firmaet Thomas B. Thrige). Danish patent, cl. 21 d^1, 35, No. 79957, October 10, 1955.

H. M. Ogle and C. N. Hood, "Magnetic Amplifier Circuit," (General Electric Co.) U. S. Patent, cl. 323-89, No. 2.768.345, October 23, 1956.

W. F. Steagal, "Ring Counter Utilizing Magnetic Amplifiers," (Remington Rand Inst.) U. S. patent, cl. No. 2710952, June 14, 1955; Referat. Zhur. Elektrotekh. 1, 1362P (1957).

J. Stone, "Magnetic Amplifier System," Canadian patent No. 517.705, October 18, 1955 (Warren, Webster and Co.)

O. Werner, "Durch Vormagnetisierung regelbare Drosselanordnung," (Simens-Schuckert Akt. Ges.) FRG patent, cl. 21 c, 67/70, No. 926866, December 29, 1955; Referat. Zhur. Elektrotekh. 12, 22082 P (1956).

H. H. Woerdemann, "Ring Modulator Magnetic Amplifier," (North American Aviation Inc.) U. S. patent, cl. 179-171, No. 2.767,257, October 16, 1956.

4. Design of Magnetic Amplifiers

D. I. Ageikin, S. P. Kolosov and N. P. Udalov, Design Handbook for Automatic Control Units [in Russian] (Oborongiz, Chapter 4, 1957).

R. Kh. Bal'ian, "Design of self-saturating magnetic amplifiers," Elektrichestvo 9, 63-67 (1956) 7 fig., 3 Bibl.

A. V. Basharin, "Calculation of a magnetic amplifier's characteristics when magnitized by a dc and an ac field," Elektrichestvo 1, 17-20 (1956) 9 fig., 4 tables.

P. A. Varlashkin, "The design of optimum choke-input magnetic amplifiers," Trudy MEI Issue 16, 99-112 (1956) 14 fig., 5 Bibl.

N. P. Vasil'eva, "Design of push-pull power amplifiers," Automation and Remote Control (USSR) 17, 1, 53-65 (1956) 7 fig., 2 tables, 1 Bibl. Addendum to article, No. 4, Page 361.*

S. Ia. Dunaevskii, "Design constant of magnetic amplifiers," Elektrichestvo (USSR) 2, 15-20 (1956) 7 fig., 3 Bibl.; Referat. Zhur. Elektrotekh. 12, 22054 (1956).

A. Ia. Pisarev, "The design of saturable reactors for a controlled asynchronous servo," Elektrichestvo 5, 10-14 (1956); Referat. Zhur. Elektrotekh. 11 (1956).

M. E. Pokrovskii, "Grapho-analytical design of push-pull magnetic amplifier characteristics," Elektrichestvo 7, 57-60 (1956) 7 fig., 6 Bibl.

L. V. Safris, "The design of a magnetic amplifier from linearized magnetization curves," Collection of Scientific Papers, Rostov Institute IZhDT [in Russian] (Issue 20, 89-106, 1956) 13 fig., 4 Bibl.

L. V. Safris, "The calculation of current in an inductive load connected through a bridge rectifier," Collection of Scientific Papers, Rostov Institute IZhDT [in Russian] 20, 1956).

O. A. Sedykh, "The design of magnetic amplifiers with toroidal cores," Automation and Remote Control (USSR) 17, 5, 445-459 (1956)9 fig., 3 Bibl.*

T. Kh. Stefanovich, "The design of magnetic amplifiers and magnetic relays with the help of universal characteristics," Collection of papers of the MEP on the Automation of home appliances [in Russian] p. 134-141 (1956) 7 fig.; Vestnik Elektropromyshlennosti 6, 45-51 (1956) 7 fig. 10 Bibl; Referat. Zhur. Elektrotekh. 1, 1191 (1957).

V. N. Shestopalov, "The determination of the optimum dimensions of a magnetic amplifier with a Z-type core," Trudy Elektro-tekhniki AN UKr. SSR 13, 146-152, 1956, 1 fig. 1 Bibl.; Referat. Zhur. Elektrotekh. 12, 22055 (1956).

5. Applications

a) For the control of electric motors.

O. I. Aven, E. D. Demidenko, S. M. Domanitskii and E. K. Krug, "Variable speed, electrical actuating device," Automation and Remote Control (USSR) 17, 3, 238-249 (1956) 16 fig. 1 Bibl.*

O. I. Aven, S. M. Domanitskii and A. Ia. Lerner, "Twin-choke circuit of reversible control by a push-push asynchronous motor," Automation and Remote Control (USSR) 17, 8, 717-721 (1956) 7 fig., 3 Bibl.*

D. A. Alenchikov, "The application of power saturable reactors for a regulated actuator with an asynchronous motor," Collection of Papers of the MEP on the mechanization and automation of home appliances [in Russian] p. 155-158 (1956) 5 fig.

* See English translation.

V. I. Artemenko, "Regulated Reversible Actuator," [in Russian] Avt. sv. klass $12d^1$ 35, No. 103630. (452666/6419, January 22nd, 1955) Biull. izobr., No. 6 (1956).

V. I. Artemenko. Speed Control of Electrical Collector Servo Motors by Means of Magnetic Amplifiers (Dissertation) [in Russian] (Moscow 1956).

P. I. Dekhterenko, "Concerning a single choke magnetic amplifier," Avtomatika, Akad. Nauk Ukr. SSR 1, 84-88 (1956) 5 fig. 4 Bibl. Referat. Zhur. Elektrotekh. 1, 850 (1957).

A. G. Efanov, B. M. Gutkin and Iu. R. Reingol'd, "The application of magnetic amplifiers in actuators," Elektrichestvo, 2, 9-14 (1956) 10 fig.; Referat. Zhur. Elektrotekh. 1, 852 (1957).

V. I. Kliuchev. Circuit of Asynchronous Actuator with Saturable Reactors and Excitation of Motor (Dissertation) [in Russian] (MEI, Moscow, 1955).

G. G. Markvarot, Commutatorless Single-Phase Motor. Avt. sv. kl. $21d^2$, 41, No. 103632 (452668/6586, May 4th, 1955) Biull. izobr., No. 6 (1956).

V. D. Nagorskii, "A power tracking actuator with asynchronous motor," Trudy Zhukovskii VVIA 560, 116 (1955), 77 fig., 33 Bibl.

S. S. Roizen and K. Ia. Goosen, "The application of magnetic amplifiers to the automation of electric actuators with direct current motors," Elektrichestvo 2, 59-62 (1956) 5 fig.; Referat. Zhur. Elektrotekh. 1, 854 (1957) [continued in next number].

M. G. Chilikin, M. M. Sokolov and V. I. Kliuchev, "Regulated asynchronous actuator with saturable reactors and excitation of the motor," Elektrichestvo 1, 21-26 (1956) 6 fig., 1 Bibl.

J. H. Chiles, Jr. and A. M. Harrison, "Static control for regulators," Westinghouse Engineer, 15, 5, 162-164 (1955).

M. H. Fischer, Magnetic Amplifier Creeping Speed Control, (Westinghouse Electric Corp.) Canadian Patent No. 509349, January 18, 1955; Referat. Zhur. Elektrotech. 11 (1956).

Fr. S. Malick and C. L. Mershon, Magnetic Amplifier Electrical Position Control System, (Westinghouse Electric Corp.) U.S.A. Patent, cl. 323-89, No. 2725513, November 29, 1955; Referat. Zhur. Elektrotekh. 2, 3945 (1957).

W. Güttinger, "Die Anwendung elektronischer und magnetischer Verstärker für die Steuerung von Antrieben," Bull. Assoc. Suisse des Electr. 47, 2, 45-47 (1956) 8 fig.

J. J. Suozzi, "Magnetic amplifier two-speed servosystem," Electronics, 2, 140-143 (1956) 8 fig., 5 tables.

E. Tománek, B. Dudáš and G. Krůšek, "Transduktorový regulátor pro svařováni pod tavidlem," Elektrotechnik, 1, 2-8 (1956) 16 fig., 5 Bibl.; Engineering, 184, 4696 (1956); Referat. Zhur. Elektrotekh. 11 (1956).

J. F. Young, "Electronic and magnetic amplifier voltage and frequency regulators for electrical machines," Electricity in Industry, 9, 4-8 (1956) 11 fig.

J. Bergh, "Besturen en regelen VI," Polytechn. Tijdschr., All, N 3-4, 73a-76a (1956); Referat. Zhur. Elektrotekh. 2, 21630 (1956).

J. Bergh, "Modern regelingsen bekrachtigingsmethoden voor synchrone draaistrom generatoren," Polytechn. tijdschr., All, N 13-M, 284-287 (1956); Referat. Zhur. Elektrotekh. 12, 21631 (1956).

H. R. Zeller, "Transistor preamplifier feeds tubeless servo," Electronics, 29, 2, 168-169; Referat. Zhur. Elektrotekh. 2, 3844 (1957).

Current-limit Control in Ward-Leonard Drive, (Westinghouse Electric Corp.) Australian Patent, cl. 04.7., No. 165065, September 22, 1955; Referat. Zhur. Elektrotekh. 11 (1956).

H. Roth and W. C. Kaldenberg, "Commutatorless exciter works well," Electrical World, 5 (1956).

M. H. Fisher, "Magnetic amplifier regulated drives in the paper industry," Tappi, 38, 9, 513-522 (1955).

"Application of control regulators to steel operations," Iron and Steel Engr. 32, 8, 132-142 (1955).

E. A. Browning, "Electrical drive systems for modern rolling mills," Blast Furnace and Steel Plant, 44, 3, 299-308 (1956); Referat. Zhur. Elektrotekh. 11, 20140 (1956).

E. F. Boening and J. Kostelac, "Controlling process lines for transformer steel," Electrical Review, 4th Quarter (1955).

Al. Mozina, "Magnetic amplifiers on a high speed accuracy singlestand reversing mill," Blast Furnace and Steel Plant, 6 (1956).

b. For Rectifier Control

I. I. Ratgauz, "Stabilized selenium rectifiers," Elektrichestvo 4, 55-60 (1956) 5 fig.

E. P. Khmel'nitskii, "The use of magnetic amplifiers in the control and protection of power rectifiers by means of electronic pulse circuits," Vestnik Sviazi 3, 10-11 (1956) 2 fig.; Referat. Zhur. Elektrotekh. 12, 22057 (1956).

W. A. Derr and E. J. Cham, "Rectifier Systems and Protective Apparatus therefore," (Westinghouse Electric Corp. U. S. Patent, cl. 321-12, No. 2728043, December 20, 1955; Referat. Zhur. Elektrotekh. 1, 1673 (1957).

Sven Eric Hedström and Robert Svensson, "Transduktorrebler (Allmänna Svenska Elektriska Aktiebolaget) FRG Patent, cl. 21c, 67/70, No. 933102, September 15, 1955; Referat. (Zhur. Elektrotekh.) 12, 22083 P (1956).

Sven Eric Hedstrom and Uno Lamm, "Gleichrichter mit spannungsregelndem Transduktor.," (Allmänna Svenska Elektriska Aktiebolaget) FRG Patent, cl. 21c, 67/10, No. 933101, December 15th, 1955; Referat. Zhur. Elektrotekh. 12, 22085 P (1956).

F. Germann, "Magnetisch geregelte Gleichrichter zum Laden und Puffen von Battreien," Elektrotechn. Z., 8, 4, 116-118 (1956); Referat. Zhur. Elektrotekh. 2, 4304 (1957).

W. Schilling, "Die transduktorgesteuerten oder – geregelten Hochspannungs – Gleichrichter für elektrische Gasreinigung Gasreinigung," Energie (München), 7, 12, 484-487 (1955).

c. In Measuring Circuits

A. V. Kaliaev, "Unit for DC voltage or current measurement," Avt. sv. cl. 21e, 27_{01}, No. 103544 (452585/K-595, November 14, 1953); Biull. izobr., 6, (1956).

L. Borg, "Device for Measuring Direct Current," (Almänna Svenska Elektriska Aktiebolaget) U. S. Patent, cl. 324-127, No. 2712635, July 5, 1955; Referat. Zhur. Elektrotekh. 11 (1956).

L. E. Leikhter, "Magnetic Phase Demodulator," Avt. svid. cl. $24a^4$. 39, No. 103621 (452657/A-8002, December 1, 1954); Biull. izobr., 6, (1956).

Nagano Sakurai, "Magnetic amplifier for phase-shift measurements," Dziki gakkai dzassi, J. Inst. Electr. Engrs. (Japan) 75, 2, 125-128 (1955).

M. Tanaka, J. Yamaguchi and Y. Sacurai, "Magnetic amplifier type recording instrument for electrolysis survey," Corrosion, 12, 11, 33-36 (1956) 7 fib.

R. K. West, "Magnetic amplifiers as applied in instrumentation," Instrum. Practice, 10, 5, 417-420 (1956) 6 fig.; ISA Journ., 3, 3, 93-96 (1953).

d. In Other Automatic Control Systems

C. Bennett, "Automatic arc control," Welding Engr., 40, 4, 34-35 (1955).

J. H. Burnett, "A magnetic thyratron grid control circuit," IRE Convent. Rec., 3, 9, 16-23 (1955); Referat. Zhur. Elektrotekh. 11 (1956).

S. J. Campbell, "The use of magnetic amplifiers in the paper industry," Southern Pulp and Paper Manufacturer, 19, 1, 84-87, (1955); Referat. Zhur. Elektrotekh. 1, 887 (1957).

D. E. Musgrave, "The selection and application of saturable reactors for electric furnace control, "Industr. Heat., 22, 5, 926-928, 930, 934, 936, 1088, 1090, 1092 (1955).

Thermostatensteuerung durch Transduktorrelais, Dtsch. Elektro-Handwerk, 31, 2, 32, Al. 5 (1956); Referat. Zhur. Elektrotekh. 11 (1956).

5. Magnetic Contactless Units

1) Contactless magnetic relays and generators.

N. A. Poliakova, "Contactless Maximum Current Relay," Avt. svid. cl. 21c., 68_{60}, No. 103098 (452173/6455, February 23, 1955) Biull. izobr., 4 (1956).

L. V. Safris, "Transient processes in contactless magnetic relays," Collection of scientific papers of the Rostov Institute IZhDT [in Russian] Issue 20, 113-124 (1956) 14 fig., 7 Bibl.

N. V. Khrushcheva. Characteristics of a Magnetic Relay Operating in a Pulse Circuit (dissertation) [in Russian] (Inst. Elektrotekhniki Akad. Nauk Ukr. SSR, Kiev, 1956).

I. B. Negnevitskii, "Magnetic signal generator," Trudy MEI Issue 18, 211-228 (1956) 11 fig. 3 Bibl.

2) Direct current "transformers." Transformers with excitations.

Gleichspannungswandler mit Transistoren, Elektronik, 5, 10, 271-273 (1956) 7 fig., 2 Tables.

"Combined control voltage regulator," Avtomatika, Akad. Nauk Ukr. SSR 1, 94-95 (1956); Referat. Zhur. Elektrotekh. 2, 3841 (1957).

O. G. Shapovalenko, "Transformers with shunting magnetic flux (new type of magnetic amplifiers)," Avtomatika, Akad. Nauk Ukr. SSR 1, 40-51 (1956) 5 fig., Russian resume, 2 Bibl.

A. D. Drozdov, "Transformer directional, differential, and remote relays," Elektrichestvo 1, 41-49 (1956) 12 fig. 3 Bibl.

D. I. Mikhailov, "Contactless Magnetic Relay," Avt. svid. cl. 21c, 68_{60}, No. 103065 (452143/6790, August 13, 1955); Biull. izobr. 4 (1956).

3) Logical and memory magnetic units.

V. A. Zhozhikashvili, "Telemetering decoders using magnetic units having rectangular hysteresis loops," Automation and Remote Control (USSR) 17, 1, 87-95 (1956)* 6 fig., 2 tables.

L. I. Gutenmakher, Components and Circuits in Contactless Automation Systems [in Russian] (Izd. AN SSSR, 1955).

K. I. Petukhov. The Application of Magnetic Memory Units in Transport Automation Systems (Dissertation) [in Russian] (LETIIZhD, 1956).

I. L. Auerbach, "Applications of bistable ferromagnetic elements," Tele-Tech., 15, 4, 74-75, 160-163 (1956) 5 fig.

I. L. Auerback and S. B. Disson, "Magnetic elements in arithmetic and control circuits," Electrical Engineering 74, 9, 766-770 (1955).

W. J. Dunnet, "Circuit means for selecting the highest or lowest of a plurality of signals," (Westinghouse Electric Corp.) U. S. Patent cl. 340-172, No. 2725549, November 29, 1955.

W. G. Evans, W. G. Hall and R. L. Van Nice, Magnetic Logic Circuits for Industrial Control Systems (Westinghouse Electric Corp.) Pap. 56-91, AIEE General Meeting, 30, 1-32 (1956); Electrical Engineering, 1, 75, (1956); Applications and Industry, 25, 166-171 (July 1956) 9 fig., 3 Bibl.

E. F. Dunkin and D. L. Johnson, Electronic Engineering, 144-150 (1956), Translation in: Vestnik inform. 14, 10-13 (1956).

J. A. Rajchman and A. W. Lo, "The transfluxor," Proc. IRE, p. 321-332 (March 1956). Translation in: Vestnik inform. 23, 1-6 (1956) 16 fig.

*See English translation.

L. P. Hunter and E. W. Bayer, "High speed coincident flux magnetic storage principles," Journal of Applied Physics, 27, 11, 1257-1261 (1956) 6 fig.; Ekspressinf. Issue 12, VT-46-47 (March 1957).

6. Description of Magnetic Amplifier Series. Company Reports on Magnetic Amplifiers and Contactless Elements

D. G. Rozenblit, "Type PMU intermediate magnetic amplifiers," Vestnik Elektropromyshlennosti 11, 21-27, (1956) 10 fig.

T. Kh. Stefanovich, A. M. Liubavin and D. G. Rozenblit, "A series of magnetic amplifiers," Papers of the MEP on the Mechanization and Automation of Household Appliances [in Russian] p. 142-154 (1956) 12 fig.

"Magnetic amplifiers with high power gain," Electronics, 28, 8, 250 (1955).

"Compact control elements," (Westinghouse Electric Corp.) Anal. Chemistry, p. 29A (25th Exposition of Chem. Industries) (1956).

"Cypak systems," Toolings and Prod., 21, 3, 71-76 (1955); Referat Zhur. Elektrotekh. 12, 22201 (1956).

"Cypak systems– Neue Elemente für die Steuertechnik," Regelungstechnik, 4, 6, 150-151 (1956).

"Cypak – the most revolutionary industrial control advance in 25 years," Control Engineering 16-17 (April 1956) 2 fig.

"Improved controls for aircraft ac systems – magnetic amplifier voltage regulator," Westinghouse Engineer, 1, 27 (1956).

"Magamps watch for the breaks," Westinghouse Engineer, 1, 23 (1955).

"Magnetic amplifiers capture more business," Westinghouse Engineer, 2, 61 (1956).

"Magamp quarterbacks improved drive," Westinghouse Engineer, 2, 29 (1956).

"Miniature saturable reactors use ferro-ceramic cores," Electr. Manufact. 55, 6, 142, 144 (1955) 2 fig.

"New control system uses no moving parts," Electrified Ind., 19, 5, 60 (1955).

"New 'brains' for industry," Westinghouse Engineer, 16, 1, 25 (1956).

"New miniature servo magnetic amplifiers," (Magnetic Amplifiers Inc., N. Y.) Electronics, 2, 274 (1956).

"New products: 1) two staged MU, 2) modulator, 3) MU, 400 cycles, 15 watts," Control Engineering, 2, 8, 90-104, 107-109 (1955).

"Rival of transistors: magnistors," Amer. Aviat., 18, 22, 77 (1955).

"Saturable reactor replaces vacuum tubes for many functions," Mach. Design, 28, 20, 136, 138, (1956) 1 fig.

"Stable magnetic amplifier," (Airpax Design Engineers) Control Engineering, 3, 6, 19 (1956).

"Servo amplifier with instantaneous response," Electronics, 29, 1, 270-271 (1956).

"This is Cypak – the most revolutionary industrial control advance in 25 years," Automation, 3, 5, 14-15 (1956).

"This is Cypak, to eliminate maintenance on industrial control," Product Engineering, p. 32 (1956).

"This is Cypak, for more flexible industrial control," Product Engineering, 5, 443 (1956).

"Transistors, magamps present wide new horizons," Westinghouse Engineer, 1, 37 (1955).

"Voltage regulator is magnetic amplifier type," Aviat. Age, 24, 5, 120 (1955); Referat. Zhur. Elektrotekh. 2, 3938 (1957).

G. V. Subbotina